

**UNIVERSIDADE NOVE DE JULHO
PROGRAMA DE PÓS GRADUAÇÃO STRICTO SENSU
DOUTORADO EM CIÊNCIAS DA REABILITAÇÃO**

RENATA KELLY DA PALMA

**Estudo do comportamento da mecânica vascular
no processo de descelularização pulmonar.**

**São Paulo
2015**

RENATA KELLY DA PALMA

**Estudo do comportamento da mecânica vascular
no processo de descelularização pulmonar**

Tese apresentada ao Programa de Pós Graduação Stricto Sensu da Universidade Nove de Julho como requisito para obtenção do título de Doutor em Ciências da Reabilitação.

Orientador: Prof. Dr. Luis Vicente Franco de Oliveira.

Co-orientador: Prof. Dr. Ramon Farrè.

Universidade de Barcelona (Espanha).

São Paulo

2015

Palma, Renata Kelly da.

Estudo do comportamento da mecânica vascular no processo de descelularização pulmonar./ Renata Kelly da Palma. 2015.

125 f.

Tese (doutorado) – Universidade Nove de Julho - UNINOVE, São Paulo, 2015.

Orientador (a): Prof. Dr. Luis Vicente Franco de Oliveira.

1. Mecânica vascular. 2. Pulmões. 3. Bioengenharia de órgãos. 4. Descelularização. 4. Perfusão pulmonar.

I. Oliveira, Luis Vicente Franco de.

II. Título

CDU 615.8

São Paulo, 07 de outubro de 2015.

TERMO DE APROVAÇÃO

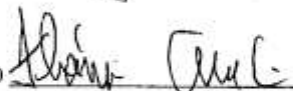
Aluno(a): Renata Kelly da Palma

Título da Tese: "Estudo do comportamento da mecânica vascular no processo de descelularização".

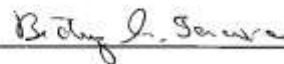
Presidente: PROF. DR. LUIS VICENTE FRANCO DE OLIVEIRA



Membro: PROF. DR. FLAVIO AIMBIRE SOARES DE CARVALHO



Membro: PROFA. DRA. BEATRIZ MANGUEIRA SARAIVA



Membro: PROFA. DRA. LUCIANA MARIA MALOSÁ SAMPAIO



Membro: PROF. DR. RODOLFO DE PAULA VIEIRA



DEDICATÓRIA

Dedico a minha mãe.

AGRADECIMENTOS

Para chegar ao final dessa longa caminhada percorri caminhos com muito trabalho e dedicação. Chego aqui hoje podendo dizer que muitas pessoas participaram desse processo, dessa forma deixo minhas palavras de agradecimento.

Primeiramente minha eterna gratidão á minha querida mãe, mulher de fibra, guerreira que me ensinou a viver em um mundo onde as coisas não acontecem se não existir muito trabalho e persistência. Ensinou-me o valor da verdade, lealdade e dignidade.

Agradeço minha base familiar que me deixa cair levantando-me em seguida, pois a queda faz parte da aprendizagem. Minha Vó Ina, por me permitir ter uma infância maravilhosa regada a mimos e carinhos, uma adolescência com os melhores conselhos e um presente com muito apoio e incentivo na vida acadêmica.

Ao meu irmão que sempre me apoiou e incentivou em todas minhas escolhas.

Aos meus companheiros de vida que estiveram ao meu lado nessa caminhada, compreendendo minha distância nesse momento: Miriam, Infinita, Panga, Goran e Dri.

Aquele que apostou todas as fichas e confiou em mim sem me conhecer e hoje me orgulho em dizer que fui orientada pelo Prof. Dr. Luis Vicente Franco de Oliveira. Um cara que adota seus alunos e tem um coração enorme me mostrando o tipo de pesquisadora que eu almejo me tornar.

Aos amigos e colegas do Laboratório do Sono. Obrigada por me receberem de braços abertos com esse meu jeito meio maluco. Em especial minhas alunas Jessica e Letícia.

Als amics i col·legues del laboratori de biofísica de la Universitat de Barcelona. Gràcies per l'any increïble en termes d'aprenentatge professional, d'intercanvi cultural i de totes les cerveses dels divendres. Especialment al Prof. Dr. Ramón Farre, a la Noelia, a la Maeba, a en Juan, a en Vinicius, a la Paula, a la Marta, a en Ig, a la Valentina.

Aos amigos e colegas do Laboratório de Imunologia Pulmonar e do Exercício. Obrigada pelas horas compartilhadas durante o “tec tec” da mecânica pulmonar. Em especial ao Prof Dr Rodolfo de Paula Vieira por ceder um espaço em seu laboratório para nossos experimentos e as alunas Nicole e Léia.

Aos meus eternos amigos do Laboratório de Fisiologia Translacional que sempre me apoiaram e incentivaram nessa minha mudança de caminho.

As pessoas especiais que a pesquisa me deu de presente. Cat pelas horas de conversa, parceria e amizade em momentos únicos. Flávia por todo suporte científico e emocional nessa reta final, obrigada!!!!

Obrigada a todos que fizeram parte dessa conquista direta ou indiretamente.

Agradeço a Coordenação de Aperfeiçoamento de Pessoal de Nível Superior(CAPES) pelo suporte financeiro.

RESUMO

A geração artificial de órgãos é uma alternativa potencial na obtenção de órgãos viáveis para o transplante humano. Obter *scaffolds* perfeitos para serem recelularizados é um grande desafio e um passo fundamental na bioengenharia de pulmões. A técnica de perfusão de agentes descelularizantes através da artéria pulmonar (AP) tem se apresentado muito eficaz no processo entretanto, a pressão e o fluxo de perfusão vascular variam ao longo do processo de descelularização pulmonar. Estes fatores ainda não se encontram totalmente compreendidos, sendo muito importantes na otimização do processo, assegurando a integridade dos *scaffolds*. Os objetivos foram caracterizar a relação pressão/fluxo vascular pulmonar associado a variação de resistência vascular (RV), de acordo com o controle da perfusão (pressão ou fluxo) no momento da infusão de diferentes agentes descelularizantes na AP e determinar o comportamento da RV em relação a diferentes pressões de insuflação pulmonar (pressão traqueal) e de perfusão (artéria pulmonar). Para o primeiro estudo, foram utilizados 43 pulmões de camundongos machos saudáveis (C57/BL6) com idade de 7-8 semanas e no segundo estudo, pulmões de 5 ratos machos saudáveis (Sprague- Dawley) com idade de 7-8 semanas. No primeiro estudo, após excisão e canulação da traqueia e da artéria pulmonar, os pulmões foram insuflados a uma pressão de 10 cmH₂O na via aérea e submetidos ao processo convencional de descelularização sendo perfundidos através da AP. Para o segundo estudo, os pulmões descelularizados foram submetidos a variações de pressão traqueal (0 à 15 cmH₂O) e pressão vascular (5 à 30 cmH₂O). A pressão na artéria pulmonar (P_{PA}) e o fluxo da artéria pulmonar (V'_{PA}) foram continuamente mensurados. A RV ($RV = P_{PA} / V'_{PA}$) variou consideravelmente ao longo do processo de descelularização pulmonar, particularmente na perfusão por pressão controlada, quando comparado a perfusão controlada por fluxo. Concluímos que o monitoramento da mecânica de perfusão ao longo do processo de descelularização fornece informações relevantes na otimização do processo, assegurando um limite para pressão vascular, preservando a integridade do *scaffold*. Somado a estes achados um resultado relevante demonstrou que a pressão arterial pulmonar tem mais influência no comportamento da RV nos pulmões descelularizados do que pressão positiva nas vias aéreas, fornecendo informações importantes para futuro manejo no processo de recelularização utilizando a RV como um facilitador na distribuição celular através do arcabouço celular pulmonar.

Palavras-chave: mecânica vascular, pulmões, bioengenharia de órgãos, descelularização, perfusão pulmonar.

ABSTRACT

Organ biofabrication is a potential future alternative for obtaining viable organs for transplantation. Achieving intact scaffolds to be recellularized is a key step in lung bioengineering. The decellularizing agent perfusion technique via the pulmonary artery (PA) has been shown very effective in the process however; vascular perfusion pressure and flow vary along the pulmonary decellularization process. These factors are not fully understood it being very important in the optimization process, ensuring the integrity of the scaffold. The objectives were to characterize the pressure / pulmonary vascular flow associated with variation in vascular resistance (VR), according to the control of the infusion (pressure or flow) at the time of the infusion of different decellularizing agents in PA and determine the VR's behavior in relation to different pressures of lung inflation (tracheal pressure) and perfusion (pulmonary artery). For the first study, were used 43 lungs of the healthy mice (C57/BL6) with 7–8 weeks old and in the second study, lungs of the 5 healthy rat (Sprague- Dawley) with 7-8 weeks old. In the first study, after excision and tracheal cannulation, lungs were inflated at 10 cmH₂O airway pressure and subjected to conventional decellularization process being perfused through PA. For the second study, the decellularized lungs were subjected to variations in tracheal pressure (0 to 15 cmH₂O) and vascular pressure (5 to 30 cmH₂O). Pressure (P_{PA}) and flow (V'_{PA}) at the pulmonary artery were continuously measured. The VR ($VR=P_{PA}/V'_{PA}$) considerably varied throughout lung decellularization, particularly for pressure controlled perfusion, as compared with flow-controlled perfusion. This study shows that monitoring perfusion mechanics throughout decellularization provides information relevant for optimizing the process time while ensuring that vascular pressure is kept within a safety range to preserve the organ scaffold integrity. Moreover, arterial lung pressure has more influence on behavior of vascular resistance in decellularized lungs than positive airway pressure, providing information that could be relevant for future cell repopulation by using the vascular resistance as a facilitator cell distribution throughout pulmonary circuit.

Keywords: vascular mechanics, lungs, bioengineering, decellularization, lung perfusion.

SUMÁRIO

LISTA DE FIGURAS	x
LISTA DE ABREVIATURAS	xii
1.CONTEXTUALIZAÇÃO	1
1.1. Bioengenharia de órgãos	1
1.1.1 O tratamento final para falência de órgãos	1
1.1.2. Engenharia de órgãos e tecidos complexos	1
1.1.3. Matriz extracelular como um scaffold biológico	2
1.1.4. Princípios e métodos de descelularização	4
1.2. Bioengenharia pulmonar	8
1.2.1Potencial da Bioengenharia de pulmão nas doenças respiratórias	8
1.2.2. Técnicas de descelularização pulmonar	8
1.2.3. Uso potencial de células-tronco na engenharia de pulmões	10
1.3. Jutificativa	11
2. OBJETIVOS	12
2.1. Objetivo geral	12
2.1.1. Objetivos específicos	12
3. MÉTODOS	13
3.1. Escopo do estudo	13
3.2. Caracterização do estudo	13
3.3. Caracterização da Amostra	13
3.4. Aspectos Éticos e Legais	14
3.5. Protocolo experimental para avaliar a resistência vascular	14
3.6. Descelularização dos Pulmões	17
3.7. Avaliação do processo de descelularização	19
3.7.1. Quantificação de DNA e dos componentes da matriz extracelular (ECM) nos pulmões descelularizados	19

3.7.2. Microscopia de contraste de fase	20
3.8. Avaliação da elastância pulmonar	20
3.9. Protocolo experimental para avaliar a resistência vascular sob diferentes pressões traqueais e vasculares	22
3.10. Análise estatística	22
4. RESULTADOS	23
4.1. Estudo I	23
4.1.1. Introdução	23
4.1.2. Resultados	25
4.1.3. Discussão	33
4.1.4. Conclusão	35
4.2. Estudo II	36
4.2.1. Introdução	36
4.2.2. Resultados	37
4.2.3. Discussão	38
4.2.4. Conclusão	38
5. CONSIDERAÇÕES FINAIS	39
6. REFERÊNCIAS BIBLIOGRÁFICAS	41
7. APÊNDICES	54
8. ANEXOS	79
Comitê de Ética – CEUA – UNINOVE	79
Publicações durante o doutorado	81
• Increased upper airway collapsability in a mouse model of Marfan Syndrome	81
• Respiratory mechanics study in experimental animal model of venom-induced acute lung injury: a new proposal for an olds technique	84
• Mechanical properties of acellular mouse lungs after sterilization by gamma irradiation	89
• Decellularized lung scaffolds for bioengineed organs	99
• Mathematical models for measuring mechanical properties in experimental animal lung: a literature review	104

LISTA DE FIGURAS

Figura 1. Fluxograma dos estudos_____	14
Figura 2. Diagrama de descelularização de pulmão por perfusão através da artéria pulmonar (A) e representação das resistências capilares de série e resistências transmembranares paralelas (B). _____	15
Figure 3. Desenho experimental do estudo. _____	16
Figura 4. Descelularização por perfusão 20cmH ₂ O _____	18
Figura 5. Descelularização por perfusão fluxo 0.2 e 0.5 ml/min_____	18
Figura 6. Pulmão fresco(direita) e pulmão descelularizados (esquerda)____	18
Figura 7. Curvas fluxo e pressão traqueal em relação ao tempo_____	21
Figura 8. Coloração fluorescente de corante 4`-6-diamidino-2-finilindol em pulmões nativos e descelularizados. _____	26
Figura 9. Elastâncias estática (Est) e dinâmica (Edyn) pulmonar computadas por meio de oclusão ao final da expiração durante a ventilação mecânica convencional. _____	27
Figura 10. Pressão e fluxo na artéria pulmonar durante a descelularização pulmonar por perfusão de pressão constante, com veia pulmonar aberta para atmosfera. _____	29
Figura 11. Pressão e fluxo na artéria pulmonar durante a descelularização pulmonar por perfusão de fluxo constante, com veia pulmonar aberta para atmosfera. _____	30

Figura 12. Pressão e fluxo na artéria pulmonar durante a descelularização pulmonar por perfusão de fluxo constante, com veia pulmonar aberta para atmosfera. _____ **31**

Figura 13. Fluxo através da artéria pulmonar durante o processo de descelularização por perfusão de pressão constante, com veia pulmonar aberta para atmosfera (●) e veia pulmonar ligada (■). _____ **32**

Figura 14. Pressão e fluxo mensurados na artéria pulmonar de pulmão descelularizado submetido a variações de pressões arteriais e pressões positivas contínuas. _____ **37**

LISTA DE ABREVIATURAS

- 3D: tridimensional
- CPAP: pressão positiva nas vias aéreas
- CHAPS: detergente 3 - [(3-colamidopropil) dimetilamônio] -1-propanossulfonato
- DAPI: corante 4'-6-diamidino-2-finilindol
- DNA: ácido desoxirribonucleico
- DPOC: doença pulmonar obstrutiva crônica
- DP1: queda rápida pressão traqueal
- DP2: queda lenta pressão traqueal
- EDTA: ácido etilenodiamino tetra-acético
- Edyn: elastância dinâmica
- EGTA: ácido etilenglicol tetraacético
- EPM: erro padrão da média
- Est: elastância estática
- GAGS: glicosaminoglicanos
- H₂O : água deionizada
- MEC: matriz extracelular
- P_{alv}: pressão aveolar
- PBS: tampão fosfato salino
- PEL: platô pressãp traqueal
- Pi: ponto de inflexão
- Po: pressão pré-inspiratória
- P_{PA}: pressão na artéria pulmonar
- P_{PV}: pressão na veia pulmonar
- Rv: resistência vascular
- SDS: detergente sullfato dodecil de sódio
- SNP: nitropussiato de sódio
- Tr: canulação traqueal
- V_{TM}: fluxo na membrana alviolo-capilar
- V_{PA}: fluxo artéria pulmonar
- V_{PV}: fluxo na veia pulmonar
- pH: potencial hidrogeniônico
- OCT: Optimal Cutting Temperature compound

1. CONTEXTUALIZAÇÃO

1.1. Bioengenharia de órgão

1.1.1 O tratamento final para falência de órgãos

A falência de órgãos de pacientes em fase terminal é um grave e dispendioso problema que apresenta altas taxas de crescimento no mundo. Atualmente, o transplante alogênico se apresenta como uma única opção de tratamento definitivo. A doença cardíaca coronária¹, a insuficiência renal², a insuficiência hepática³ e a doença pulmonar obstrutiva crônica (DPOC)⁴ contabilizam como sendo as patologias com maior índice de mortalidade em países ocidentais desenvolvidos.

O número de transplantes de órgãos vem crescendo a cada ano, assim como o número de pacientes em lista de espera. No caso do transplante pulmonar, esse número de pacientes no aguardo de um novo órgão duplicou em apenas 10 anos. Além disso, a população nos países desenvolvidos ocidentais está em um processo progressivo de envelhecimento, e isto significa que no futuro menos doadores estarão disponíveis e mais pacientes necessitarão de transplante⁵.

Os pacientes que obtêm sucesso na lista e recebem um órgão do doador, são obrigados a lidar com um tratamento imunossupressor ao longo da vida, além do risco de rejeição crônica e morbimortalidade associada⁶. Dada a necessidade urgente de um maior número de órgãos viáveis para transplante e diante da escassez de doadores, a engenharia de tecidos parece ser uma solução viável como método alternativo na resolução dos problemas de rejeição, devido a utilização de células autólogas⁷.

1.1.2. Engenharia de órgãos e tecidos complexos

Durante décadas vários materiais de *scaffolds* têm sido empregados na tentativa de construir tecidos biológicos⁷. No entanto, atualmente *scaffolds* sintéticos são incapazes de recriar a complexa arquitetura 3D dos tecidos originais. Nos últimos anos avanços significativos têm sido realizados no desenvolvimento da engenharia de tecidos como nos vasos sanguíneos^{1,8}, bexiga⁹ e traquéia¹⁰.

No entanto, estes tecidos apresentam a particularidade de não necessitarem do acoplamento à circulação sanguínea no momento da implantação. Ao lidar com órgãos completos, este recurso não pode ser obtido devido a necessidade de uma rede vascular intacta para conectar a circulação do receptor.

Portanto, existe uma necessidade eminente de uma estratégia em medicina regenerativa assegurando que a substituição de um órgão por completo torne-se possível para os pacientes com doenças em fase crônica final¹¹.

Atualmente, uma abordagem promissora para a substituição de órgãos funcionais é a descelularização prévia de órgão. Os órgãos alogênicos ou xenogênicos, tais como coração¹², fígado¹³ e pulmões¹⁴⁻¹⁶ fornecem, após o processo de descelularização, um *scaffold* natural que pode ser subsequentemente repopulados com células tronco. O objetivo, visando a clínica, é a utilização da matriz extracelular do órgão descelularizado para ser recelularizado com células autólogas obtidas do próprio paciente, evitando a necessidade de tratamento com imunossuppressores. Até o momento, a literatura aponta resultados encorajadores, uma vez que a formação de neotecido funcional tem sido demonstrada em modelos pré-clínicos com animais^{9,13,14}. Estes resultados nos permitem considerar a hipótese de que a engenharia de órgãos é um caminho viável em relação à complexa engenharia de tecido tridimensional^{13,14}.

Para o sucesso da engenharia de órgãos, vários parâmetros primordiais ainda necessitam de ajustes tais como, a determinação da espécie dos candidatos a partir do órgão a ser retirado (diferente de doadores humanos), quais os melhores protocolos para a descelularização, a otimização do processo de recelularização, o tipo celular mais adequado para a recelularização, a endotelização da matriz vascular e o desenvolvimento de biorreatores adequados ao processo de recelularização.

1.1.3. Matriz extracelular como um *scaffold* biológico.

Os tecidos e órgãos são formados por células associadas a matriz extracelular (MEC), que por sua vez, é sintetizada por células residentes únicas e específicas do tecido. Tradicionalmente, os tecidos foram considerados como células apoiadas por um estroma estático e em oposição a esta idéia, a MEC é dinâmica, agindo de forma recíproca as células que a estão formando^{17,18}. As células residentes da MEC são influenciadas pelas condições do microambiente, tais como a concentração de oxigênio do meio, o potencial de hidrogeniônico (pH), as forças mecânicas e a composição bioquímica específica¹¹. Estes fatores irão direcionar o seu perfil genético, o proteoma e a sua funcionalidade. Por sua vez, as células secretam componentes adequados e moléculas que podem garantir a sua sobrevivência, função e comunicação com outras células. Essa interação recíproca assegura a manutenção de um estado de homeostase tecidual que quando alterado conduz a um dano¹⁹⁻²¹.

Além da participação na homeostase tecidual, a MEC participa do remodelamento tecidual pós lesão^{22,23}. Os processos envolvidos nesta resposta compreendem em liberação de quimiocinas e citocinas²⁴, modulando o sistema imune²⁵, fornecendo sinais moleculares específicos do tecido agindo no fenótipo e na função celular^{14,26,27}. A MEC também influencia a migração, a proliferação e a diferenciação celular²⁸, etapas necessárias durante o processo de recelularização. Portanto, a MEC nativa é um *scaffold* ideal para a engenharia de tecidos e órgãos²⁸.

A literatura científica já provou que órgãos completos descelularizados demonstraram aderência de subtipos celulares adultos em locais anatômicos corretos e também foi verificada uma diferenciação em fenótipos celulares específicos durante o processo de recelularização¹²⁻¹⁴. É provável que a estrutura 3D, a topologia de superfície, a apresentação de ligantes, de moléculas bioativas e a composição da MEC, participem e contribuam para o processo de recelularização local específico²⁹.

Outra vantagem das matrizes descelularizadas é que estas induzem uma resposta angiogênica *in vivo*, propriedade crucial na implantação do tecido, garantindo a revascularização para o fornecimento de nutrientes e oxigênio^{30,31}.

Portanto, a retenção de componentes da MEC é essencial no processo de decelularização. Entretanto, ainda é desconhecida qual combinação de proteínas deve permanecer para manter a sinalização para as funções celulares. O protocolo de descelularização a ser utilizado, deve ao mesmo tempo assegurar uma remoção eficaz da população de células nativas e garantir que todos estes componentes da matriz tenham uma alteração mínima, com uma atenção especial a célula acoplada ao ligante¹¹. Nesse sentido, devemos nos ater para que substâncias como detergentes biológicos possam ativar as metaloproteinases da matriz e, potencialmente exacerbar a degradação dos epítomos de ligação nas proteínas da MEC restantes³².

Dentre as moléculas estruturais mais relevantes da MEC que permanecem após a descelularização destacamos os glicosaminoglicanos (GAGs), colágenos, elastina, fibronectina, laminina e vitronectina^{29,32-34}. Os colágenos são componentes estruturais do MEC responsáveis pela resistência mecânica global. A elastina é uma importante proteína que participa nos processos de distensão e fornece as propriedades intrínsecas de recuo de tecidos tais como as encontradas no pulmão. Os GAGs ajudam no controle macromolecular e no movimento celular na lâmina basal do epitélio e pode desempenhar um papel de mecânica em alguns tecidos.

Todas estas proteínas são altamente conservadas juntamente com os organismos eucariotas, o qual poderia explicar a ausência de uma resposta imunológica adversa sobre o xenotransplante³⁵⁻³⁸.

1.1.4. Princípios e métodos de descélularização

Nos últimos anos, inúmeras técnicas surgiram como propostas para descélularizar órgãos completos, preservando a sua estrutura 3D em conjunto com os principais componentes da MEC³⁹. Ainda não existe na literatura científica um protocolo ideal que propicie a completa remoção do material celular sem comprometer a estrutura, a atividade biológica e ou as propriedades mecânicas da MEC restante.

É de grande importância levar em consideração que cada passo do processo de remoção celular poderá alterar as propriedades da MEC, podendo causar alguma ruptura na sua estrutura. Portanto, evitar totalmente estes danos passa a ser um dos grandes desafios na bioengenharia de órgãos³⁹.

Vale ressaltar que ainda não existe um protocolo ideal que possa ser utilizado no processo de descélularização de todos os tipos de tecidos e órgãos, uma vez que a descélularização irá depender de diversos fatores, incluindo a celularidade do tecido (fígado vs. tendão), a densidade (derme vs. tecido adiposo), o teor lipídico (cerebral vs. bexiga urinária) e a espessura dos tecidos (derme vs. pericárdio)²⁹.

Os protocolos de descélularização baseiam-se na utilização de diferentes combinações de métodos físicos, iônicos, químicos e enzimático e, diversas constantes de tempo (horas ou semanas)¹¹. As diferentes técnicas buscam uma ruptura das células, com consequente liberação de seu conteúdo e remoção destes detritos celulares. Apesar da variedade de métodos e protocolos, é extremamente difícil obter uma completa descélularização e na maioria dos casos o *scaffold* produzido retém ácido desoxirribonucleico (DNA) residual^{40,41}.

Além da eliminação do DNA, a remoção eficaz dos epítomos antigênicos, presentes nas membranas celulares e citoplasma das células, se faz necessário para minimizar a possível resposta imunogênica no momento da implantação de novas células, devido fato de que os antígenos alogênicos e xenogênicos poderiam ser reconhecidos pelo hospedeiro e induzirem uma resposta inflamatória com provável rejeição⁴²⁻⁴⁴.

- **Agente Físico**

A temperatura é o agente físico mais comumente empregado, sendo utilizado através de ciclos de congelamento-descongelamento, uma vez que por meio desse processo se consegue o rompimento das células pela formação de cristais durante as etapas de congelamento. Estes ciclos auxiliam a redução da resposta imune em *scaffolds* de MEC vasculares⁴⁴. Além disso, não há perda de proteínas da MEC produzida⁴⁵ e o efeito sobre as propriedades mecânicas do *scaffold* é mínimo^{46,47}. Após estas etapas de congelamento-descongelamento, os detritos celulares irão ficar retidos no tecido necessitando a associação de outro processo de descclularização nessa amostra.

Outra estratégia consiste na aplicação de abrasão mecânica em combinação com enzimas, solução salina hipertônica ou agentes quelantes visando facilitar a dissociação celular a partir da membrana basal⁴⁸. Isto é muito eficaz em tecidos como da bexiga urinária, intestino delgado ou pele, nos quais as superfícies são distintas e acessíveis durante a sua manipulação⁴⁸.

Finalmente, outras abordagens menos empregadas, são a pressão hidrostática e a eletroforese irreversível não térmica. A pressão hidrostática tem sido aplicada na descclularização de vasos sanguíneos e tecidos da córnea^{49,50}. A eletroforese irreversível não térmica consiste em indução de microporos sobre as células quando se aplica potenciais elétricos através da membrana, podendo ser utilizada apenas em tecidos menores por razões de limitação de tamanho.

- **Agentes biológicos**

Os agentes biológicos são divididos em agentes enzimáticos e não enzimáticos. Dentre as enzimas temos as nucleases, desoxirribonuclease (DNase) e as ribonucleases (RNases), que auxiliam na limpeza das sequências de ácido nucleico após a lise celular^{49,51,52}; a tripsina, que é geralmente utilizada como um passo inicial para tecidos densos, mas que pode causar grave ruptura na estrutura; as colagenases, que pode ser empregada quando a preservação do colágeno não é crítica; as lipases, que são insuficientes, se utilizadas isoladamente, mas ajudam quando combinadas com outros reagentes^{53,54} e a dispase, que é geralmente mais eficaz quando combinada com a tripsina na descclularização de tecidos mais espessos como a derme⁵⁵.

Os agentes não enzimáticos são o quelante e os inibidores da protease serina. Os agentes quelantes tais como ácido etilenodiamino tetra-acético (EDTA) e o ácido etilenglicol tetra-acético (EGTA) são utilizados muito frequentemente porque auxiliam na dissociação de células da MEC por sequestro de íons^{56,57}.

A utilização do EGTA sem associação é insuficiente na eliminação das células, de modo que eles são normalmente aplicados em combinação com enzimas como a tripsina^{49,52,58-61}.

- **Agentes químicos**

Uma grande variedade de agentes químicos é utilizada nos protocolos de descclularização. Eles podem ser divididos pela sua natureza em ácidos e bases, solução hipertônica e hipotônica, detergentes, álcoois e outros solventes. Os ácidos e as bases podem promover ou catalisar a degradação de biomoléculas. O periacético e o ácido acético são comumente utilizados, sendo o primeiro menos prejudicial para a MEC em relação ao segundo⁶²⁻⁶⁴. O hidróxido de cálcio, o sulfureto de sódio e o hidróxido de sódio também são empregados, mas com cuidado porque podem comprometer as propriedades mecânicas da MEC e eliminar os fatores de crescimento tecidual⁶⁵.

As soluções salinas hipertônicas atuam dissociando o DNA das proteínas e as soluções hipotônicas são úteis para romper as células por um efeito osmótico produzindo um mínimo impacto sobre a MEC⁶⁶. Visando o aumento do efeito de osmose, normalmente realizava-se a imersão do tecido em soluções hipotônicas e hipertônicas, em ciclos repetidos⁶⁶. Os detergentes biológicos, que podem ser iônicos, não iônicos e zwitteriônico, tem a função de remoção do material celular do tecido por solubilização de células e dissociação de DNA-proteína^{67,68}. A sua eficiência aumenta com o tempo de exposição^{51,55,69}, variando com o tecido e idade do doador^{45,70,71}.

O detergente não iônico Triton X-100 é normalmente utilizado em tecidos mais espessos⁵⁸, sendo mais eficaz do que os detergentes iônicos em processos envolvendo tecidos com alto teor de lipídeos. Os detergentes iônicos solubilizam as membranas celulares e compostos nucleicos e tendem a desnaturar as proteínas. O dodecilsulfato de sódio (SDS) é o detergente mais comum utilizado em protocolos de descclularização e tem sido aplicado em tecidos mais espessos como o de rins ou pulmões^{72,73} sendo muito apropriado quando a conservação das propriedades mecânicas dos tecidos se faz necessária, embora possa provocar rompimento em estruturas^{16,74,75} e eliminação do fator de crescimento⁶⁵.

Os detergentes zwitteriônicos, tais como o 3-[(3-Cholamidopropyl)dimethylammonio]-1-propanesulfonate hydrate (CHAPS), apresentam propriedades de ambos os detergentes, iônicos e não iônicos, e eles são normalmente aplicados à descclularização de tecidos mais finos, como o de pulmão¹⁶, córnea⁶⁹ ou nervos⁷⁶.

Por vezes, os detergentes são utilizados em combinação, a fim de aproveitar a vantagem das propriedades de ambos os compostos como, por exemplo a utilização de um protocolo de SDS e CHAPS concomitantemente⁷⁷.

Quando se utilizam detergentes como agentes de descclularização é extremamente importante lavar muito bem os tecidos antes de que a recelularização aconteça. Os produtos químicoempregados podem penetrar na MEC, especialmente em tecidos espessos, e se não forem bem removidos, a citotoxicidade pode ocorrer no momento da recelularização^{78,79}.

Finalmente, os álcoois tais como o glicerol, o isopropanol, o etanol, o metanol e outros solventes como as acetonas podem ser úteis em tecidos com um elevado teor de lípidos, tais como o tecido adiposo^{54,80,81}. A desvantagem do uso de solventes como etanol e metanol é que eles são utilizados para fins de fixação em histologia. Isto significa que eles podem alterar as propriedades da MEC, geralmente na ligação cruzada das proteínas, tornando a matriz mais rígida e também induzindo a precipitação de proteína⁸².

A fim de uma melhor utilização dos agentes acima citados, algumas características do tecido terão que ser observadas (espessura, tamanho, densidade e aplicação futura). É de grande importância considerar que a duração e a complexidade do protocolo de descclularização irão depender do grau desejado de conservação do tecido a ser recelularizado.

Quando se trabalha com órgãos completos é comum realizar a perfusão do agente descclularizante através da vasculatura. Além de preservar a arquitetura dos órgãos, a perfusão pode auxiliar na melhor distribuição de agentes descclularizantes por todo o tecido e na completa remoção dos detritos celulares. A utilização da perfusão para otimizar o processo de descclularização foi descrito pela primeira em modelo de descclularização de corações^{61,83}, de pulmões¹⁴⁻¹⁶, de fígados^{13,84} e de rins^{25,85,86}.

No entanto, o protocolo de perfusão nem sempre é possível devido a especificidades de alguns tecidos que não apresentam uma vasculatura acessível. Nestes casos, a única maneira de otimizar a descclularização é adicionando a agitação com as amostras imersas. Este tem sido o caso de uma grande variedade de tecidos, tais como válvulas cardíacas^{58,54,78}, vasos sanguíneos^{44,77,81}, músculos esqueléticos^{31,87} e tendões⁸⁸⁻⁹⁰. Quando se aplica a agitação, a velocidade deve ser de acordo com as amostras de tecidos que serão agitadas, uma vez que a remoção do DNA e a perda de componentes da MEC ocorrem em função da velocidade de agitação durante o processo³².

1.2. Bioengenharia pulmonar

1.2.1 Potencial da Bioengenharia de Pulmão nas Doenças Respiratórias

As doenças do sistema respiratório tais como a DPOC (enfisema e bronquite crônica), a fibrose pulmonar idiopática, a hipertensão arterial pulmonar primária, a doença intersticial pulmonar, a fibrose cística e a deficiência de α -1-antitripsina resultam em danos pulmonares estruturais irreversíveis, tendo o transplante pulmonar como indicação terapêutica quando a doença atinge uma progressão avançada⁹¹. Infelizmente, o sucesso do transplante pulmonar é limitado, principalmente devido à escassez do número de doadores de órgãos e incidência de bronquiolite obliterante resultante de uma resposta aloimune provocada pelas disparidades entre o doador e os antígenos do receptor. A taxa de sobrevivência de 50% após o transplante de pulmão está confinada a aproximadamente cinco anos⁹¹.

As atuais limitações em relação às doações requerem estratégias no sentido de aumentar a disponibilidade de órgãos para transplante. Necessidade esta, reforçada pelo envelhecimento progressivo da população, o que aumenta a lista de espera de pacientes com doenças respiratórias graves incapacitantes terminais. Por exemplo, a DPOC está prevista para ser a terceira principal causa de morte no ano de 2020^{92,93}. Neste contexto, a bioengenharia de pulmões é considerada uma alternativa terapêutica em potencial, porém as pesquisas atuais se encontram em estágios preliminares e esforços científicos mais intensos são necessários⁹⁴.

1.2.2. Técnicas de descellularização pulmonar

Devido à grande complexidade estrutural de órgãos completos, a abordagem atual para a engenharia de órgãos é baseada na utilização da MEC natural do pulmão descellularizado como partida para a reconstrução do órgão por recellularização em um biorreator¹⁴⁻¹⁶.

A matriz de órgãos descellularizados potencialmente mantém a arquitetura tridimensional e a composição bioquímica, bem como a microvasculatura do tecido original. Estas propriedades únicas tornam o pulmão descellularizado natural, muito promissor para a fabricação bioartificial de pulmões funcionais, uma vez que proporciona uma melhor recriação do microambiente *in vivo*. A técnica de descellularização, como descrito anteriormente, foi utilizada para a engenharia de uma diversidade de tecidos, incluindo ossos, esôfago, artérias, bexiga, traquéia e coração^{12,15,95-100}.

Comparado a outros órgãos, a estrutura do pulmão é particularmente complexa, dificultando o processo de bioengenharia. Apesar dessa complexidade, tem sido demonstrado que com a utilização de protocolos adequados, o pulmão pode ser completamente descelularizado para obter uma estrutura acelular preservada^{101,102}. A descelularização com detergentes biológicos é uma abordagem frequentemente utilizada e pode ser aplicada tanto por perfusão vascular quanto por via traqueal. O método de descelularização por perfusão ocorre por meio da rede vascular intrínseca sendo a forma mais eficiente de distribuir os agentes descelularizantes, até mesmo para tecidos mais espessos, uma vez que diminui consideravelmente a distância da difusão do agente descelularizante, preservando a macroestrutura e microestrutura 3D¹².

Melo et al.¹⁰³, recentemente observaram que a descelularização por perfusão com detergentes SDS ou CHAPS não induziu alterações significativas nas propriedades micromecânicas de pulmões acelulares. Além disso, estudos anteriores demonstraram que esse método por perfusão não comprometeu a arquitetura de vias aéreas ou estrutura vascular de pulmões descelularizados^{14,26,104}. Entretanto todos esses estudos foram realizados por perfusão com pressão constante e mesmo que os métodos alternativos de descelularização tenham sido explorados, nenhuma comparação direta entre a descelularização por perfusão de pressão constante e fluxo constante foi realizada. Além disso, não foi observado na literatura, a descrição do comportamento da resistência vascular pulmonar durante o processo de descelularização e se esse comportamento pode gerar danos a macro e microarquitetura pulmonar¹⁰².

A perfusão de agentes descelularizantes através da artéria pulmonar é um processo que pode ser realizado manualmente, como já demonstrados em estudos anteriores^{32,105-107}. No entanto, este processo não permite controlar a quantidade de agentes na infusão, aumentando o risco de danificar os pulmões. Alternativamente, essa perfusão pode ser controlada de maneira automática através do controle da pressão e ou do fluxo junto a artéria pulmonar. Atualmente existem estudos limitados sobre estes procedimentos, nos quais sugerem que tanto perfusão por fluxo ou pressão controlado pode resultar em um *scaffold* bem descelularizado e com as estruturas preservadas. Alguns poucos estudos recentes têm comparado métodos de perfusão (pressão vs. fluxo controlado e automatizado vs. manual), em termos de eliminação de detritos de células doadoras no *scaffold*, na preservação da composição e da estrutura da MEC do *scaffold* acelular como substrato para posterior cultura de células. Mesmo assim, a resistência vascular pulmonar não foi investigada em nenhum desses estudos¹⁰⁸⁻¹¹¹.

Notavelmente, cada procedimento de perfusão tem suas próprias vantagens e inconvenientes do ponto de vista da mecânica de fluidos. Por um lado, controlar a pressão de perfusão na artéria pulmonar garante que nenhum barotrauma ocorra no *scaffold*, mas o acúmulo de detritos causados por células rompidas poderia reduzir fortemente o fluxo ou mesmo interrompê-lo em caso de pressão insuficiente. Por outro lado, controlar o fluxo infundido na artéria pulmonar garante uma boa quantidade de meios na circulação, mas - também devido ao acúmulo de detritos - pode induzir a uma pressão aumentada dentro dos vasos pulmonares, com risco de danificar a membrana alvéolo-capilar¹⁰¹. No entanto, nenhum estudo detalhado investigou estas questões profundamente. A compreensão da dinâmica de fluidos na perfusão durante o processo de descelularização pulmonar pode fornecer conhecimentos para aperfeiçoar esse processo, tanto para fins de investigação como também para facilitar a otimização na produção de *scaffold* pulmonares.

A preservação das redes vasculares intactas e outras arquiteturas essenciais dos órgãos após o processo de descelularização provê uma base ideal para recelularização¹⁰³. Price et al.¹⁵ relataram que o pulmão descelularizado pode ser recelularizado com células fetais pulmonares submetidas à ventilação simulada. Além disso, Ott et al.¹⁶ e Petersen et al.¹⁴ recelularizaram estruturas descelularizadas de pulmões de roedores com células epiteliais e alveolares para obter um pulmão através de bioengenharia mostrando a funcionalidade das trocas gasosas a curto prazo, após a implantação *in vivo*.

1.2.3. O uso potencial de células-tronco na engenharia de pulmões

Como mencionado por Ott et al.¹⁶ e Petersen et al.¹⁴, a utilização de células indiferenciadas para semear uma MEC pode ser uma estratégia mais prática para bioengenharia pulmonar devido a possibilidade de expansão destas células e sua capacidade de se diferenciar em diferentes fenótipos. Esta abordagem, no entanto, exige células-tronco para serem diferenciadas em fenótipos pulmonares necessários nos locais específicos dentro da estrutura do órgão.

Uma prova de conceito da viabilidade potencial desta abordagem foi recentemente publicada por Cortiella et al.²⁶ demonstrando que após cultivar células-tronco embrionárias murinas em pulmões descelularizados, as estruturas formadas pela diferenciação das células-tronco secretaram os componentes da MEC ausentes no pulmão anteriormente acelular.

Além disso, em culturas de 21 dias de pulmão, a diferenciação local-específica de células-tronco foi evidenciada pela geração de discretos focos de células expressando α -actina de músculo liso, citoqueratina-18 e CC10 em regiões de traquéia e brônquios. Os autores detectaram camadas de células ao longo da superfície interna da traquéia e dos brônquios que expressaram marcadores de células epiteliais como TTF-1, citoqueratina-18, ou CC10, que também incluiu algumas células ciliadas.

Estes dados sugerem que o pulmão descelularizado preserva os sinais biológicos mediados pela estrutura pulmonar descelularizada, suficientes para direcionar as células-tronco a linhagens específicas de pulmão e orientar o desenvolvimento de tecido pulmonar específico *in vitro*, demonstrando a capacidade dos sinais da MEC em influenciar a diferenciação das células-tronco embrionárias de forma local específica. No entanto, é notável que estes resultados promissores tenham sido obtidos por uma estrutura de pulmão recelularizado que não foi submetido aos estímulos físicos associados com os principais processos no pulmão: ventilação e perfusão.

Os estímulos físicos mais notáveis aplicados as células pulmonares são a) um substrato do microambiente com variada viscoelasticidade e estrutura 3D nos diferentes locais do pulmão; b) *cyclic stretch* causado pela mudança contínua do volume pulmonar durante a respiração; c) *shear stress* devido à circulação de fluidos pelas vias aéreas e vasos; d) existência de uma interface ar-líquido no epitélio das vias aéreas e e) diferentes níveis de pressão parcial de oxigênio sobre as várias seções da arquitetura nas trocas gasosas (vias aéreas superiores e inferiores, alvéolos, superfície arterial e venosa dos capilares). Os estímulos físicos, quando aplicados isoladamente ou em combinação com fatores solúveis pró-diferenciação, demonstram modular a diferenciação das células-tronco tanto embrionárias como mesenquimais derivadas da medula óssea, ambas *in vitro*¹⁶⁻¹⁸.

1.3. Jutificativa

Considerando as atuais limitações em relação ao transplante pulmonar, torna-se eminente a busca por estratégias para aumentar a disponibilidade de órgãos para transplante. Dentre as muitas questões em aberto nesta área, a presente tese visou comparar métodos automatizados de descelularização por perfusão (pressão vs. fluxo) hipotetizando que o comportamento da resistência vascular poderia influenciar na produção do *scaffold* pulmonar, pois existe a dúvida se o aumento da resistência vascular durante o processo de descelularização pode gerar danos nesse *scaffold*. Portanto, para responder a essa questão caracterizamos a resistência vascular.

Sabendo que as células pulmonares experimentam diferentes estímulos físicos durante a respiração, o *scaffold* pulmonar deve ser submetido a estímulos que mimetizam a respiração normal, a ventilação e a perfusão, a fim de proporcionar um ambiente fisiológico ideal para que as células sejam cultivadas no pulmão descelularizado. No entanto, dados sobre a variação da resistência circulatória em função das variações das pressões das vias aéreas e vascular são atualmente desconhecidas. Esta informação é de interesse considerável desde a distribuição adequada de células durante a recelularização do *scaffold* e *homing* celular subsequente poderiam ser modulados pela resistência vascular.

Diante do exposto, essa tese foi dividida em dois estudos para caracterizar a mecânica vascular do pulmão descelularizado. Inicialmente, foi realizado um estudo que caracterizou a relação pressão/fluxo na vasculatura pulmonar e verificou como a variação da resistência vascular é dependente da perfusão aplicada, pressão ou fluxo controlados durante o processo de descelularização pulmonar. O segundo estudo, determinou o comportamento da resistência vascular de acordo com a insuflação pulmonar (pressão traqueal) e perfusão (arterial pulmonar). Dessa forma buscar um protocolo eficaz na descelularização e obter parâmetros para futura recelularização.

2. OBJETIVOS

2.1- Objetivo geral

Caacterizar a relação pressão/fluxo vascular pulmonar associado a variação de resistência vascular, de acordo com o controle de perfusão (pressão ou fluxo) no momento da infusão de diferentes agentes descelularizantes na artéria pulmonar e determinar o comportamento da resistência vascular em relação a diferentes pressões de insuflação pulmonar (pressão traqueal) e de perfusão (artéria pulmonar).

2.1.1- Objetivos Específicos

- Avaliar a resistência vascular pulmonar durante o processo de descelularização por perfusão da artéria pulmonar de camundongos;
- Comparar as estruturas das vias aéreas e vasculares de pulmões descelularizados por perfusão arterial por meio pressão ou fluxo constante;
- Avaliar as propriedades viscoelásticas de pulmões descelularizados por perfusão arterial por meio pressão ou fluxo constante;

- Determinar a variação da resistência vascular dependendo da insuflação pulmonar (pressão traqueal) e perfusão (arterial pulmonar).
- Estabelecer um protocolo de descelularização pulmonar;

3. MÉTODOS

3.1. Escopo do estudo

Inicialmente, um primeiro estudo experimental foi realizado para verificar se existe diferença nas estruturas de via aérea e vasculares de pulmões descelularizados pelo detergente dodecil-sulfato de sódio (SDS) por meio de perfusão arterial por pressão constante ou fluxo constante (Estudo 1). Dessa maneira estabelecendo um protocolo adequado para descelularização. Posteriormente, um segundo estudo foi realizado para avaliar a variação da resistência vascular dependente da insuflação pulmonar (pressão traqueal) e perfusão (arterial pulmonar) em pulmões descelularizados, visando estabelecer um protocolo ideal de bioengenharia de pulmão, que promova a proliferação de uma matriz extracelular mais organizada mecanicamente para futura recelularização.

3.2. Caracterização do estudo

Estudo controlado experimental animal, com o envolvimento do Laboratório de Biofísica e Bioengenharia do Departamento de Ciências Fisiológicas da Faculdade de Medicina da Universidade de Barcelona, na cidade de Barcelona – Espanha e do Laboratório Experimental de Mecânica Cardiorrespiratória do Programa de Pós-Graduação Mestrado e Doutorado em Ciências da Reabilitação da UNINOVE.

3.3. Caracterização da Amostra

Foram utilizados 43 camundongos machos da raça C57/BL6, com peso de 17-20 g para o primeiro estudo e cinco ratos machos da raça Sprague- Dawley, com peso de 250–300 g para o segundo estudo. Os animais foram acondicionados nos biotérios do Departamento de Ciências Fisiológicas da Universidade de Barcelona e da UNIVOVE mantidos em ambiente limpo e seco, com luminosidade natural, respeitando o ciclo claro/escuro de 12h, temperatura e umidade relativa do ar adequado. A ração e a água permaneceram *ad libitum* e monitoramento diário para troca de palha e água, até o momento do experimento. Os animais foram distribuídos em grupos, conforme fluxograma da figura 1.

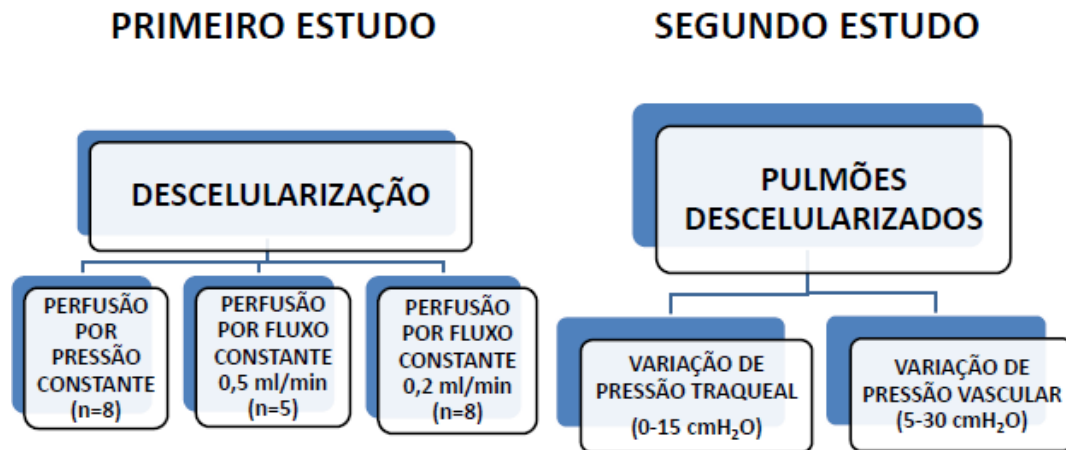


Figura 1. Fluxogramas dos estudos.

3.4. Aspectos Éticos e Legais.

O projeto do estudo foi aprovado pelo Comitê de Ética em Pesquisa (COEP) da UNINOVE, sob protocolo de número 0038/2011. Foram seguidos os Princípios Éticos na Experimentação Animal, editados pelo Colégio Brasileiro de Experimentação Animal – COBEA/Junho de 1991 para os experimentos a serem realizados no Brasil.

3.5. Protocolo experimental

Um sistema experimental foi desenvolvido para medir a mecânica vascular pulmonar durante todo processo de descclularização. A figura 2A representa o diagrama dos capilares e alvéolos pulmonares quando a descclularização do órgão ocorre por perfusão através da artéria pulmonar. A pressão e o fluxo na artéria pulmonar são P_{PA} e V'_{PA} , respectivamente. O fluxo que se movimenta dos capilares para os alvéolos (a uma pressão P_{alv}) através da membrana alveolo-capilar é V'_{TM} . V'_{PV} é o fluxo de saída dos pulmões através da veia pulmonar ($V'_{PA} = V'_{TM} + V'_{PV}$).

A figura 2B corresponde a representação em termos de resistências do circuito de passagem do fluido, onde as resistências em série e em paralelo são representadas pelos capilares e as vias de circulação transmembranar, respectivamente. A descclularização pulmonar ocorre mantendo a veia pulmonar aberta para a atmosfera ($P_{PV} = 0$). Assim, mensurando continuamente a V'_{PA} e a P_{PA} calcula-se a resistência vascular (R_V), onde $R_V = P_{PA} / V'_{PA}$. No experimento o qual a descclularização por perfusão ocorre através da artéria pulmonar com a veia pulmonar ligada ($V'_{PV} = 0$; $V'_{PA} = V'_{TM}$), a R_V avaliada corresponde à da via transmembranar.

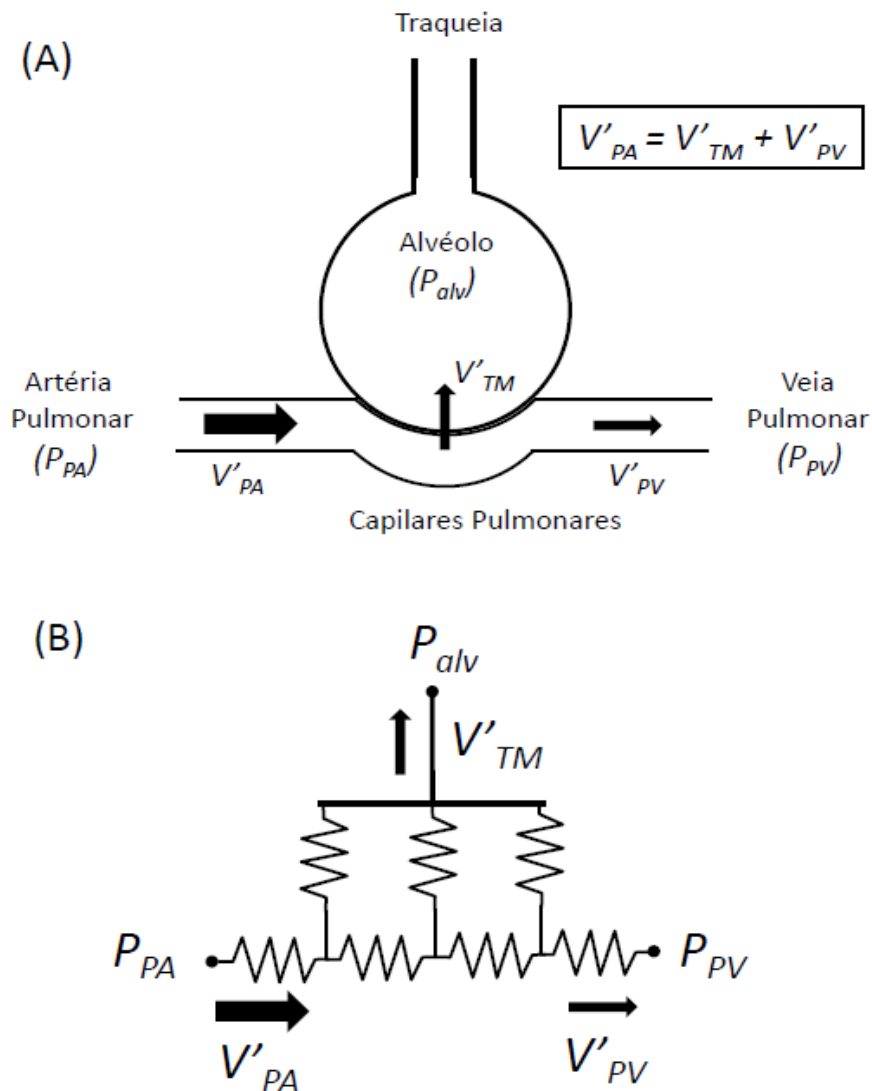


Figura 2. Diagrama de descclularização de pulmão por perfusão através da artéria pulmonar. P_{PA} e V'_{PA} são pressão e fluxo na artéria pulmonar. P_{PV} e V'_{PV} são pressão e o fluxo na veia pulmonar. V'_{TM} é o fluxo médio deixando os capilares para os alvéolos através da membrana alvéolo-capilar. P_{alv} é a pressão alveolar (A). Resistências capilares de série e resistências transmembranares paralelas correspondentes ao circuito (B). Nota: figura do autor.

Para caracterizar as propriedades mecânicas vasculares ao longo do processo de descclularização pulmonar realizada sob diferentes condições de perfusão foi utilizado o sistema experimental mostrado no diagrama da figura 2. A traqueia foi canulada e conectada a um gerador de fluxo contínuo de pressão positiva nas vias aéreas (CPAP) para fornecer uma pressão traqueal (transpulmonar) de 10 cmH₂O, insuflando os pulmões a um volume fisiológico e evitando atelectasias. A pressão traqueal foi verificada por um transdutor de pressão (ICU Medical Inc., San Clemente, CA, EUA).

O fluxo transmembranar V'_{TM} de entrada nas vias aéreas dos capilares saiu do pulmão através de uma porta na entrada da cânula traqueal. A artéria pulmonar foi canulada e ligada a uma das duas possíveis fontes de perfusão controlada, de pressão constante (nível gravimétrica) ou de fluxo constante gerado por uma bomba de infusão (Harvard Apparatus, Holliston, MA, EUA). Em ambos os casos, um transdutor de pressão (ICU Medical Inc., San Clemente, CA, EUA) foi utilizado para mensurar a P_{PA} . A veia pulmonar foi mantida aberta para a atmosfera para permitir que a saída de V'_{PV} ou, alternativamente, ligada sendo $V'_{PV}=0$. Quando a perfusão foi realizada a P_{PA} constante, V'_{PA} foi quantificada a partir da variação do peso registrado por uma balança eletrônica $V'_{TM}+V'_{PV}$ ou somente V'_{TM} (no caso da veia pulmonar ligada), de acordo com a figura 3.

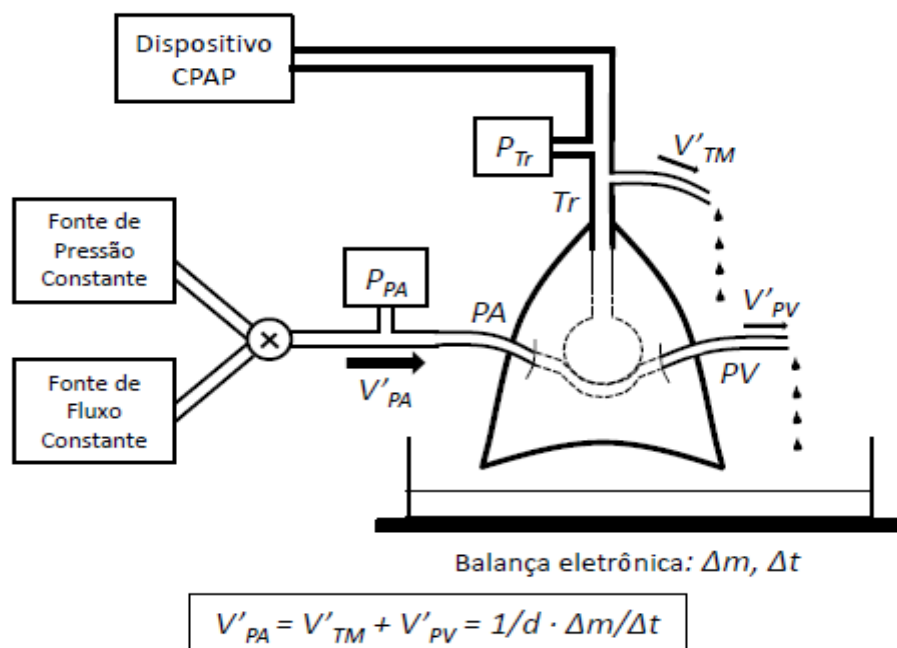


Figure 3. Desenho experimental do estudo.

Nota: CPAP: pressão positiva contínua na via aérea. Ptr: transdutor de pressão para mensurar a pressão traqueal. Tr: cânula traqueal. PA e PV: artéria pulmonar e veia pulmonar canuladas, respectivamente. PPA: transdutor de pressão para medir a pressão da artéria pulmonar. V'_{PA} e V'_{PV} : fluxo na artéria e veia pulmonar, respectivamente. V'_{TM} : fluxo deixando os capilares para os alvéolos através da membrana alvéolo-capilar. Δm alteração do peso medido na balança eletrônica durante um intervalo de tempo Δt . d : densidade do meio de perfusão. Figura da autora.

3.6. Descelularização dos pulmões

Inicialmente, os camundongos foram anestesiados com uretano (1 mg/kg, intraperitoneal), de acordo com protocolo padrão adotado pelo laboratório e posteriormente eutanasiados por exsanguinação da aorta¹¹². Imediatamente após a eutanásia, o diafragma foi perfurado e a caixa torácica rebatida para a visualização dos pulmões.

Os pulmões dos camundongos foram perfundidos através do ventrículo direito com uma solução tampão de fosfato (PBS) contendo 50 U/ml heparina e 1µg/ml de nitroprussiato de sódio (Sigma Chemical Co. ., St. Louis, MO, USA) para evitar formação de coágulos sanguíneos.

A seguir, a traquéia, o esôfago, o coração e os pulmões foram retirados e os tecidos limpos para remover esôfago, tecidos linfáticos e conjuntivos anexos. O protocolo de descelularização dos pulmões compreendeu as etapas de coleta, limpeza, congelamento e descongelamento, lavagem com SDS e PBS²⁶.

Os pulmões foram armazenados a -80° C até que o processo de descelularização fosse iniciado. Os pulmões foram, posteriormente, descongelados em banho-maria a 40°C e congelados rapidamente em gelo seco, seguido por descongelamento. Este processo foi repetido quatro vezes para aumentar a quebra celular e facilitar a sua remoção.

Após a canulação da traqueia e da artéria pulmonar, estas foram conectadas ao sistema experimental adotando a seguinte sequência de meios descelularizantes, perfundidos através da artéria pulmonar, (1) PBS 1x, durante 30 minutos, (2) água deionizada durante 15 minutos, (3) 1% de SDS, durante 150 min e (4) PBS durante 30 minutos.

O processo de descelularização foi realizado em diferentes condições mecânicas, enquanto se mantinha a veia pulmonar aberta (sendo procedimento convencional), os agentes descelularizantes eram perfundidos de acordo com (1) uma pressão constante de $P_{PA}=20$ cmH₂O (8 pulmões), e (2) com fluxos constantes V'_{PA} de 0,2 ml/min (8 pulmões) e de 0,5 ml/min (5 pulmões).

Também foi realizada uma outra sequência de descelularizações pulmonares, a uma pressão constante de $P_{PA}=20$ cmH₂O de tal modo que a veia pulmonar foi ciclicamente mantida aberta e ligada a cada 5 minutos, permitindo assim a comparação de V'_{TM} e V'_{PV} ao longo de todo o processo de descelularização.



Figura 4. Descelularização por perfusão 20cmH₂O



Figura 5. Descelularização por perfusão fluxo 0.2 e 0.5 ml/min

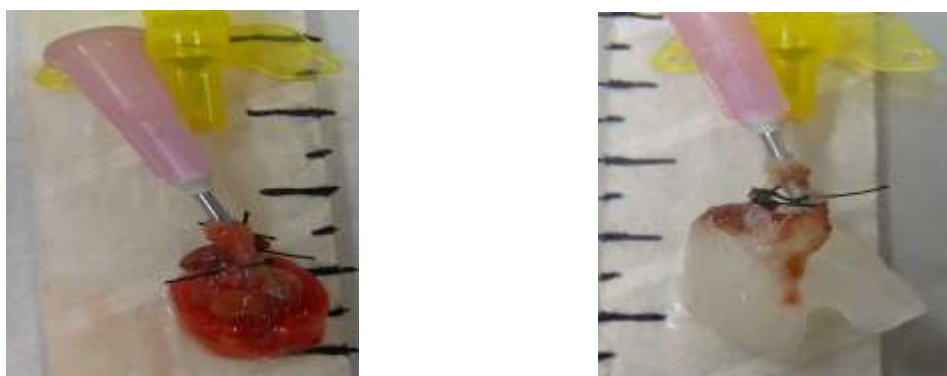


Figura 6. Pulmão fresco(direita) e pulmão descelularizado (esquerda)

3.7. Avaliação do processo de descelularização

3.7.1. Quantificação de DNA e dos componentes da matriz extracelular nos pulmões descelularizados

Após o processo de descelularização, os pulmões (assim como 3 pulmões nativos para comparação) foram divididos em lobos e fixados por infusão bronquial de composto de temperatura ótima para corte (*Optimal Cutting Temperature compound-OCT, Sakura Finetek Inc., USA*) e PBS em uma proporção de 3:1, depois foram submetidos a um congelamento rápido em nitrogênio líquido, sendo posteriormente armazenados a -80°C . As criosecções (10-15 μm) de amostras congeladas de pulmões foram obtidas em um criomicrotomo (*Cryostats, Thermo Fisher Scientific, Waltham, MA, USA*). Para verificar a ausência de DNA celular após o processo de descelularização, foi realizada a coloração fluorescente com o corante 4'-6-diamidino-2-fenilindol (DAPI).

As criosecções foram lavadas com PBS, a fim de remover o OCT e mantidos em solução DAPI (Sigma-Aldrich Co. LLC, USA), a uma concentração de $1\mu\text{g/ml}$, por dez minutos. As proteínas de matriz extracelular, o colágeno, a elastina e a laminina nos pulmões descelularizados foram avaliadas por coloração imunofluorescente para cortes. Para este fim, as amostras após serem lavadas com PBS, foram fixadas a 70% de metanol mais 30% de acetona por 5 minutos em temperatura ambiente, então bloqueadas com PBS 1x e 10% soro fetal bovino por 30 minutos e incubadas durante a noite com anticorpos primários.

Foram utilizados os anticorpos anti-colágeno-I (Abcam Plc, Cambridge, UK), anti-laminina (Sigma-Aldrich Co. LLC, USA), anti-colágeno-III (Abcam Plc, Cambridge, UK), anti-colágeno-IV (*Santa Cruz Biotechnology Inc., Texas, USA*), anti-elastina (*Santa Cruz Biotechnology Inc., Texas, USA*). Os anticorpos primários foram detectados utilizando-se anticorpos secundários apropriados e as criosecções lavadas três vezes com PBS 1x por 5 minutos cada lavagem. Os anticorpos secundários diluídos em PBS 1x e incubados por 60 minutos.

As imagens das regiões de interesse foram obtidas com uma câmera digital (*CCD-EM C9100 Hamamatsu, Tokyo, Japan*) acoplado a um microscópio invertido fluorescente (*Ti-Eclipse Nikon, Tokyo, Japan*) com uma ampliação de 10x e operado por um *software* comercial (NIS-Elements C Microscope Imaging Software, Nikon Instruments Inc, *Tokyo, Japan*).

Os níveis restantes de DNA no *scaffold* após os procedimentos de perfusão foram avaliados em três pulmões descelularizados selecionados aleatoriamente e em um pulmão nativo. Uma amostra do lóbulo direito de cada pulmão foi seca e pesada e o seu DNA genômico total foi isolado usando *spin-column* baseado no PureLinks® Mini Kit de Genomic DNA (Invitrogen™, Thermo Fisher Scientific, Waltham, MA, USA.) de acordo com as instruções do fabricante. A cadeia dupla de DNA foi mensurada por espectrofotometria (NanoDrop 1000, Thermo Fisher Scientific, Waltham, MA, USA) e normalizada pelo peso do tecido.

3.7.2. Microscopia de contraste de fase

As imagens de contraste de fase foram realizadas depois de completa eliminação do OCT e as amostras mantidas em PBS 1 x em temperatura ambiente durante a aquisição de imagem. A obtenção das imagens foi através de uma câmera digital (Marlyn F145, Allied V.T., Germany) operado por um *software Vision Assistant* (National Instruments, Texas, USA) e acoplado a um microscópio invertido óptico modelo TE2000 (Nikon, Tokyo, Japan).

3.8. Avaliação da elastância pulmonar

Para avaliar as potenciais alterações induzidas pelo procedimento de perfusão sobre as propriedades mecânicas do órgão foi analisado o comportamento da elastância pulmonar. As elastâncias dinâmica (Edyn) e estática (Est) pulmonares foram avaliadas em órgãos adicionais (3 pulmões nativos e 11 pulmões acelulares) imediatamente após o processo de descelularização. Para caracterizar a relação pressão-volume em condições mecânicas semelhantes às da respiração fisiológica normal, os pulmões foram submetidos à ventilação mecânica convencional, seguindo um protocolo já descrito detalhadamente na literatura^{47,113-114}.

Os pulmões foram canulados pela traqueia, suspensos verticalmente por ação da gravidade e colocados dentro de uma câmara (32°C e 100% de humidade). Um pneumotacógrafo foi conectado a entrada da cânula para mensurar o fluxo traqueal pela sensibilidade de queda pressórica através do pneumotacógrafo com um transdutor diferencial de pressão (Hans Rudolph Inc., Shawnee, USA). A pressão traqueal foi verificada através da conexão de um transdutor de pressão na porta lateral localizada entre o pneumotacógrafo e a cânula.

A entrada do pneumotacógrafo foi conectada à uma peça em Y de um ventilador mecânico volumétrico (MV215, Montevideo, UY) projetado para a ventilação artificial de roedores¹¹⁵. Os pulmões foram submetidos à ventilação mecânica convencional com um padrão quasi-sinusoidal de fluxo com um volume corrente de 10 ml/kg de peso do camundongo, uma frequência respiratória de 100 ciclos/min e uma pressão expiratória positiva final de 2 cmH₂O, para contrabalançar a ausência da pressão pleural fisiológica negativa em repouso. Os sinais de fluxo e de pressão dos transdutores foram analogicamente filtrados, amostrados e armazenados para posterior análise.

As Est e Edyn foram verificadas por meio da técnica de oclusão ao final da expiração realizada suprimindo um botão correspondente no ventilador mecânico, como demonstrado na figura 4. Após a oclusão ao final da expiração, observa-se uma queda rápida da pressão traqueal (DP1) até um ponto de inflexão (com pressão Pi), a partir daí ocorre uma queda lenta (DP2) lenta que decorre até um platô (PEL) o qual equivale à pressão de retração elástica do pulmão. Considerando que DP1 está associada com a pressão dissipada contra a resistência pulmonar, DP2 reflete propriedades viscoelásticas do tecido ou o fenômeno de *pendelluft*. Levando-se em conta o valor de pressão pré-inspiratória (Po), a elastância estática pulmonar (Est) é calculada como o ajuste da pressão de platô (Pel-Po) gravada após 5s de oclusão dividida pelo volume corrente.

A Edyn é mensurada dividindo-se a pressão do ponto de inflexão ajustada (Pi-Po) pelo volume corrente^{47,113}. Para cada pulmão nativo e descelularizado, as Est e Edyn foram obtidas a partir de cinco oclusões ao final da inspiração, cada uma realizada depois de 1 min de ventilação mecânica normal. Podemos observar as curvas de fluxo e pressão traqueal em relação ao tempo de acordo com o protocolo de cálculo através do método da pausa inspiratória na figura 4.

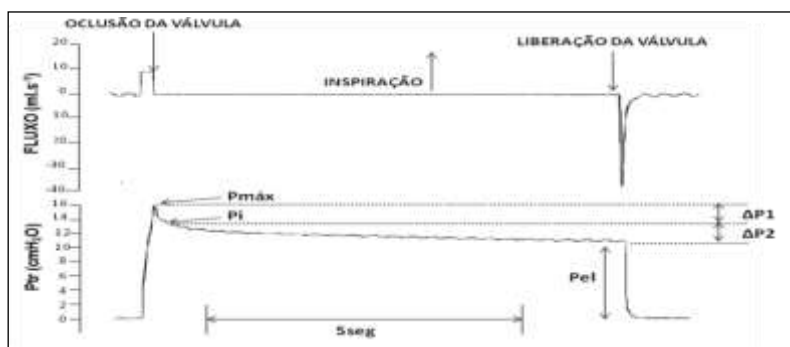


Figura 7. Curvas fluxo e pressão traqueal em relação ao tempo.

3.9. Protocolo experimental para avaliar a resistência vascular sob diferentes pressões traqueais e vasculares

Para mensurar o comportamento da mecânica vascular de pulmões de ratos decelularizados, a traqueia, após ter sido canulada foi conectada a um gerador de fluxo CPAP para fornecer uma pressão traqueal (transpulmonar) variando de 0 a 15 cmH₂O. A artéria pulmonar foi canulada e conectada a um sistema de perfusão com pressão constante, controlada por nível gravimétrico, de infusão de PBS variando de 5 a 30 cmH₂O. Em sequência, um transdutor de pressão (ICU Medical Inc., San Clemente, CA, EUA) e um transdutor de pressão diferencial (ICU Medical Inc., San Clemente, CA, EUA) permitindo verificar a pressão (P_{PA}) e o fluxo (V'_{PA}) na entrada da artéria pulmonar, respectivamente. Estes sinais dos transdutores foram analogicamente filtrados, amostrados e armazenados para análise posterior. Assim, aferindo continuamente V'_{PA} e P_{PA} foi possível realizar o cálculo da resistência vascular (R_v) como $R_v = P_{PA} / V'_{PA}$.

3.10. Análise estatística

Estudo 1

A análise estatística foi realizada no software Sigma stat 2.0. Todos os valores foram expressos em média e erro padrão da média (EPM). Os valores de resistência vascular (R_v) foram comparados com os valores no início e no final do processo, pelas médias do testes-t pareado. Foi utilizada a ANOVA de dois caminhos na comparação das alterações no fluxo (V'_{TM} vs. V'_{PV}), sob perfusão de pressão constante, sendo o tempo decelularização e ligadura das veias pulmonares o dois fatores analisados. A ANOVA de um caminho foi utilizada para avaliar as alterações nas elastâncias pulmonares induzidas pelos diferentes procedimentos de perfusão. A significancia estatística foi considerada quando o valor de $p < 0.05$.

Estudo 2

A análise estatística foi realizada no software Sigma stat 2.0. Todos os valores foram expressos em média e erro padrão da média (EPM). Os valores de resistência vascular (R_v) e fluxo (V'_{PA}) foram comparados com os valores em cada pressão na artéria pulmonar (5 a 30 cmH₂O) e traqueal (0 a 15 cmH₂O) por meio de testes-t pareados.

4. RESULTADOS

Os resultados da presente tese estão apresentados no formato de artigos. O estudo I, intitulado ‘Pressure and flow-controlled media perfusion differently modify vascular mechanics in lung decellularization’ foi publicado no periódico *Journal of the Mechanical Behavior of Biomedical Materials* e o estudo II, intitulado “Behaviour of vascular resistance undergoing various pressure insufflation and perfusion on decellularized lungs” foi submetido para publicação no periódico Plos One.

4.1- Estudo I

Perfusão por pressão e fluxo controlados modificam o comportamento da mecânica vascular na descélularização pulmonar?

4.1.1- Introdução

A bioengenharia pulmonar surgiu recentemente como uma potencial alternativa na obtenção de órgãos disponíveis para o transplante nos próximos anos^{16,104,116,117}. De acordo com essa abordagem, os pulmões gerados biologicamente gerados ajudariam na redução das atuais longas filas de espera para transplante e também atenderiam ao aumento da demanda por órgãos causada pelo envelhecimento progressivo da população em ambos os países desenvolvidos e em desenvolvimento⁹¹. Apesar de estudos experimentais já terem estabelecido provas convincentes sobre a viabilidade de bioengenharia de pulmão^{16, 104}, vale ressaltar que se trata de um campo de conhecimento novo e pouco explorado cientificamente.

Dada a complexidade estrutural do pulmonar, que apresenta tipicamente 300 milhões de alvéolos, cada um com um diâmetro de 300 milímetros, separados a partir dos capilares com um diâmetro de 10 mm e por uma membrana com uma espessura de 3 mm e a superfície aproximada de 70 m² e a incapacidade das tecnologias atuais para a construção de uma estrutura 3D em micro-escala, a abordagem da bioengenharia pulmonar baseia-se na utilização de *scaffolds* pulmonares obtidos a partir de órgãos naturais^{15, 26}.

O conceito da biofabricação pulmonar parte inicialmente da descélularização de um órgão que não estaria disponível para o transplante e, em seguida, usar o seu *scaffold* acelular como uma matriz para o cultivo de células tronco, que após a sua proliferação e diferenciação, regenerariam um novo pulmão^{16,104,118}.

O procedimento para descelularização pulmonar, ou de qualquer outro órgão deve ser suficientemente agressivo no sentido da eliminação de todo o material celular do órgão doador e ao mesmo tempo deve ser bastante conservador no sentido de preservar a estrutura e a composição da sua matriz extracelular¹¹. O processo de obtenção de pulmões acelulares ainda não está claramente estabelecido, pois diferentes protocolos publicados na literatura têm demonstrado a viabilidade de fornecer *scaffolds* pulmonares com qualidade razoável em termos de baixa carga de DNA do doador associados a uma matriz extracelular com estrutura e composição preservada^{16,106,107,119}.

O procedimento de perfusão com diferentes agentes descelularizantes (água deionizada, detergentes e enzimas) através do circuito vascular do órgão é um procedimento convencional na eliminação de materiais celulares do doador uma vez que uma ampla distribuição da rede capilar dentro do órgão permite tanto a distribuição dos agentes descelularizantes por difusão a curta distância de qualquer célula, quanto à lavagem dos detritos resultantes. Especificamente para os pulmões, vários estudos experimentais em órgãos de animais e em humanos têm demonstrado que a perfusão de agentes descelularizantes através da artéria pulmonar permite a descelularização adequada não somente das paredes do vaso, mas também na eliminação de células do parênquima pulmonar e das paredes das vias aéreas^{108-110,120-121}.

A perfusão de agentes descelularizantes através da artéria pulmonar é um processo que pode ser realizado manualmente^{32,105-107}. No entanto, este processo não permite controlar facilmente a taxa de infusão, podendo gerar danos aos pulmões. Alternativamente, agentes descelularizantes podem ser infundidos, de maneira controlada por pressão ou fluxo na artéria pulmonar.

As evidências científicas atuais são limitadas quanto a estes procedimentos sugerindo que tanto por fluxo quanto por pressão controlados podem resultar em *scaffolds* pulmonares descelularizados e bem conservados. De fato, estudos recentes compararam métodos de perfusão (pressão vs. fluxo controlado e manual vs. automatizado) em termos de eliminação dos materiais celulares do doador no *scaffold*, preservação da composição e estrutura da matriz extracelular, e a adequação do *scaffold* como substrato acelular para a futura cultura de células tronco¹⁰⁸⁻¹¹¹. No entanto, nenhum desses estudos investigou o comportamento da resistência vascular pulmonar. Notavelmente, cada protocolo de perfusão apresenta vantagens e desvantagens do ponto de vista da mecânica dos fluidos.

Por um lado, controlar a pressão de perfusão na artéria pulmonar garante que nenhum barotrauma seja induzido no *scaffold*, porém, o acúmulo de detritos gerados pela lise das células poderia reduzir fortemente o fluxo ou mesmo interrompê-lo em caso de pressão insuficiente. Por outro lado, controlar o fluxo infundido na artéria pulmonar garante uma quantidade de agentes descelularizantes, mas - também devido ao acúmulo de detritos - pode induzir um aumento de pressão dentro dos vasos pulmonares com risco de danificar a membrana alvéolo-capilar. No entanto, de acordo com o nosso conhecimento, nenhum estudo ainda investigou esta questão.

Acreditamos que compreender a dinâmica de fluidos com perfusão de agentes descelularizantes durante o processo de descelularização pulmonar pode fornecer conhecimentos que busquem otimizar o processo, tanto para fins de investigação científica quanto para viabilizar a automação de alto rendimento na produção de *scaffolds* pulmonares. Assim, este estudo objetivou caracterizar a relação pressão/fluxo na vasculatura pulmonar e estudar o comportamento da resistência vascular dependente da pressão ou fluxo controlados, quando aplicados diferentes protocolos de perfusão por agentes descelularizantes no processo de descelularização pulmonar.

4.1.2- Resultados

Como esperado a partir de estudos anteriores¹⁰⁸, o protocolo de descelularização por pressão vs. fluxo controlados não resultou em diferenças aparentes em termos de manutenção da estrutura do *scaffold* e composição dos principais componentes da matriz extracelular (Figura 8). De fato, quando comparados os pulmões nativos aos *scaffolds* não foi observada a presença de núcleos celulares, de acordo com a análise DAPI. O conteúdo de genoma de DNA no *scaffold* descelularizado foi de 29.377.0 ng/mg (abaixo de 50 ng/mg sugerido por Crapo et al.²⁸) que representa 7,5% do conteúdo de DNA no pulmão nativo (392,8 ng/mg).

Além disso, podemos observar também na Figura 8 que componentes relevantes da matriz extracelular como a elastina, a laminina e os colágenos I, III e IV mantiveram-se praticamente inalterados nos pulmões descelularizados e as estruturas alveolares e vasculares também foram preservadas.

Observando os dados sobre elastância pulmonar, foi observado que os diferentes processos de descelularização utilizados não induziram alterações significativas nas propriedades mecânicas do órgão.

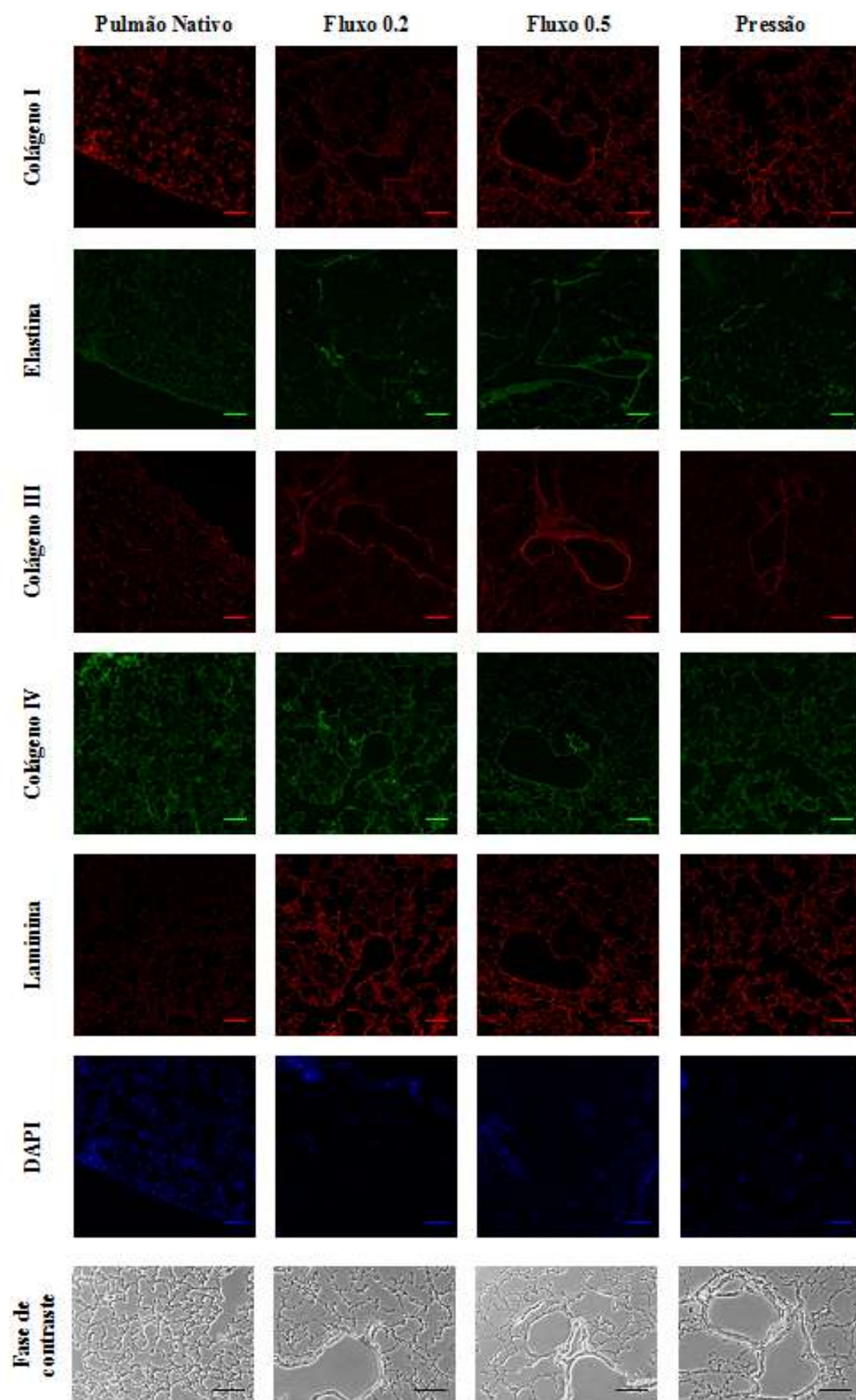


Figura 8. Coloração fluorescente de DAPI em pulmões nativos e descelularizados.

Nota: Os pontos azuis (ausentes no pulmão descelularizado) correspondem aos núcleos celulares. A coloração com azul difusa no pulmão acelular corresponde a autofluorescência da matriz extracelular (MEC). As imagens de imunofluorescência em pulmões nativos e descelularizados por perfusão (fluxo e pressão controlados) apresentaram marcações para diferentes componentes da MEC (colágeno I, III e IV, laminina e elastina) e imagens de contraste de fase. Barra de escala = 100 μm .

Como mostrado na Figura 9, os valores das elastâncias pulmonares (Est e Edyn) mensurados nos órgãos acelulares foram muito próximos em relação aos procedimentos de perfusão por pressão constante e fluxo constante, sendo que estes estão ligeiramente mais baixos do que os correspondentes ao pulmão nativo.

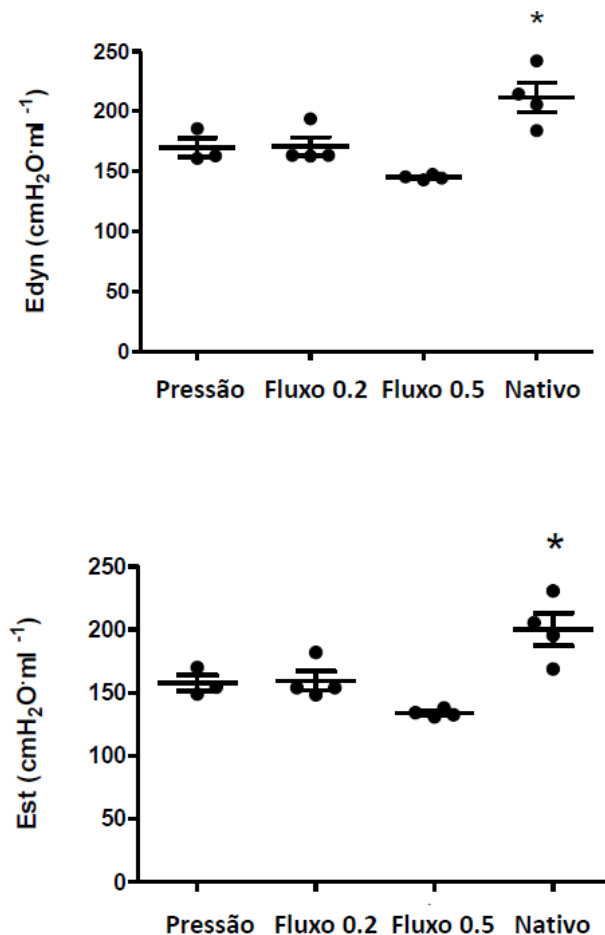


Figura 9. Elastâncias estática (Est) e dinâmica (Edyn) pulmonar computadas por meio de oclusão ao final da expiração durante a ventilação mecânica convencional.

Nota: As medidas foram realizadas em pulmões nativos e descelularizados por perfusão de pressão constante (Pressão) e por perfusão de fluxo constante de 0,2 ml/min e 0,5 ml/min (Fluxo 0,2 e Fluxo 0,5; respectivamente). Os asteriscos indicam $p < 0,05$.

A Figura 10 demonstra a evolução no tempo do fluxo V'_{PA} durante o processo de descelularização pulmonar através de pressão de perfusão constante (veia pulmonar aberta para a atmosfera). A V'_{PA} apresentou uma considerável redução quando a água deionizada foi perfundida e esta redução de fluxo persistiu durante a perfusão com o detergente SDS. Com a perfusão final de PBS, foi observado um aumento considerável do fluxo, com um V'_{PA} final similar à anterior ao processo de descelularização.

Consistentemente, a resistência vascular correspondente a R_v apresentou um aumento repentino e considerável de $29,1 \pm 3,0$ cm H₂O/(ml/min) (perfusão anterior de água deionizada) para um máximo de $664,1 \pm 164,3$ cmH₂O/(ml/min) ($p < 0,05$), durante a perfusão de meios descelularizantes, regredindo ao final do processo para um valor ($47,8 \pm 6,5$ cm H₂O / (ml/min) próximo aos valores iniciais do processo de descelularização ($p > 0,05$).

A descelularização por perfusão de fluxo constante (Figuras 11 e 12) resultou em um aumento considerável na pressão da artéria pulmonar (P_{PA}) para valores até $42,4 \pm 14,1$ cmH₂O e $66,4 \pm 2,2$ cmH₂O para V'_{PA} de 0,2 ml/min e 0,5ml/min, respectivamente. No entanto, após a perfusão final com PBS, a P_{PA} retomou aos valores próximos àqueles anteriores a aplicação dos meios descelularizantes. Em comparação ao observado na perfusão de pressão constante (Figura 10), os valores máximos de resistência vascular (R_v) ($211,7 \pm 70,5$ cmH₂O/(ml/min) e ($114,4 \pm 13,9$ cmH₂O/(ml/min) de V'_{PA} 0,2 ml/min e 0,5 ml/min; respectivamente) aumentaram ($p < 0,05$ em ambos os casos) em relação aos valores pré-descelularização ($79,5 \pm 5,1$ cmH₂O / (ml/min) e ($49,9 \pm 3,3$ cm H₂O / (ml/min) para V'_{PA} de 0,2 ml/min e 0,5 ml/min, respectivamente).

No entanto, os aumentos de R_v por perfusão de fluxo constante foram muito menores do que os obtidos por perfusão de pressão constante (Figura 10). Notavelmente, o aumento de R_v observado em $V_{PA} = 0,5$ ml/min foi particularmente baixo. Ao final do processo de descelularização por constante de fluxo, os valores de R_v foram ($57,5 \pm 7,9$ cmH₂O / (ml/min) e $39,5 \pm 3,2$ cmH₂O / (ml/min) para V'_{PA} de 0,2 ml/min e 0,5 ml/min, respectivamente) semelhantes aos inicial ($p > 0,05$ em ambos os casos).

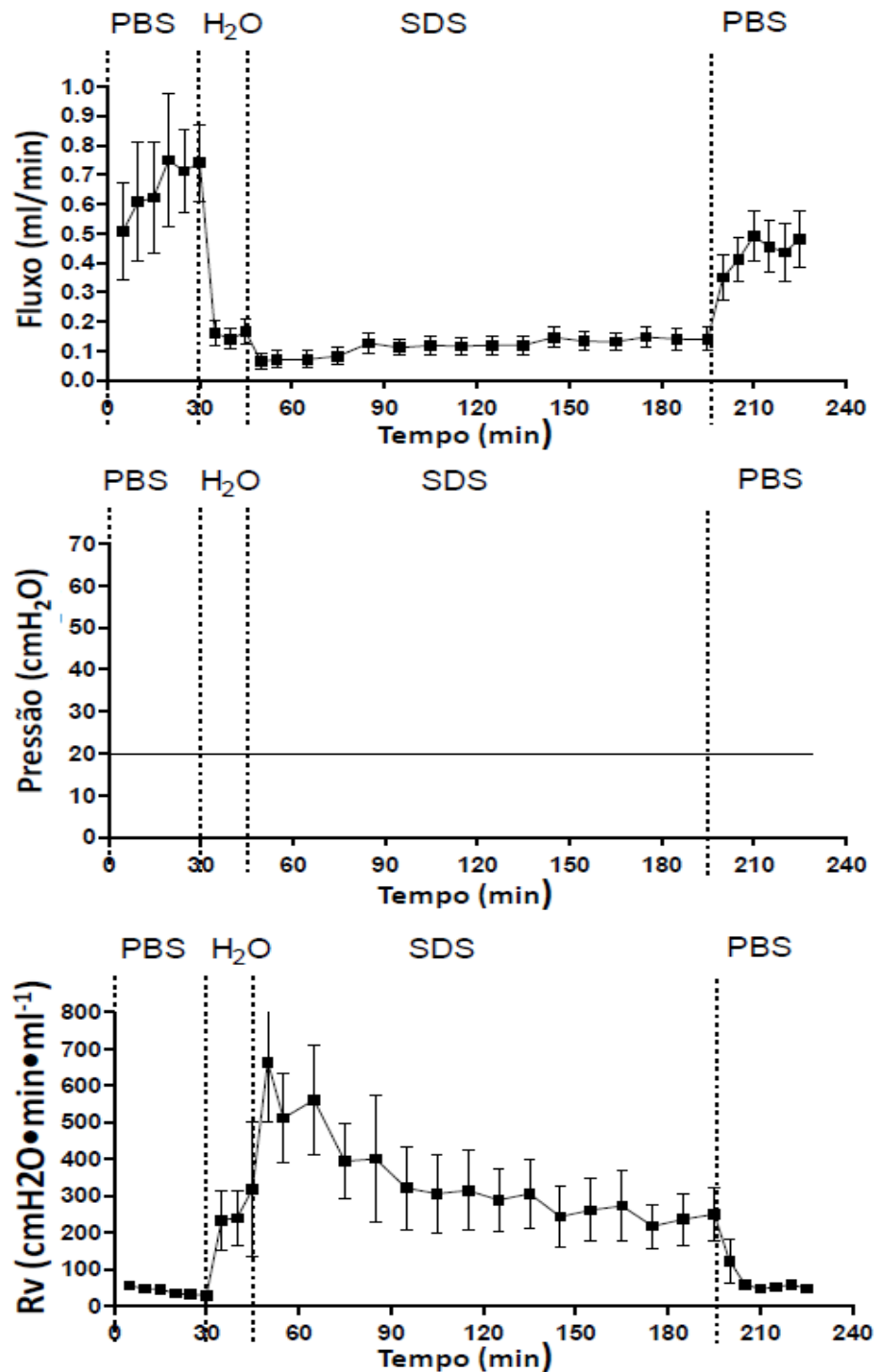


Figura 10. Pressão (P_{PA}) e fluxo (V'_{PA}) na artéria pulmonar durante a descélularização pulmonar por perfusão de pressão constante ($P_{PA}=20$ cmH₂O), com veia pulmonar aberta para atmosfera. Nota: Correspondente a resistência vascular (R_v). Os dados estão expressos em média±EPM. PBS (solução de tampão fosfato), H₂O (água deionizada) e de SDS (detergente dodecil sulfato de sódio) indicam os tempos de perfusão com o diferentes descélularizantes.

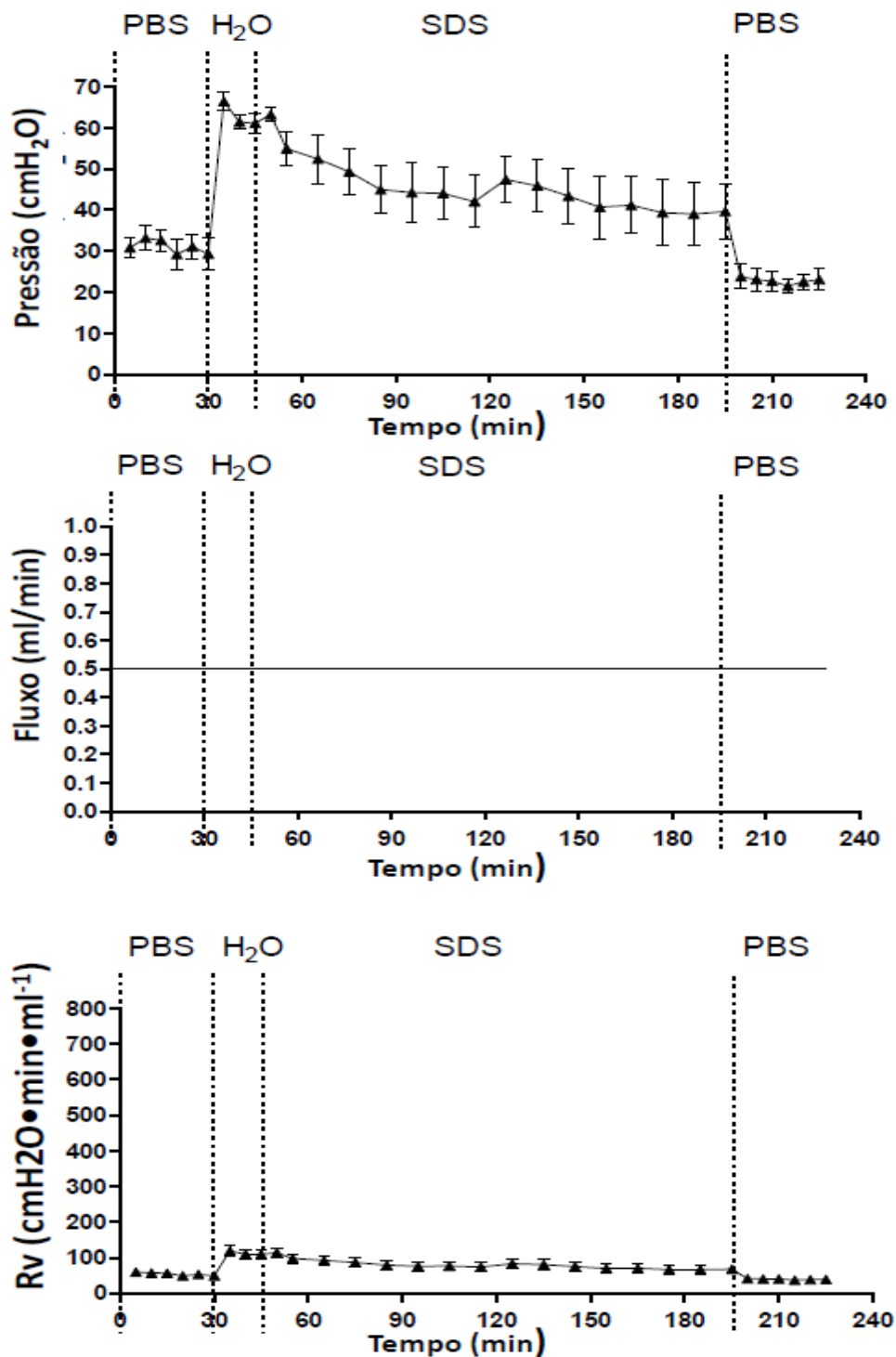


Figura 11. Pressão (P_{PA}) e fluxo (V'_{PA}) na artéria pulmonar durante a descclularização pulmonar por perfusão de fluxo constante ($V'_{PA}=0.5$ ml / min), com veia pulmonar aberta para atmosfera. Nota: Correspondente a resistência vascular (R_v). Os dados estão expressos em média \pm EPM. PBS (solução de tampão fosfato), H₂O (água deionizada) e de SDS (detergente dodecil sulfato de sódio) indicam os tempos de perfusão com o diferentes agentes descclularizantes.

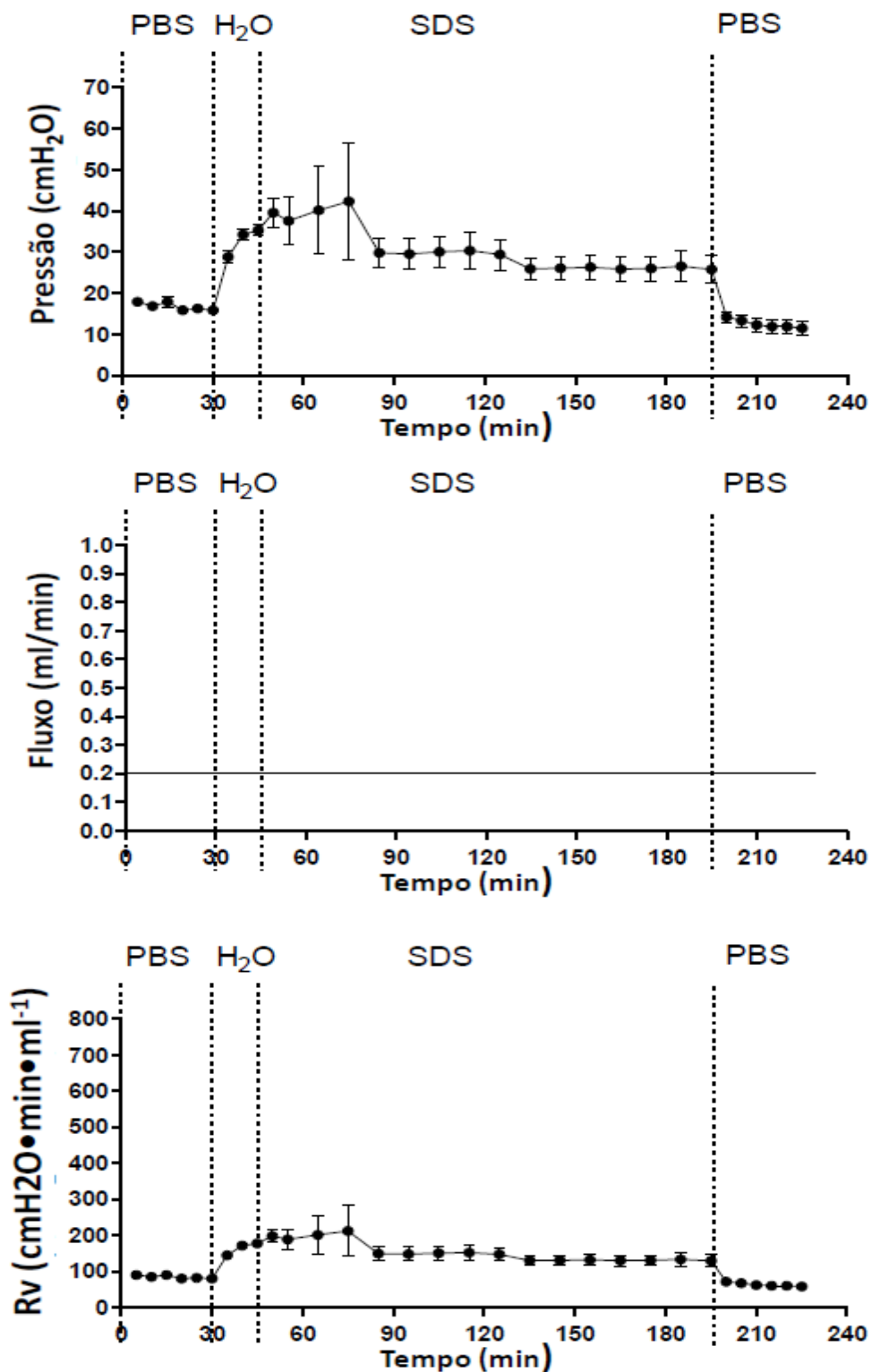


Figura 12. Pressão (P_{PA}) e fluxo (V'_{PA}) na artéria pulmonar durante a descélularização pulmonar por perfusão de fluxo constante ($V'_{PA}=0.2$ ml / min), com veia pulmonar aberta para atmosfera. Nota: Correspondente a resistência vascular (R_v). Os dados estão expressos em média \pm EPM. PBS (solução de tampão fosfato), H₂O (água deionizada) e de SDS (detergente dodecil sulfato de sódio) indicam os tempos de perfusão com o diferentes agentes descélularizantes.

Na figura 10 podemos observar a comparação do fluxo V'_{PA} medido em todo processo de descelularização por perfusão com pressão constante ($P_{PA}=20$ cmH₂O), quando a veia pulmonar estava aberta ($V'_{PA}=V'_{TM} + V'_{PV}$) e quando ela foi ligada ($V'_{PV} = 0$). Tal como esperado, o fluxo variou significativamente com ao longo do processo de descelularização ($p>0,05$) e não houve diferença significativa se a veia pulmonar estivesse aberta ou não ($p>0,05$). Tendo em conta o esquema de circuito na Figura 2B, que mostra a distribuição de V'_{PA} em V'_{TM} e V'_{PA} , a semelhança de fluxo mensurado em ambas as condições indicam que a via através da membrana alvéolo-capilar foi a principal rota de trânsito de agentes descelularizante durante a descelularização, especialmente quando a água deionizada e detergente SDS foram infundidos.

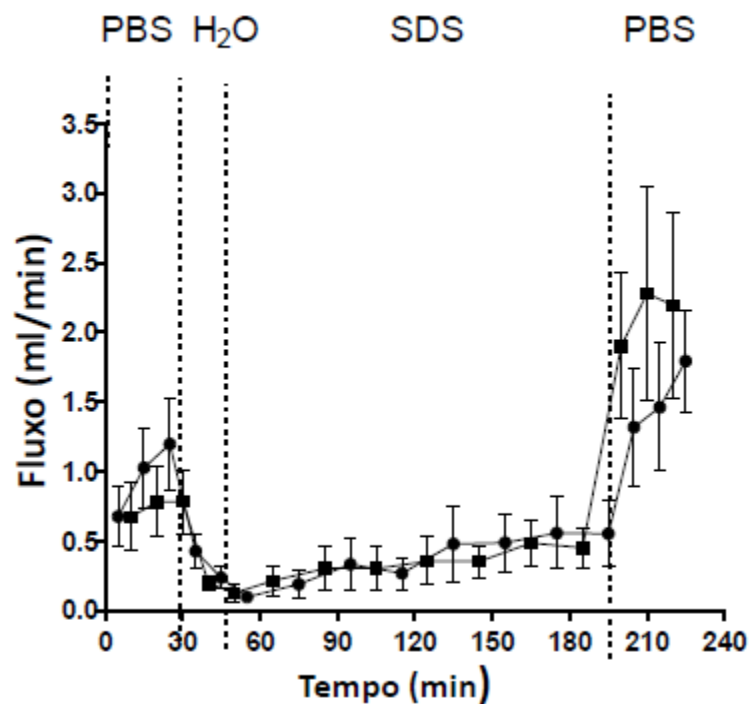


Figura. 13. Fluxo através da artéria pulmonar (V'_{PA}) medida durante o processo de descelularização pulmonar por perfusão de pressão constante ($P_{PA}=20$ cmH₂O), com veia pulmonar aberta para atmosfera (●) e com veia pulmonar ligada (■).

Nota: Os dados estão expressos em média±SE. PBS (solução de tampão fosfato), H₂O (água deionizada) e de SDS (detergente dodecil sulfato de sódio) indicam os tempos de perfusão com o diferentes agentes descelularizantes.

4.1.3 - Discussão

De acordo com o nosso conhecimento, este é o primeiro estudo que avalia o comportamento das variáveis da dinâmica dos fluidos vasculares envolvidas no processo de descelularização pulmonar. Mensurar a relação pressão-fluxo ao longo de todo o processo de descelularização sob diferentes regimes de perfusão, pressão e fluxo controlados, permitiu caracterizar um importante processo na bioengenharia de pulmão para a obtenção de um *scaffold* acelular que se baseia na circulação dos meios ao longo de toda a rede vascular e de vias aéreas do órgão.

Especificamente, três principais afirmações foram extremamente relevantes para o estudo. Em primeiro lugar, a resistência vascular apresentou variações consideráveis ao longo do processo de descelularização, particularmente para a perfusão controlada por pressão. Segundo, a perfusão por controle de fluxo aumentou a pressão no interior do sistema vascular, mas, dada a dependência da resistência de pressão inversa, a pressão vascular foi menor do que o esperado a partir dos valores de resistência vascular medidas sob regime controlado por pressão. Em terceiro, os meios descelularizantes infundidos pela artéria pulmonar circulam principalmente para o compartimento de vias respiratórias através da membrana alveolo-capilar, deixando uma menor fração para o circuito vascular pulmonar através da veia pulmonar.

Existem evidências científicas concretas de que os pulmões podem ser descelularizados através de diferentes protocolos que consistem em uma combinação de técnicas aplicadas na obtenção de *scaffolds* acelulares em órgãos e tecidos^{14-16,32,73,122,123}. Apesar destas evidências, a comparação de protocolos de descelularização pulmonares ainda não foi mostrada e, portanto, não há nenhuma conclusão de qual seja o protocolo ideal. De fato, essa comparação exige o uso de combinações quase infinitas de agentes físicos, químicos e enzimáticos, incluindo diferentes concentrações possíveis de cada agente descelularizante associada a diversos tempos de cada etapa.

Embora este fato possa ser visto como uma desvantagem, experiências práticas já publicadas consolidaram diferentes protocolos que realmente podem ser aplicados na obtenção de *scaffolds* pulmonares viáveis de camundongos,¹⁰⁷ ratos^{103,121}, porcos¹²⁰, primatas^{124,125} e até em órgãos humanos^{109,110,119,126}. Independentemente da definição da sequência específica de agentes descelularizantes a ser empregada, o qual pode ser diferente entre laboratórios, um problema comum é que estes agentes são perfundidos através do órgão.

A idéia é conseguir a melhor distribuição possível dos agentes descclularizantes dentro do órgão visnado alcançar todas as células presentes. Na maioria dos órgãos (coração, rim, pulmão), a única rota disponível é a circulatória. O pulmão, no entanto, tem um percurso adicional possível para os agentes descclularizantes que pode ser através da traqueia. Na verdade, ambas as rotas (traqueia ou artéria pulmonar) isoladas ou combinadas têm sido utilizadas para descclularizar efetivamente os pulmões^{47,103,108-110,113,114,120,123}.

Este estudo foi focado em perfundir os agentes descclularizantes através da rede vascular, uma vez que é a rota mais convencional nos pulmões e a única disponível em outros órgãos relevantes. A perfusão pela artéria pulmonar foi realizada utilizando os valores comuns na literatura¹⁵, tanto pela aplicação de baixa pressão fisiológica de 20 cmH₂O (~15 mmHg) na artéria pulmonar ou os fluxos correspondentes em condições normais (0,2-0,5 ml / min)¹²⁷.

O acúmulo de detritos celulares gerados pela aplicação de água deionizada (ruptura da membrana da célula por choque osmótico) causou um aumento de 10 vezes na resistência vascular. De fato, como demonstrado na Figura 7, o fluxo de perfusão se apresenta ligeiramente aumentado ao longo dos primeiros 30 minutos de perfusão com PBS, provavelmente pela a eliminação de componentes sanguíneos restantes após a excisão do pulmão. Imediatamente após a aplicação de água deionizada, o fluxo reduziu consideravelmente e manteve-se baixo com subsequente discreto aumento durante toda a perfusão do detergente.

Por fim, quando o PBS foi aplicado para lavar o circuito, o fluxo aumentou (a resistência vascular diminuiu) como resultado de uma redução na viscosidade após a eliminação de SDS^{128,129}, recuperando os valores de fluxo e de resistência vascular próximos aos verificados antes de se iniciar o processo de descclularização. É interessante notar que tal como refletido na Figura 10, praticamente todo o fluxo perfundido através da membrana alveolo-capilar deixa o circuito vascular através da veia pulmonar.

Este fato explica porque a descclularização por perfusão através da rede vascular do órgão funciona. Na situação em que a maioria dos agentes descclularizantes circula no circuito vascular, eles não seriam capazes de atingir toda a extensão do órgão, desse modo não permitindo o completo processo de descclularização do parênquima dos órgãos e as paredes das vias respiratórias.

De acordo com o valor da resistência vascular encontrada durante a aplicação de água deionizada sob regime de pressão controlada seriam esperados valores elevados de pressão vascular a um um fluxo constante (Figura 7). Por exemplo, para um fluxo de perfusão de 0,5 ml/min, se a resistência vascular foi ~ 600 cmH₂O/(ml/min), a pressão durante o fluxo controlado atingiria ~ 300 cmH₂O. No entanto, o pico de pressão observado quando a água deionizada foi perfundida, foi muito menor (60 cmH₂O), indicando que a resistência ao fluxo através da membrana alveolo-capilar reduziu ou que manteve um elevado fluxo de 0,5 ml/min, permitindo uma melhor lavagem dos detritos celulares devido a indução de uma redução na resistência vascular mantendo a pressão relativamente baixa (Figura 8).

De acordo com a Figura 9, podemos observar que a perfusão a um fluxo constante de 0,2 ml/min induziu um pico de pressão de ~ 40 cmH₂O. Esta relação negativa observada entre a pressão vascular e resistência - que é o esperado de um circuito de fluxo típico não-linear e parede rígida - explica por que o *scaffold* de pulmão é razoavelmente bem preservado, independentemente se a descelularização do pulmão foi por fluxo ou pressão controlados^{14,15,108}.

Como este estudo foi dirigido para a descelularização pulmonar, as suas principais conclusões sobre as propriedades mecânicas do circuito vascular durante o processo de descelularização por perfusão de agentes através da rede circulatória, acreditamos que o mesmo possa ser aplicado para protocolos de descelularização de outros órgãos. De fato, tanto a perfusão vascular por pressão ou fluxo controlado são utilizados para a obtenção de *scaffolds* acelular de rim^{130,131}, fígado¹³²⁻¹³⁴ ou de coração^{12,135,136} com valores fisiológicos de pressão e fluxo, assim como neste estudo.

A única diferença entre estes órgãos e o pulmão é que a membrana capilar sistêmica está envolvida em vez da membrana alveolo-capilar, não induzindo uma diferença substancial entre os órgãos na dinâmica de fluidos perfundidos, como refletido pelo fato de que tanto a pressão e fluxo controlados alcançaram adequada descelularização da membrana com a preservação do *scaffold*^{108-111,145}.

4.1.4. Conclusão

Este estudo demonstrou que a análise do comportamento da dinâmica de fluidos na perfusão durante todo processo de descelularização, geralmente negligenciado na engenharia de tecidos, fornece relevantes informações garantindo que o processo será mantido sob uma área segura das variáveis na preservação do *scaffold*.

Podemos inferir que, parece razoável que o monitoramento mecânico deva ser incorporado nos procedimentos de controle de qualidade automatizado e em futuras linhas de produção de *scaffolds* pulmonares acelulares. Além disso, o monitoramento do comportamento da mecânica dos fluidos pode ser útil para planejar os procedimentos automáticos otimizados para alcançar *scaffolds* viáveis com um tempo de processo reduzido e, conseqüentemente com menores custos. Sendo assim, em vez de aplicar um procedimento simples de pressão ou de fluxo controlados, poderia ser possível conceber estratégias combinadas para aplicação de um processo de perfusão mais eficaz à cada um dos passos de todos os agentes descelularizantes.

4.2. Estudo II

Comportamento da resistência vascular submetida a diferentes pressões de insuflação e de perfusão em pulmões descelularizados

4.2.1 Introdução

Em 2012, mais de 1300 pacientes se encontravam em lista de espera para um transplante pulmonar nos Estados Unidos¹³⁸ devido a reduzida oferta de doadores de pulmões. Considerando que os transplantes pulmonares são complicados devido a rejeição crônica e por efeitos adversos do tratamento com imunossupressor^{139,140}, novas estratégias se fazem necessárias no sentido de aumentar a disponibilidade de órgãos. Recentemente, a geração de órgãos bioartificiais a partir de *scaffolds* tem sido proposta como uma potencial opção alternativa¹⁰⁶. No entanto, para resultar em novos órgãos funcionais esses *scaffolds* devem preservar sua estrutura oferecendo um macro e micro-ambiente ideal para facilitar a fixação das futuras células a serem implantadas através do processo de recelularização¹¹.

Considerando que as células pulmonares sofrem a ação de diferentes estímulos físicos durante a respiração, o *scaffold* pulmonar também deveria ser submetido aos mesmos estímulos de ventilação e perfusão, mimetizando uma respiração normal proporcionando um ambiente fisiológico adequado ao cultivo celular no pulmão descelularizado. Em estudo prévio do nosso grupo, demonstramos que existem diferenças consideráveis na resistência vascular ao longo do processo de descelularização¹⁴⁰. No entanto, dados sobre o comportamento da resistência circulatória em função das variações das pressões das vias aéreas e vasculares são atualmente desconhecidas.

Esta informação é de considerável interesse desde que a distribuição adequada de células durante a recelularização do *scaffold* e *homing* celular subsequente poderiam ser modulados pela resistência vascular. O monitoramento do comportamento da resistência vascular poderia ser uma ferramenta útil no controle de qualidade do *scaffold* para uma futura produção de alto rendimento¹⁴⁰. Dessa forma, este trabalho teve como objetivo determinar como a resistência vascular varia dependendo das pressões de insuflação pulmonar (pressão traqueal) e de perfusão (arterial pulmonar).

4.2.2. Resultados

Como mostrado na Fig. 11, a resistência vascular no pulmão descelularizado diminuiu de $\sim 6-7 \text{ cmH}_2\text{O}\cdot\text{min}\cdot\text{ml}^{-1}$ para $\sim 3 \text{ cmH}_2\text{O}\cdot\text{min}\cdot\text{ml}^{-1}$ quando a pressão arterial pulmonar foi aumentada de 5 a 20 cmH_2O , mantendo-se constante até a 30 cmH_2O no sistema arterial pulmonar. Os valores de resistência vascular não dependeram dos valores de pressão positiva contínua nas vias aéreas (CPAP).

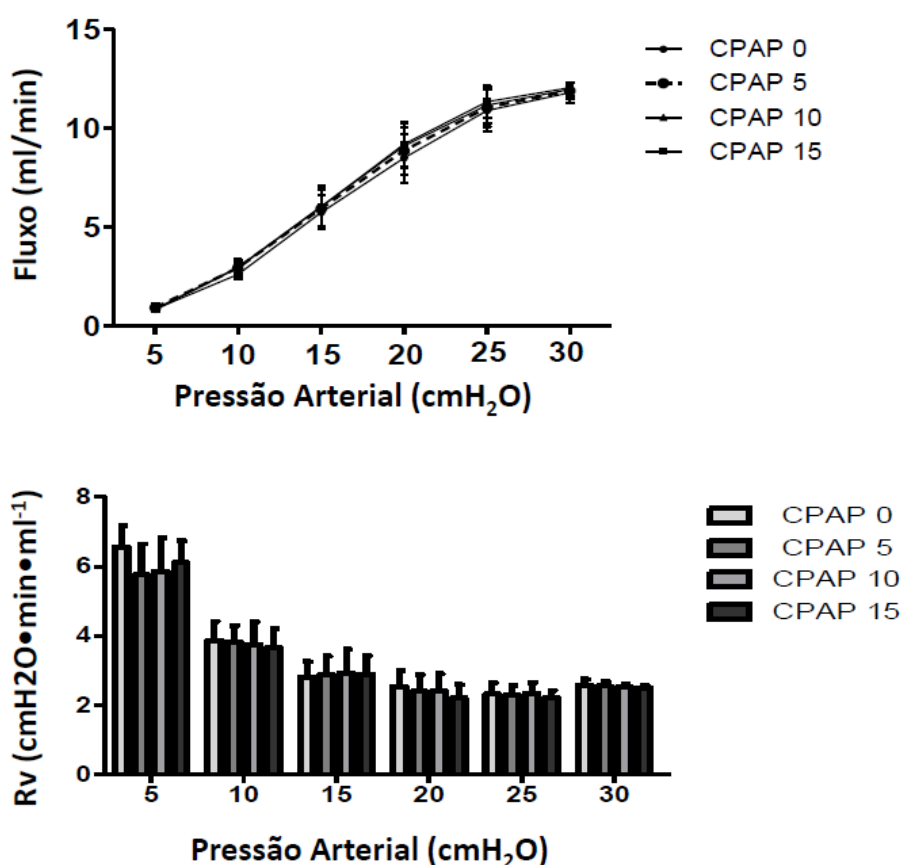


Figura 14. Pressão (P_{PA}) e fluxo (V'_{PA}) na artéria pulmonar do pulmão descelularizado submetido a variações de pressões arteriais (5-30 cmH_2O) e pressões positivas contínua nas vias aéreas (0- 15 cmH_2O). Nota: resistência vascular (R_v). Os dados estão expressos como média \pm EPM.

4.2.3. Discussão

De acordo com uma extensa revisão bibliográfica, este é o primeiro estudo que descreve o comportamento da resistência vascular nos pulmões descelularizados em função de variações nas pressões arteriais e das vias aéreas pulmonares. Sabe-se que a falta de surfactante nos pulmões descelularizados pode induzir a um colapso alveolar, assim, em um estudo anterior foi utilizado o CPAP de 10 cmH₂O para manter os pulmões insuflados durante o processo de descelularização¹⁵⁹. No entanto, não se sabe ainda a influência do CPAP sobre a resistência vascular no pulmão acelular. Neste estudo foi observado que a resistência vascular no pulmão acelular é quase constante dentro de valores de CPAP de 0-15 cm H₂O, desde que a pressão na artéria pulmonar seja superior a 15 cmH₂O.

Alguns estudos obtiveram sucesso no transplante pulmonar após a reconstrução com células-tronco, no entanto esses pulmões realizaram as trocas gasosas no máximo até 7 dias^{14,16}. Parece claro, contudo, que a diferenciação e maturação celular necessitam ser aperfeiçoadas. Portanto, poderia ser esperado que variações nas pressões arteriais e alveolares poderiam influenciar na adesão celular, considerando que quanto menor o fluxo no circuito pulmonar menor será a distribuição celular. Assim, de acordo com este estudo, podemos sugerir que o valor ideal de fluxo e resistência vascular para uma a dinâmica ideal é obtida por valores fisiológicos de pressão arterial pulmonar (15-30 cmH₂O).

O processo de descelularização elimina completamente células epiteliais alveolares tipo II que secretam surfactante pulmonar, tornando esse pulmão mais complacente como descrito anteriormente^{132,160}. Com menores valores de elastância, o pulmão descelularizado não fornece uma grande força na parede alveolar capaz de alterar a resistência vascular, o que pode explicar por que o CPAP apresenta menor influência na resistência vascular.

4.2.4 Conclusão

De acordo com nossos resultados, podemos concluir que a pressão arterial pulmonar exerce maior influência sobre o comportamento da resistência vascular nos pulmões descelularizados do que a pressão positiva nas vias aéreas. Este estudo fornece informações que podem ser relevantes para uma futura recelularização utilizando a resistência vascular como um facilitador na distribuição celular por todo o circuito pulmonar.

5. CONSIDERAÇÕES FINAIS

Como descrito na seção de contextualização, a bioengenharia pulmonar ainda é um assunto pouco explorado na pesquisa. Embora, avanços relevantes tenham sido relatados recentemente, existe uma considerável gama de questões fundamentais e práticas que permanecem em aberto. Os dados disponíveis na literatura refletem conhecimentos sobre o processo de descelularização, entretanto existe uma necessidade de um protocolo automatizado afim de beneficiar o processo de produção em grande escala de *scaffolds* pulmonares integros e viáveis para recelularização.

A contribuição deste trabalho de doutoramento pode ser dividido em dois momentos, um deles centrado no processo de descelularização e um segundo sobre o comportamento vascular do *scaffold* visando uma futura recelularização. No primeiro momento, os parâmetros de resistência vascular durante a descelularização foram estudados a partir do ponto de vista mecânico. A variável analisada foi o método de perfusão utilizado para descelularizar, pressão ou fluxo constante. Além de avaliar o comportamento desta variável, o estudo nos permitiu adaptar esse protocolo para pulmões de ratos, visto que foi padronizado em pulmões de camundongo. Como resposta a hipótese inicial, ambas as metodologias produziram um *scaffold* ausente de DNA do doador com sua MEC preservada, contradizendo alguns autores, provavelmente porque foram realizados métodos de descelularização controlados.

Subsequentemente a este estudo sobre a metodologia de descelularização pulmonar, procedeu-se a caracterização da mecânica vascular do *scaffold* aplicando diferentes pressões traqueais e vasculares para uma potencial abordagem em futuros projetos que visam a recelularização de um pulmão acelular. A hipótese era de que ambas as pressões (traqueal e vascular) poderiam influenciar a resistência desse *scaffold* pulmonar e, surpreendentemente somente pressão vascular influenciou na resistência, provavelmente devido a falta de surfactante que induz a um aumento da complacência desse *scaffold*.

Dado que a bioengenharia de pulmão é uma nova linha de pesquisa no mundo e, principalmente no Brasil, a primeira tarefa após o período de 12 meses no laboratório de Biofísica da Faculdade de Medicina, na Universidade de Barcelona, foi implementar o protocolo aqui apresentado de descelularização pulmonar, afim de dar continuidade aos estudos no Brasil.

Considerando o aumento da qualidade de vida da população em geral e o crescente aumento no número de idosos temos como uma das consequências o aumento do número de doenças pulmonares crônicas que está diretamente ligado ao aumento dos custos do Sistema Único de Saúde em relação a medicação, atendimento de urgência e emergência, seguridade social, o que consequentemente gera um aumento do número de pacientes na fila de espera por um órgão, levando muitos ao óbito pela dificuldade em receber um órgão viável e compatível. Acreditamos que, os resultados da presente tese possam contribuir de maneira eficaz tornando o processo de obtenção de um órgão para o transplante mais rápido, mais viável e mais acessível a toda população, reduzindo assim o número de mortes ao redor do mundo. Dessa forma, esses resultados, mesmo que de forma inicial, trazem avanços para área da reabilitação pulmonar.

6. REFERÊNCIAS BIBLIOGRÁFICAS

1. Shin'oka T, Imai Y, Ikada Y. Transplantation of a tissue-engineered pulmonary artery. *The New England journal of medicine*. 2001;344(7):532-3.
2. US Renal Data System 2014 Annual Data Report: Epidemiology of Kidney Disease in the United States. 2015; 66(1): S1-S306.
3. Heron M. Deaths: leading causes for 2008. *National vital statistics reports : from the Centers for Disease Control and Prevention, National Center for Health Statistics, National Vital Statistics System* 2012; 60(6):1-94.
4. Roger VL, Go AS, Lloyd-Jones DM, Benjamin EJ, Berry JD, Borden WB, et al. Heart disease and stroke statistics-2012 update: a report from the American Heart Association. *Circulation* 2012; 125(1):e2-e220.
5. Christie JD, Edwards LB, Kucheryavaya AY, Benden C, Dipchand AI, Dobbels F, et al. The Registry of the International Society for Heart and Lung Transplantation: 29th adult lung and heart-lung transplant report-2012. *The Journal of heart and lung transplantation* 2012;31(10):1073-86.
6. Orens JB, Garrity ER, Jr. General overview of lung transplantation and review of organ allocation. *Proceedings of the American Thoracic Society* 2009;6(1):13-9.
7. Lee SJ, Atala A. Scaffold technologies for controlling cell behavior in tissue engineering. *Biomedical materials* 2013;8(1):010201.
8. L'Heureux N, McAllister TN, de la Fuente LM. Tissue-engineered blood vessel for adult arterial revascularization. *The New England journal of medicine* 2007;357(14):1451-3.
9. Atala A, Bauer SB, Soker S, Yoo JJ, Retik AB. Tissue-engineered autologous bladders for patients needing cystoplasty. *Lancet* 2006;367(9518):1241-6.
10. Macchiarini P, Jungebluth P, Go T, Asnaghi MA, Rees LE, Cogan TA, et al. Clinical transplantation of a tissue-engineered airway. *Lancet* 2008;372(9655):2023-30.
11. Badylak SF, Weiss DJ, Caplan A, Macchiarini P. Engineered whole organs and complex tissues. *Lancet* 2012;379(9819):943-52.
12. Ott HC, Matthiesen TS, Goh SK, Black LD, Kren SM, Netoff TI, et al. Perfusion decellularized matrix: using nature's platform to engineer a bioartificial heart. *Nature medicine* 2008;14(2):213-21.

13. Uygun BE, Soto-Gutierrez A, Yagi H, Izamis ML, Guzzardi MA, Shulman C, et al. Organ reengineering through development of a transplantable recellularized liver graft using decellularized liver matrix. *Nature medicine* 2010;16(7):814-20.
14. Petersen TH, Calle EA, Zhao L, Lee EJ, Gui L, Raredon MB, et al. Tissue engineered lungs for in vivo implantation. *Science* 2010;329(5991):538- 41.
15. Price AP, England KA, Matson AM, Blazar BR, Panoskaltsis-Mortari A. Development of a decellularized lung bioreactor system for bioengineering the lung: the matrix reloaded. *Tissue engineering Part A*. 2010;16(8):2581-91.
16. Ott HC, Clippinger B, Conrad C, Schuetz C, Pomerantseva I, Ikononou L, et al. Regeneration and orthotopic transplantation of a bioartificial lung. *Nature medicine* 2010;16(8):927-33.
17. Bissell MJ, Hall HG, Parry G. How does the extracellular matrix direct gene expression? *Journal of theoretical biology* 1982;99(1):31-68.
18. Bornstein P MJ, Sage H. Synthesis and secretion of structural macromolecules by endothelial cells in culture. In: Nosel HL VH, editor. *Pathobiology of the endothelial cell*. New York: Academic Press 1982. p. 215-28.
19. Nelson CM, Bissell MJ. Of extracellular matrix, scaffolds, and signaling: tissue architecture regulates development, homeostasis, and cancer. *Annual review of cell and developmental biology* 2006;22:287-309.
20. Hynes RO. The extracellular matrix: not just pretty fibrils. *Science* 2009;326(5957):1216-9.
21. Bornstein P, Sage EH. Matricellular proteins: extracellular modulators of cell function. *Current opinion in cell biology* 2002;14(5):608-16.
22. Raghov R. The role of extracellular matrix in postinflammatory wound healing and fibrosis. *FASEB journal: official publication of the Federation of American Societies for Experimental Biology* 1994;8(11):823-31.
23. Eckes B, Nischt R, Krieg T. Cell-matrix interactions in dermal repair and scarring. *Fibrogenesis & tissue repair* 2010;3:4.
24. Tottey S, Corselli M, Jeffries EM, Londono R, Peault B, Badylak SF. Extracellular matrix degradation products and low-oxygen conditions enhance the regenerative potential of perivascular stem cells. *Tissue engineering Part A*. 2011;17(1-2):37-44.

25. Valentin JE, Stewart-Akers AM, Gilbert TW, Badylak SF. Macrophage participation in the degradation and remodeling of extracellular matrix scaffolds. *Tissue engineering Part A*. 2009;15(7):1687-94.
26. Cortiella J, Niles J, Cantu A, Brettler A, Pham A, Vargas G, et al. Influence of acellular natural lung matrix on murine embryonic stem cell differentiation and tissue formation. *Tissue engineering Part A*. 2010;16(8):2565-80.
27. Allen RA, Seltz LM, Jiang H, Kasick RT, Sellaro TL, Badylak SF, et al. Adrenal extracellular matrix scaffolds support adrenocortical cell proliferation and function in vitro. *Tissue engineering Part A*. 2010;16(11):3363-74.
28. Crapo PM, Gilbert TW, Badylak SF. An overview of tissue and whole organ decellularization processes. *Biomaterials* 2011;32(12):3233-43.
29. Baiguera S, Gonfiotti A, Jaus M, Comin CE, Paglierani M, Del Gaudio C, et al. Development of bioengineered human larynx. *Biomaterials* 2011;32(19):4433-42.
30. Wang L, Johnson JA, Chang DW, Zhang Q. Decellularized musculofascial extracellular matrix for tissue engineering. *Biomaterials* 2013;34(11):2641-54.
31. Wallis JM, Borg ZD, Daly AB, Deng B, Ballif BA, Allen GB, et al. Comparative assessment of detergent-based protocols for mouse lung decellularization and recellularization. *Tissue engineering Part C, Methods* 2012;18(6):420-32.
32. Badylak SF, Taylor D, Uygun K. Whole-organ tissue engineering: decellularization and recellularization of three-dimensional matrix scaffolds. *Annual review of biomedical engineering* 2011;13:27-53.
33. Faulk DM, Carruthers CA, Warner HJ, Kramer CR, Reing JE, Zhang L, et al. The effect of detergents on the basement membrane complex of a biologic scaffold material. *Acta biomaterials* 2014;10(1):183-93
34. Bernard MP, Chu ML, Myers JC, Ramirez F, Eikenberry EF, Prockop DJ. Nucleotide sequences of complementary deoxyribonucleic acids for the pro alpha 1 chain of human type I procollagen. Statistical evaluation of structures that are conserved during evolution. *Biochemistry* 1983;22(22):5213-23.
35. Bernard MP, Myers JC, Chu ML, Ramirez F, Eikenberry EF, Prockop DJ. Structure of a cDNA for the pro alpha 2 chain of human type I procollagen. Comparison with chick cDNA for pro alpha 2(I) identifies structurally

- conserved features of the protein and the gene. *Biochemistry* 1983;22(5):1139-45.
36. Constantinou CD, Jimenez SA. Structure of cDNAs encoding the triple-helical domain of murine alpha 2 (VI) collagen chain and comparison to human and chick homologues. Use of polymerase chain reaction and partially degenerate oligonucleotide for generation of novel cDNA clones. *Matrix* 1991;11(1):1-9.
 37. Exposito JY, D'Alessio M, Solursh M, Ramirez F. Sea urchin collagen evolutionarily homologous to vertebrate pro-alpha 2(I) collagen. *The Journal of biological chemistry* 1992;267(22):15559-62.
 38. Arenas-Herrera JE, Ko IK, Atala A, Yoo JJ. Decellularization for whole organ bioengineering. *Biomedical materials* 2013;8(1):014106.
 39. Gilbert TW, Freund JM, Badylak SF. Quantification of DNA in biologic scaffold materials. *The Journal of surgical research* 2009;152(1):135-9.
 40. Derwin KA, Baker AR, Spragg RK, Leigh DR, Iannotti JP. Commercial extracellular matrix scaffolds for rotator cuff tendon repair. Biomechanical, biochemical, and cellular properties. *The American Journal of bone and joint surgery* 2006;88(12):2665-72.
 41. Erdag G, Morgan JR. Allogeneic versus xenogeneic immune reaction to bioengineered skin grafts. *Cell transplantation* 2004;13(6):701-12.
 42. Gock H, Murray-Segal L, Salvaris E, Cowan P, D'Apice AJ. Allogeneic sensitization is more effective than xenogeneic sensitization in eliciting Gal-mediated skin graft rejection. *Transplantation* 2004;77(5):751-3.
 43. Ross JR, Kirk AD, Ibrahim SE, Howell DN, Baldwin WM, 3rd, Sanfilippo FP. Characterization of human anti-porcine "natural antibodies" recovered from ex vivo perfused hearts--predominance of IgM and IgG2. *Transplantation* 1993;55(5):1144-50.
 44. Lehr EJ, Rayat GR, Chiu B, Churchill T, McGann LE, Coe JY, et al. Decellularization reduces immunogenicity of sheep pulmonary artery vascular patches. *The Journal of thoracic and cardiovascular surgery* 2011;141(4):1056-62.
 45. Patel N, Solanki E, Picciani R, Cavett V, Caldwell-Busby JA, Bhattacharya SK. Strategies to recover proteins from ocular tissues for proteomics. *Proteomics* 2008;8(5):1055-70.

46. Jackson DW, Grood ES, Wilcox P, Butler DL, Simon TM, Holden JP. The effects of processing techniques on the mechanical properties of bone-anterior cruciate ligament-bone allografts. An experimental study in goats. *The American journal of sports medicine* 1988;16(2):101-5.
47. Nonaka PN, Campillo N, Uriarte JJ, Garreta E, Melo E, de Oliveira LV, et al. Effects of freezing/thawing on the mechanical properties of decellularized lungs. *Journal of biomedical materials research Part A*. 2014;102(2):413-9
48. Hopkinson A, Shanmuganathan VA, Gray T, Yeung AM, Lowe J, James DK, et al. Optimization of amniotic membrane (AM) denuding for tissue engineering. *Tissue engineering Part C Methods* 2008;14(4):371-81.
49. Funamoto S, Nam K, Kimura T, Murakoshi A, Hashimoto Y, Niwaya K, et al. The use of high-hydrostatic pressure treatment to decellularize blood vessels. *Biomaterials* 2010;31(13):3590-5.
50. Sasaki S, Funamoto S, Hashimoto Y, Kimura T, Honda T, Hattori S, et al. In vivo evaluation of a novel scaffold for artificial corneas prepared by using ultrahigh hydrostatic pressure to decellularize porcine corneas. *Molecular vision* 2009;15:2022-8.
51. Elder BD, Kim DH, Athanasiou KA. Developing an articular cartilage decellularization process toward facet joint cartilage replacement. *Neurosurgery* 2010;66(4):722-7.
52. Yang B, Zhang Y, Zhou L, Sun Z, Zheng J, Chen Y, et al. Development of a porcine bladder acellular matrix with well-preserved extracellular bioactive factors for tissue engineering. *Tissue engineering Part C, Methods* 2010;16(5):1201-11.
53. Flynn LE. The use of decellularized adipose tissue to provide an inductive microenvironment for the adipogenic differentiation of human adipose-derived stem cells. *Biomaterials* 2010;31(17):4715-24.
54. Brown BN, Freund JM, Han L, Rubin JP, Reing JE, Jeffries EM, et al. Comparison of three methods for the derivation of a biologic scaffold composed of adipose tissue extracellular matrix. *Tissue engineering Part C, Methods* 2011;17(4):411- 21.
55. Chen RN, Ho HO, Tsai YT, Sheu MT. Process development of an acellular dermal matrix (ADM) for biomedical applications. *Biomaterials* 2004;25(13):2679-86.

56. Klebe RJ. Isolation of a collagen-dependent cell attachment factor. *Nature* 1974;250(463):248-51.
57. Gailit J, Ruoslahti E. Regulation of the fibronectin receptor affinity by divalent cations. *The Journal of biological chemistry* 1988;263(26):12927-32.
58. Meyer SR, Chiu B, Churchill TA, Zhu L, Lakey JR, Ross DB. Comparison of aortic valve allograft decellularization techniques in the rat. *Journal of biomedical materials research Part A*. 2006;79(2):254-62.
59. Tudorache I, Cebotari S, Sturz G, Kirsch L, Hurschler C, Hilfiker A, et al. Tissue engineering of heart valves: biomechanical and morphological properties of decellularized heart valves. *The Journal of heart valve disease* 2007;16(5):567-73.
60. Zhou J, Fritze O, Schleicher M, Wendel HP, Schenke-Layland K, Harasztosi C, et al. Impact of heart valve decellularization on 3-D ultrastructure, immunogenicity and thrombogenicity. *Biomaterials* 2010;31(9):2549-54.
61. Wainwright JM, Czajka CA, Patel UB, Freytes DO, Tobita K, Gilbert TW, et al. Preparation of cardiac extracellular matrix from an intact porcine heart. *Tissue engineering Part C, Methods* 2010;16(3):525-32.
62. Gilbert TW, Wognum S, Joyce EM, Freytes DO, Sacks MS, Badylak SF. Collagen fiber alignment and biaxial mechanical behavior of porcine urinary bladder derived extracellular matrix. *Biomaterials* 2008;29(36):4775-82.
63. Hodde J, Janis A, Ernst D, Zopf D, Sherman D, Johnson C. Effects of sterilization on an extracellular matrix scaffold: part I. Composition and matrix architecture. *Journal of materials science Materials in medicine* 2007;18(4):537-43.
64. Dong X, Wei X, Yi W, Gu C, Kang X, Liu Y, et al. RGD-modified acellular bovine pericardium as a bioprosthetic scaffold for tissue engineering. *Journal of materials science Materials in medicine* 2009;20(11):2327-36.
65. Reing JE, Brown BN, Daly KA, Freund JM, Gilbert TW, Hsiong SX, et al. The effects of processing methods upon mechanical and biologic properties of porcine dermal extracellular matrix scaffolds. *Biomaterials* 2010;31(33):8626-33.
66. Xu CC, Chan RW, Tirunagari N. A biodegradable, acellular xenogeneic scaffold for regeneration of the vocal fold lamina propria. *Tissue engineering* 2007;13(3):551-66.

67. Cox B, Emili A. Tissue subcellular fractionation and protein extraction for use in mass-spectrometry-based proteomics. *Nature protocols*. 2006;1(4):1872-8.
68. Giusti S, Bogetti ME, Bonafina A, Fiszer de Plazas S. An improved method to obtain a soluble nuclear fraction from embryonic brain tissue. *Neurochemical research* 2009;34(11):2022-9.
69. Du L, Wu X, Pang K, Yang Y. Histological evaluation and biomechanical characterisation of an acellular porcine cornea scaffold. *The British journal of ophthalmology* 2011;95(3):410-4.
70. Nakayama Kh Fau - Batchelder CA, Batchelder Ca Fau - Lee CI, Lee Ci Fau - Tarantal AF, Tarantal AF. Decellularized rhesus monkey kidney as a three-dimensional scaffold for renal tissue engineering *Tissue Eng Part A*. 2010 Jul;16(7):2207-16.
71. Alhamdani MS, Schroder C, Werner J, Giese N, Bauer A, Hoheisel JD. Singlestep procedure for the isolation of proteins at near-native conditions from mammalian tissue for proteomic analysis on antibody microarrays. *Journal of proteome research* 2010;9(2):963-71.
72. Nakayama KH, Batchelder CA, Lee CI, Tarantal AF. Decellularized rhesus monkey kidney as a three-dimensional scaffold for renal tissue engineering. *Tissue engineering Part A*. 2010;16(7):2207-16.
73. Nichols JE, Niles J, Riddle M, Vargas G, Schilagard T, Ma L, et al. Production and assessment of decellularized pig and human lung scaffolds. *Tissue engineering Part A*. 2013;19(17-18):2045-62.
74. Courtman DW, Pereira CA, Kashef V, McComb D, Lee JM, Wilson GJ. Development of a pericardial acellular matrix biomaterial: biochemical and mechanical effects of cell extraction. *Journal of biomedical materials research* 1994;28(6):655-66.
75. Kasimir MT, Rieder E, Seebacher G, Silberhumer G, Wolner E, Weigel G, et al. Comparison of different decellularization procedures of porcine heart valves. *The International journal of artificial organs* 2003;26(5):421-7.
76. Hudson TW, Liu SY, Schmidt CE. Engineering an improved acellular nerve graft via optimized chemical processing. *Tissue engineering* 2004;10(9-10):1346-58.
77. Gui L, Chan SA, Breuer CK, Niklason LE. Novel utilization of serum in tissue decellularization. *Tissue engineering Part C, Methods* 2010;16(2):173-84.

78. Cebotari S, Tudorache I, Jaekel T, Hilfiker A, Dorfman S, Ternes W, et al. Detergent decellularization of heart valves for tissue engineering: toxicological effects of residual detergents on human endothelial cells. *Artificial organs* 2010;34(3):206-10.
79. Feil G, Christ-Adler M, Maurer S, Corvin S, Rennekampff HO, Krug J, et al. Investigations of urothelial cells seeded on commercially available small intestine submucosa. *European urology* 2006;50(6):1330-7.
80. Lumpkins SB, Pierre N, McFetridge PS. A mechanical evaluation of three decellularization methods in the design of a xenogeneic scaffold for tissue engineering the temporomandibular joint disc. *Acta biomaterialia* 2008;4(4):808-16.
81. Montoya CV, McFetridge PS. Preparation of ex vivo-based biomaterials using convective flow decellularization. *Tissue engineering Part C, Methods*. 2009;15(2):191-200.
82. Jamur MC, Oliver C. Cell fixatives for immunostaining. *Methods in molecular biology* 2010;588:55-61.
83. Henderson PW, Nagineni VV, Harper A, Bavinck N, Sohn AM, Krijgh DD, et al. Development of an acellular bioengineered matrix with a dominant vascular pedicle. *The Journal of surgical research* 2010;164(1):1-5.
84. Shupe T, Williams M, Brown A, Willenberg B, Petersen BE. Method for the decellularization of intact rat liver. *Organogenesis* 2010;6(2):134-6.
85. Baptista PM, Orlando G, Mirmalek-Sani SH, Siddiqui M, Atala A, Soker S. Whole organ decellularization - a tool for bioscaffold fabrication and organ bioengineering. *Conference proceedings: Annual International Conference of the IEEE Engineering in Medicine and Biology Society IEEE Engineering in Medicine and Biology Society Conference*. 2009;2009:6526-9.
86. Sullivan DC, Mirmalek-Sani SH, Deegan DB, Baptista PM, Aboushwareb T, Atala A, et al. Decellularization methods of porcine kidneys for whole organ engineering using a high-throughput system. *Biomaterials* 2012;33(31):7756-64.
87. Gillies Ar Fau - Smith LR, Smith Lr Fau - Lieber RL, Lieber Rl Fau - Varghese S, Varghese S. Method for decellularizing skeletal muscle without detergents or proteolytic enzymes *Tissue Eng Part C Methods*. 2011 Apr;17(4):383-9.

88. Woods T, Gratzner PF. Effectiveness of three extraction techniques in the development of a decellularized bone-anterior cruciate ligament-bone graft. *Biomaterials* 2005;26(35):7339-49.
89. Deeken CR, White AK, Bachman SL, Ramshaw BJ, Cleveland DS, Loy TS, et al. Method of preparing a decellularized porcine tendon using tributyl phosphate. *Journal of biomedical materials research Part B, Applied biomaterials* 2011;96(2):199-206.
90. Cartmell JS, Dunn MG. Development of cell-seeded patellar tendon allografts for anterior cruciate ligament reconstruction. *Tissue engineering* 2004;10(7-8):1065-75.
91. Yusen RD, et al. Lung Transplantation in the United States, 1999–2008. *Am J Transplantation* 2010;10(2):1047–1068.
92. Lopez AD, Shibuya K, Rao C, Mathers CD, Hansell AL, Held LS, et al. Chronic obstructive pulmonary disease: current burden and future projections. *The European respiratory journal* 2006;27(2):397-412.
93. Eisner MD, Anthonisen N, Coultas D, Kuenzli N, Perez-Padilla R, Postma D, et al. An official American Thoracic Society public policy statement: Novel risk factors and the global burden of chronic obstructive pulmonary disease. *American journal of respiratory and critical care medicine* 2010;182(5):693-718.
94. Nichols JE, et al. Design and development of tissue engineered lung: Progress and challenges. *Organogenesis*.2009;5:57-61.
95. Badylak SF. The extracellular matrix as a scaffold for tissue reconstruction *Cell & Developmental Biology* 2002; 13: 377–383.
96. Gilbert TW, Sellaro TL, Badylaka SF. Decellularization of tissues and organs. *Biomaterials* 2006; 27:3675–3683.
97. Badylak SF, Freytes DO, Gilbert TW. Extracellular matrix as a biological scaffold material: Structure and function. *Acta Biomaterialia* 2009; 5:1–13.
98. Gilbert TW, Gilbert S, Madden M, Reynolds SD, Badylak SF. Morphologic Assessment of Extracellular Matrix Scaffolds for Patch Tracheoplasty in a Canine Model. *Ann Thorac Surg* 2008;86:967–74.
99. Gilbert TW, Nieponice A, Spievack AR, Holcomb J, Gilbert S, Badylak SF.. Repair of the Thoracic Wall With an Extracellular Matrix Scaffold in a Canine Model. *Journal of Surgical Research*. 2008;147: 61–67.

100. Macchiarini P, Jungebluth P, Go T, Asnaghi MA, Rees LE, Cogan TA, et al. Clinical transplantation of a tissue-engineered airway. *Lancet* 2008;372:2023-30.
101. Cortiella J, Nichols JE, Kojima K, Bonassar LJ, Dargon P, Roy AK, et al. Tissue-engineered lung: an in vivo and in vitro comparison of polyglycolic acid and pluronic F-127 hydrogel/somatic lung progenitor cell constructs to support tissue growth. *Tissue Eng* 2006;12:1213-25
102. Guyette JP, Gilpin SE, Charest JM, Tapias LF, Ren X, Ott HC. Perfusion decellularization of whole organs. *Nat Protoc* 2014;9(6):1451-68
103. Melo E, Garreta E, Luque T, Cortiella J, Nichols J, Navajas D, et al. Effects of the decellularization method on the local stiffness of acellular lungs. *Tissue Eng Part C Methods* 2014;20(5):412-22.
104. Song JJ, Kim SS, Liu Z, Madsen JC, Mathisen DJ, Vacanti JP, et al. Enhanced in vivo function of bioartificial lungs in rats. *Ann Thorac Surg.* 2011;92(3):998-1005.
105. Jensen T, Roszell B, Zang F, Girard E, Matson A, Thrall R, et al. A rapid lung de-cellularization protocol supports embryonic stem cell differentiation in vitro and following implantation. *Tissue Eng Part C Methods* 2012; 18:632–646
106. Daly AB, Wallis JM, Borg ZD, Bonvillain RW, Deng B, Ballif BA, et al. Initial binding and recellularization of decellularized mouse lung scaffolds with bone marrow-derived mesenchymal stromal cells. *Tissue Eng Part A.* 2012;18(1-2):1-16.
107. Bonenfant NR, Sokocevic D, Wagner DE, Borg ZD, Lathrop MJ, Lam YW, et al. The effects of storage and sterilization on decellularized and recellularized whole lung. *Biomaterials* 2013; 34:3231–3245.
108. Girard ED, Jensen TJ, Vadasz SD, Blanchette AE, Zhang F, Moncada C, et al. Automated procedure for biomimetic de-cellularized lung scaffold supporting alveolar epithelial transdifferentiation. *Biomaterials* 2013;34(38):10043-55.
109. Wagner DE, Bonenfant NR, Sokocevic D, DeSarno MJ, Borg ZD, Parsons CS, et al. Three-dimensional scaffolds of acellular human and porcine lungs for high throughput studies of lung disease and regeneration. *Biomaterials* 2014 Mar;35(9):2664-79.

110. Wagner DE, Bonenfant NR, Parsons CS, Sokocevic D, Brooks EM, Borg ZD, et al. Comparative decellularization and recellularization of normal versus emphysematous human lungs. *Biomaterials* 2014;35(10):3281-97.
111. Guyette JP, Gilpin SE, Charest JM, Tapias LF, Ren X, Ott HC. Perfusion decellularization of whole organs. *Nat Protoc* 2014;9(6):1451-68
112. Carreras A, Rojas M, Tsapikouni T, Montserrat JM, Navajas D, Farré R. Obstructive apneas induce early activation of mesenchymal stem cells and enhancement of endothelial wound healing. *Respir Res.* 2010;11:91.
113. Nonaka PN, Uriarte JJ, Campillo N, Melo E, Navajas D, Farré R, Oliveira LV. Mechanical properties of mouse lungs along organ decellularization by sodium dodecyl sulfate. *Respir. Physiol. Neurobiol.* 2014;15(200):1–5.
114. Uriarte JJ, Nonaka PN, Campillo N, Palma RK, Melo E, de Oliveira LV, Navajas D, Farré R. Mechanical properties of acellular mouse lungs after sterilization by gamma irradiation. *J. Mech. Behav. Biomed. Mater.* 2014;40:168–177.
115. Farre R, Granell S, Rotger M, Serrano-Mollar A, Closa D, Navajas D. Animal model of unilateral ventilatorinduced lung injury. *Intensive Care Med.* 2005;31:487–490.
116. Nichols JE., Niles JA, Cortiella J. Production and utilization of acellular lung scaffolds in tissue engineering. *J Cell Biochem.* 2012;113(7):2185-92.
117. Gilpin SE, Guyette JP, Gonzalez G, Ren X, Asara JM, Mathisen DJ, et al. Perfusion decellularization of human and porcine lungs: bringing the matrix to clinical scale. *J Heart Lung Transplant* 2014;33(3):298-308.
118. Weiss D.J. Concise review: current status of stem cells and regenerative medicine in lung biology and diseases. *Stem Cells* 2014;32 (1), 16–25.
119. Gilpin SE, Guyette JP, Gonzalez G, Ren X, Asara JM, Mathisen DJ, et al. Perfusion decellularization of human and porcine lungs: bringing the matrix to clinical scale. *J. Heart Lung Transplant.* 2014;33 (3), 298–308.
120. Price AP, Godin LM, Domek A, Cotter T, D’Cunha J, Taylor DA, et al. Automated decellularization of intact, human-sized lungs for tissue engineering. *Tissue Eng. Part C: Methods* 2014;21, 94–103
121. Gilpin SE, Ren X, Okamoto T, Guyette JP, Mou H, Rajagopal J, et al. Enhanced lung epithelial specification of human induced pluripotent stem cells

- on decellularized lung matrix. In: Presented at the Fiftieth Annual Meeting of The Society of Thoracic Surgeons, Orlando, FL, 2014;98(5):1721–1729.
122. Booth A.J, Hadley R, Cornett AM, Dreffs AA, Matthes SA, Tsui JL, et al. Acellular normal and fibrotic human lung matrices as a culture system for in vitro investigation. *Am. J. Respir. Crit. Care Med.* 2012;186(9):866–876.
 123. Khalpey Z, Qu N, Hemphill C, Louis AV, Ferng AS, Son TG, et al. Rapid porcine lung decellularization utilizing a novel organ regenerative control acquisition bioreactor. *ASAIO* 2014; J.61(1):71–77.
 124. Bonvillain RW, Danchuk S, Sullivan DE, Betancourt AM, Semon JA, Eagle M.E. et al. A nonhuman primate model of lung regeneration: detergent-mediated decellularization and initial in vitro recellularization with mesenchymal stem cells. *Tissue Eng. Part A* 2012;18(23-24):2437–2452.
 125. Bonvillain RW, Scarritt ME, Pashos NC, Mayeux JP, Meshberger CL, Betancourt AM, et al. Nonhuman primate lung decellularization and recellularization using a specialized large-organ bioreactor. *J. Vis. Exp.* 2013;15(82):e50825.
 126. Price AP, Godin LM, Domek A, Cotter T, D’Cunha J, Taylor DA, et al. Automated decellularization of intact, human-sized lungs for tissue engineering. *Tissue Eng. Part C: Methods* 2015;21(1):94–103
 127. Tuchscherer HA, Webster EB, Chesler NC. Pulmonary vascular resistance and impedance in isolated mouse lungs: effects of pulmonary emboli. *Ann. Biomed. Eng.* 2006;34(4):660–668.
 128. Starov VM, Zhdanov VG. Viscosity of emulsions: influence of flocculation. *J. Colloid Interface Sci.* 2003;15(258):404–414.
 129. Dhopatkar N, Park JH, Chari K, Dhinojwala A. Adsorption and viscoelastic analysis of polyelectrolyte-surfactant complexes on charged hydrophilic surfaces. *Langmuir* 2015;31:1026–1037
 130. Orlando G, Farney AC, Iskandar SS, Mirmalek-Sani SH, Sullivan DC, Moran E, et al. Production and implantation of renal extracellular matrix scaffolds from porcine kidneys as a platform for renal bioengineering investigations. *Ann Surg.* 2012;256(2):363-70.
 131. Song JJ, Guyette JP, Gilpin SE, Gonzalez G, Vacanti JP, Ott HC. Regeneration and experimental orthotopic transplantation of a bioengineered kidney. *Nat. Med.* 2013;19(5):646–651.

132. Uygun B.E, Soto-Gutierrez A, Yagi H, Izamis ML, Guzzardi MA ,et al. Organ reengineering through development of a transplantable recellularized liver graft using decellularized liver matrix. *Nat. Med.* 2010;16(7):814–820.
133. Struecker B, Butter A, Hillebrandt K, Polenz D, Reutzel-Selke A, Tang P, et al. Improved rat liver decellularization by arterial perfusion under oscillating pressure conditions. *J Tissue Eng Regen Med.* 2014;4.
134. Struecker B, Hillebrandt KH, Voitl R, Butter A, Schmuck RB, Reutzel-Selke A, et al Porcine liver decellularization under oscillating pressure conditions: a technical refinement to improve the homogeneity of the decellularization process. *Tissue Eng Part C Methods.* 2015;21(3):303-13
135. Wainwright JM, Czajka CA, Patel UB, Freytes DO, Tobita K, Gilbert TW, et al. Preparation of cardiac extracellular matrix from an intact porcine heart. *Tissue Eng Part C Methods.* 2010;16(3):525-32.
136. Weymann A, Patil NP, Sabashnikov A, Jungebluth P, Korkmaz S, Li S, Veres G. Bioartificial heart: a human-sized porcine model—the way ahead. *PLoS One* 2014;3:9(11):e111591.
137. Organ Procurement and Transplantation Network (OPTN). <http://optn.transplant.hrsa.gov> (accessed Online 05 may 2014).
138. Lopez AD, Shibuya K, Rao C, Mathers CD, Hansell AL, Held LS, et al. Chronic obstructive pulmonary disease: current burden and future projections. *Eur Respir J* 2006;27:397-412
139. Barberà JA, Riverola A, Roca J, Ramirez J, Wagner PD, Ros D, et al. Pulmonary vascular abnormalities and ventilation-perfusion relationships in mild chronic obstructive pulmonary disease. *Am J Respir Crit Care Med* 1994;149:423–429.
140. da Palma RK, Campillo N, Uriarte JJ, Oliveira LV, Navajas D, Farré R. Pressure- and flow-controlled media perfusion differently modify vascular mechanics in lung decellularization. *J Mech Behav Biomed Mater.* 2015;49:69-79.

7. APÊNDICES

Estudo 1.

JOURNAL OF THE MECHANICAL BEHAVIOR OF BIOMEDICAL MATERIALS 49 (2015) 69–79

Available online at www.sciencedirect.com

ScienceDirect

www.elsevier.com/locate/jmbbm

Research Paper

Pressure- and flow-controlled media perfusion differently modify vascular mechanics in lung decellularization



Renata K. da Palma^{a,b}, Noelia Campillo^{a,c}, Juan J. Uriarte^{a,d},
Luis V.F. Oliveira^b, Daniel Navajas^{a,c,d}, Ramon Farré^{a,d,e,*}

^aUnitat Biofísica i Bioenginyeria, Facultat de Medicina, Universitat de Barcelona, Barcelona, Spain

^bMaster's and Doctoral Degree Programs in Rehabilitation Sciences, Nove de Julho University, Sao Paulo, Brazil

^cInstitut de Bioenginyeria de Catalunya, Barcelona, Spain

^dCIBER Enfermedades Respiratorias, Madrid, Spain

^eInstitut Investigacions Biomèdiques August Pi Sunyer, Barcelona, Spain

ARTICLE INFO

Article history:

Received 12 January 2015

Received in revised form

18 April 2015

Accepted 23 April 2015

Available online 7 May 2015

Keywords:

Tissue engineering

Lung bioengineering

Organ biofabrication

Lung scaffold

Cellular lung

Vascular resistance

Fluid mechanics

ABSTRACT

Organ biofabrication is a potential future alternative for obtaining viable organs for transplantation. Achieving intact scaffolds to be recellularized is a key step in lung bioengineering. Perfusion of decellularizing media through the pulmonary artery has shown to be effective. How vascular perfusion pressure and flow vary throughout lung decellularization, which is not well known, is important for optimizing the process (minimizing time) while ensuring scaffold integrity (no barotrauma). This work was aimed at characterizing the pressure/flow relationship at the pulmonary vasculature and at how effective vascular resistance depends on pressure- and flow-controlled variables when applying different methods of media perfusion for lung decellularization. Lungs from 43 healthy mice (C57BL/6, 7–8 weeks old) were investigated. After excision and tracheal cannulation, lungs were inflated at 10 cmH₂O airway pressure and subjected to conventional decellularization with a solution of 1% sodium dodecyl sulfate (SDS). Pressure (P_{PA}) and flow (V_{PA}) at the pulmonary artery were continuously measured. Decellularization media was perfused through the pulmonary artery: (a) at constant $P_{PA}=20$ cmH₂O or (b) at constant $V_{PA}=0.5$ and 0.2 ml/min. Effective vascular resistance was computed as $R_e=P_{PA}/V_{PA}$. R_e (in cmH₂O/(ml/min); mean±SE) considerably varied throughout lung decellularization, particularly for pressure-controlled perfusion (from 29.1±3.0 in baseline to a maximum of 664.1±164.3 ($p<0.05$), as compared with flow-controlled perfusion (from 49.9±3.3 and 79.5±5.1 in baseline to a maximum of 1144±13.9 and 211.7±70.5 ($p<0.05$, both), for V_{PA} of 0.5 and 0.2 ml/min respectively. Most of the media infused to the pulmonary artery throughout decellularization circulated to the airways compartment across the alveolar-capillary membrane. This

*Corresponding author at: Unitat Biofísica i Bioenginyeria, Facultat de Medicina, Casanova 143, 08036 Barcelona, Spain.

E-mail address: rfarre@ub.edu (R. Farré).

study shows that monitoring perfusion mechanics throughout decellularization provides information relevant for optimizing the process time while ensuring that vascular pressure is kept within a safety range to preserve the organ scaffold integrity.

© 2015 Elsevier Ltd. All rights reserved.

1. Introduction

Lung bioengineering has recently emerged as a potential alternative for obtaining available organs for transplantation in the forthcoming years (Ott et al., 2010; Song et al., 2011; Nichols et al., 2012; Garcia et al., 2012). According to this approach, biofabricated lungs would help in reducing the current long waiting lists for transplantation, and also the increased expected demands caused by the progressive aging of the population in both developed and developing countries (Yusen et al., 2010). Although experimental studies have already established convincing proof of concept on the feasibility of lung bioengineering (Ott et al., 2010; Song et al., 2011), it should be mentioned that the field is still at its scientific infancy and thus requires considerable research before reaching evidence to plan the first clinical tests.

Given the structural complexity of the lung (typically having 300 millions alveoli, each with a diameter of 300 μm , separated from capillaries with a diameter of 10 μm by a membrane with a thickness of 3 μm and surface of 70 m^2 ; all packed in a volume of 5 l) and the inability of current technologies to construct such a micron-scale 3D structure, the approach for lung bioengineering is to use lung scaffolds obtained from natural organs (Price et al., 2010; Cortiella et al., 2010). Indeed, the concept for biofabricating a lung is to first decellularize an organ that is not available for transplantation and then to use its acellular scaffold as a platform for seeding cells that, after proliferating and differentiating, regenerate the lung (Ott et al., 2010; Song et al., 2011; Weiss, 2014).

The procedure for decellularizing a lung – or any other organ – should strike a difficult balance: it must be sufficiently aggressive to eliminate all the cell material from the donor but at the same time must be smooth enough to preserve the structure and composition of its extracellular matrix (Badylak et al., 2012). Although how to optimally obtain acellular lungs has not been so far clearly established, different published protocols have shown to provide lung scaffolds exhibiting reasonable quality in terms of low DNA donor load and high preserved extracellular matrix structure and composition (Ott et al., 2010; Daly et al., 2012; Bonenfant et al., 2013; Gilpin et al., 2014a).

Perfusion of different decellularizing media (e.g. deionized water, detergents, enzymes) through the vascular circuit of the organ is a conventional procedure for eliminating donor cell material since the widespread distribution of the capillary network within the organ allows both to distribute the media to short diffusion distance from any cell and to washout the resulting debris. In the specific case of the lung, different experimental studies in animal and human organs have shown that perfusing media through the pulmonary artery allows to adequately decellularize not only the vessel

walls but also to eliminate the cells in the lung parenchyma and in the airway walls (Girard et al., 2013; Price et al., 2014; Gilpin et al., 2014a, 2014b; Wagner et al., 2014a, 2014b).

Perfusing media through the pulmonary artery is a mechanical process that could be carried out manually (Jensen et al., 2012; Wallis et al., 2012; Daly et al., 2012; Bonenfant et al., 2013). However, this procedure does not allow to easily control the rate of infusion, thereby risking lung damage. Alternatively, media perfusion can be automatically controlled by regulating pressure or flow at the entrance of the pulmonary artery. The limited knowledge currently available on these procedures suggests that both pressure- and flow-control could result in well decellularized and preserved lung scaffolds. Indeed, recent studies have compared perfusion methods (e.g. pressure- vs flow-controlled and manual vs automated) in terms of elimination of donor cell material in the scaffold, preservation of the extracellular matrix composition and structure, and suitability of the acellular scaffold as substrate for culturing cells (Girard et al., 2013; Wagner et al., 2014a, 2014b; Guyette et al., 2014). Nevertheless, none of these studies has investigated lung vascular resistance in detail. Remarkably, each perfusion procedure has its own advantages and drawbacks from a fluid mechanics viewpoint. On the one hand, controlling perfusion pressure at the pulmonary artery ensures that no barotrauma is induced within the scaffold, but accumulation of debris caused by disrupted cells could strongly reduce flow or even interrupt it in case of insufficient pressure. On the other hand, controlling the flow infused at the pulmonary artery ensures a rate of media circulation but – also owing to debris accumulation – may induce high pressure inside the lung vessels, thereby risking to damage the alveolar-capillary membrane. However, no detailed study has investigated this issue in detail.

Furthering our understanding of the fluid dynamics in media perfusion during lung decellularization may provide insights to optimize the process, both for research purposes and also to facilitate automatization for high-throughput production of lung scaffolds. Accordingly, this work was aimed at characterizing the pressure/flow relationship at the pulmonary vasculature and at studying how effective vascular resistance depends on pressure- and flow-controlled variables when applying different conventional ways of perfusing media for lung decellularization.

2. Methods

2.1. Animals and lung excision

This study was carried out on lungs excised from 43 C57BL/6 male healthy mice, 7–8 weeks old (17–18 g), following experimental procedures approved by the Ethical Committee for

Animal Research of the University of Barcelona. The mice were anesthetized with intraperitoneal urethane (1 mg/kg), heparinized 250 U/kg, and sacrificed by exsanguination through the abdominal aorta. Immediately after euthanasia, the diaphragm was punctured and the rib cage was cut to reveal the lungs. The lungs were perfused via the right ventricle with phosphate buffered saline (PBS) containing 50 U/ml heparin (Sigma) and 1 μ g/ml sodium nitroprusside (SNP, Fluka) to prevent formation of blood clots in the lung. After perfusion was complete, the heart, lungs and trachea were dissected and removed en bloc, and stored in a -80°C freezer until the decellularization process was carried out.

2.2. Experimental setting

The experimental setting was implemented to measure lung vascular mechanics throughout organ decellularization. Fig. 1A shows a diagram of the lung capillaries and alveoli when organ decellularization is carried out by perfusing media through the pulmonary artery. Pressure and flow at the entrance of the pulmonary artery are P_{PA} and V_{PA} , respectively. Flow moving from the capillaries to the alveoli (at a pressure P_{alv}) through the alveolar-capillary membrane is V_{TM} . V_{PV} is the medium flow leaving the lungs through the pulmonary vein ($V_{PA} = V_{TM} + V_{PV}$). Fig. 1B is the corresponding representation in terms of the fluid resistances circuit,

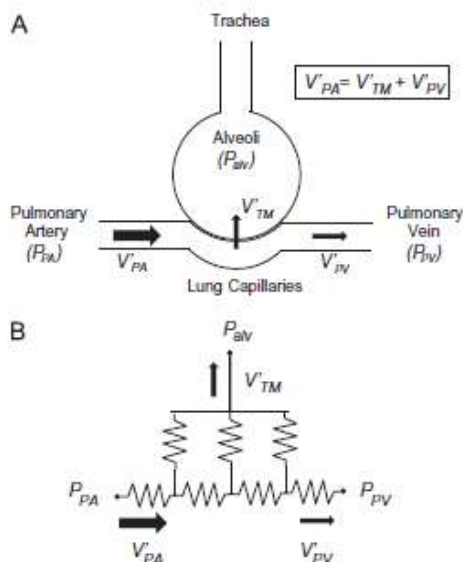


Fig. 1 – (A) Diagram of lung decellularization by perfusing media through the pulmonary artery. P_{PA} and V_{PA} are pressure and flow at the pulmonary artery. P_{PV} and V_{PV} are pressure and flow at the pulmonary vein. V_{TM} is medium flow leaving the capillaries to the alveoli through the alveolar-capillary membrane. P_{alv} is alveolar pressure. (B) Circuit corresponding to (A) representing the serial capillary resistances and the parallel transmembrane resistances.

where the serial and parallel resistances represent the capillary and transmembrane circulation pathways, respectively. Lung decellularization is usually carried out by keeping the pulmonary vein open to the atmosphere ($P_{PV} = 0$). Hence, continuously measuring V_{PA} and P_{PA} allows the computation of effective vascular resistance (R_e) as $R_e = P_{PA}/V_{PA}$. In the particular case that the decellularization is carried out by perfusing the media through the pulmonary artery with the pulmonary vein ligated ($V_{PV} = 0$; $V_{PA} = V_{TM}$), the effective vascular resistance R_e measured would correspond to that of the transmembrane pathway.

To characterize vascular mechanics throughout lung decellularization carried out under different perfusion conditions we used the experimental system shown in the diagram of Fig. 2. The trachea was cannulated and connected to a continuous positive airway pressure (CPAP) device to provide a tracheal (i.e. transpulmonary) pressure of 10 cmH₂O to inflate the lung at a physiological volume to avoid atelectasis. Tracheal pressure was measured by a pressure transducer (011-OP229-01; ICUmedical, USA). The transmembrane flow V_{TM} entering the airways from the capillaries was allowed to leave the lung through a port at the inlet of the tracheal cannula. The pulmonary artery was cannulated and could be connected to one of two possible sources of controlled perfusion: constant pressure (gravimetric level) or constant flow (55-2222 perfusion pump; Harvard Apparatus, USA). In both instances, a pressure transducer (011-OP229-01; ICUmedical, USA) allowed the measurement of P_{PA} . The pulmonary vein was kept open to the atmosphere allowing to leave V_{PV} or, alternatively, was ligated so that $V_{PV} = 0$. When perfusion was carried out at constant P_{PA} , V_{PA} was measured from the rate of change in the weight recorded by a scale collecting $V_{TM} + V_{PV}$ or only V_{TM} (in case of pulmonary vein ligation), Fig. 2.

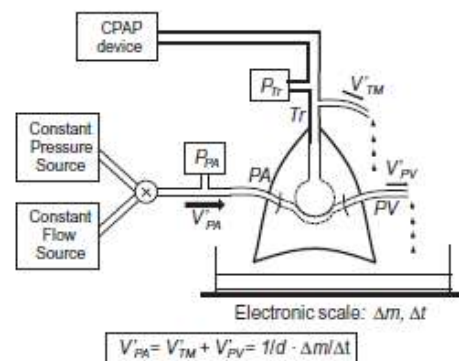


Fig. 2 – Experimental setting. CPAP: constant positive airway pressure. P_{Tr} : pressure transducer to measure tracheal pressure. T: tracheal cannulation. PA and PV: pulmonary artery and pulmonary vein cannulations, respectively. P_{PA} : pressure transducer to measure pulmonary artery pressure. V_{PA} and V_{PV} : flows at the pulmonary artery and vein, respectively. V_{TM} : flow leaving the capillaries to the alveoli through the alveolar-capillary membrane. Δm mass change measured at the electronic scale during time interval Δt . d: perfusion medium density.

2.3. Lung decellularization

Prior to placing the lungs into the experimental setting (Fig. 2), they were thawed in a bath at 37 °C and subjected to 3 additional cycles of freezing (−80 °C) and thawing (37 °C) to enhance cell membrane rupture. Once the trachea and pulmonary artery were cannulated and placed into the experimental system, the following sequence of decellularizing media was perfused through the pulmonary artery: (1) PBS 1x for 30 min, (2) deionized water for 15 min, (3) 1% sodium dodecyl sulfate (SDS) detergent for 150 min, (4) PBS for 30 min.

This decellularization process was performed under different mechanical conditions. While keeping the pulmonary vein open (which is the conventional procedure), the decellularizing media was perfused: (1) at a constant pressure of $P_{PA}=20$ cmH₂O (8 lungs), and (2) at constant flows V_{PA} of 0.2 ml/min (8 lungs) and of 0.5 ml/min (5 lungs). In addition, a series of lung decellularization at a constant pressure of $P_{PA}=20$ cmH₂O was carried out ($n=5$) in such a way that the pulmonary vein was cyclically kept open and ligated every 5 min, thus allowing the comparison of V_{TM} and V_{PV} throughout lung decellularization.

2.4. Decellularization assessment

After decellularization, lung scaffolds (as well as 3 native lungs for comparison) were divided into their lobes and fixed by bronchial infusion of a 3:1 ratio mixture of Optimal Cutting Temperature compound (OCT, Sakura) and PBS and stored at a −80 °C freezer. Subsequently, cryosections (12 μm) of frozen lung samples were obtained using a cryostat (Thermo Scientific, HM 560 CryoStat). To verify the absence of cell DNA after the process of decellularization, the cryosections were rinsed with PBS to remove the OCT and then maintained for 10 min in 1 μg/ml of 4',6-diamidino-2-phenylindole (DAPI, Sigma) fluorescence solution for staining. Sections of interest were observed with a digital camera (CCD-EM C9100, Hamamatsu, Japan) coupled to an inverted fluorescent microscope (Ti-Eclipse, Nikon, Tokyo, Japan) and driven by a conventional acquisition software (NIS Elements, Nikon Instruments Inc).

To perform conventional fluorescent imaging, cryosections of the lung (12 μm thick) obtained from each group were allowed to thaw at room temperature. Several PBS 1x rinses were done in order to remove the OCT. Tissue samples were fixed in 70% ice-cold methanol+30% acetone for 5 min, then blocked with a buffer solution containing PBS 1x and 10% fetal bovine serum (FBS) for 30 min. Primary antibodies were diluted in buffer solution. Diverse slices with different primary antibodies, rabbit anti-collagen I (1:500, Abcam), goat anti-elastin (1:200, Santa Cruz), rabbit anti-collagen III (1:200, Abcam), goat anti-collagen IV (1:200, Santa Cruz) and rabbit anti-laminin (1:25, Sigma), were incubated overnight at 4 °C. The slices were rinsed three times with the PBS 1x, for 5 min each wash. Secondary antibodies, donkey anti-rabbit Cy3 and bovine anti-goat Alexa 488 diluted (1:200, Jackson) in buffer solution, were incubated for 60 min. Three times 5-min rinses with PBS 1x were applied to eliminate unbound secondary antibodies. Finally, coverslips were mounted on each section using a non-fluorescent compound (Fluoromont G, SouthernBiotech). Images of the regions of interest were obtained with a digital

camera (CCD-EM C9100, Hamamatsu, Japan) coupled to an inverted fluorescent microscope (Ti-Eclipse, Nikon, Tokyo, Japan) with a magnification of 10× and operated by a commercial acquisition software (NIS-Elements C Microscope Imaging Software, Nikon Instruments Inc).

Phase contrast images were obtained after complete OCT elimination and samples were kept in PBS 1x at room temperature during image acquisition. Images were obtained with a digital camera (Marlyn F145, Allied V.T., Germany) operated by Vision Assistant software (National Instruments) and coupled to an inverted optical microscope (TE2000, Nikon, Tokyo).

In addition, the level of remaining DNA in the scaffold after using the perfusion procedure was assessed in three randomly selected decellularized lungs and in one native lung. A sample of the right middle lobe of each lung was dried and weighted and its total genomic DNA was isolated using the spin-column based PureLink[®] Genomic DNA Mini Kit (Invitrogen™) according to manufacturer's instructions. Double-stranded DNA yield was measured by spectrophotometry (NanoDrop 1000, Thermo Scientific) and normalized to sample tissue weight.

2.5. Assessment of lung elastance

To assess the potential changes induced by the perfusion procedures on the mechanics of the whole organ we measured lung elastance. Dynamic (E_{dyn}) and static (E_{st}) lung elastances were determined in additional organs (3 native lungs and 11 acellular lungs immediately after decellularization). To characterize the pressure–volume relationship in mechanical conditions similar to those in physiologically normal breathing, the lungs were subjected to conventional mechanical ventilation, following a procedure describe in detail elsewhere (Nonaka et al., 2014a, 2014b; Uriarte et al., 2014). Briefly, the lungs were tracheally intubated, suspended vertically by gravity and placed within a chamber (32 °C and 100% humidity). A pneumotachograph was connected to the inlet of the cannula to measure tracheal flow by sensing the pressure drop across the pneumotachograph with a differential pressure transducer. Tracheal pressure was measured by connecting a pressure transducer on a side port placed between the pneumotachograph and the cannula. The inlet of the pneumotachograph was then connected to the Y piece of a volumetric mechanical ventilator designed for the artificial ventilation of rodents (Farre et al., 2005). The lungs were subjected to conventional ventilation with a quasi-sinusoidal flow pattern with a tidal volume of 10 ml/kg of mouse body weight, a frequency of 100 breaths/min and a positive end expiratory pressure of 2 cmH₂O, to counteract the absence of the physiological negative pleural pressure at rest. Flow and pressure signals from the transducers were analogically low-pass filtered, sampled and stored for subsequent analysis.

E_{st} and E_{dyn} were measured by means of end-inspiratory airway occlusions achieved by pushing the corresponding control button of the mechanical ventilator. After an end-inspiratory occlusion, there was a fast initial drop in acellular lung pressure (DP_i) from the pre-occlusion value down to an inflection point (with pressure P_i), followed by a slow pressure decay (DP_e) until a plateau pressure (P_{pl}) corresponding to the

elastic recoil pressure of the lung is reached. Whereas DP_1 is associated with pressure dissipated against pulmonary resistance, DP_2 reflects tissue viscoelastic properties or pendelluft. Taking into account the value of pre-inspiratory pressure (P_0), lung static elastance (E_{st}) was computed as the adjusted plateau pressure ($P_{st}-P_0$) recorded after 5 s of occlusion divided by the tidal volume. E_{dyn} was computed by dividing the adjusted inflection point pressure (P_i-P_0) by the tidal volume (Nonaka et al., 2014a, 2014b). For each native and decellularized lung, E_{st} and E_{dyn} were obtained as the means from five end-inspiratory occlusions, each one carried out after 1 min of normal mechanical ventilation.

2.6. Statistical analysis

All values are expressed as mean \pm SE. Values of vascular resistance R_v were compared with values at the beginning/end of the process by means of paired t-tests. Two-way ANOVA was used to compare changes in flow (V_{TM} vs. V_{PV}) under constant-pressure perfusion, being decellularization time and pulmonary venous ligation the two analyzed factors. One-way ANOVA was used to assess changes in lung elastances induced by the different perfusion procedures. Statistical significance was considered when $p < 0.05$.

3. Results

As expected from previous data (Girard et al., 2013), pressure- vs. flow-controlled decellularization procedures performed satisfactorily and did not result in apparent differences in terms of maintenance of scaffold structure and composition of main extracellular matrix components. Indeed, as compared with native lungs, organ scaffolds lacked cellular nuclei assessed by DAPI (Fig. 3) and genomic DNA content in the decellularized scaffold was 29.3 ± 7.0 ng/mg (below the 50 ng/mg suggested by Crapo et al., 2011) representing 7.5% of DNA content in the native lung (392.8 ng/mg). Moreover, Fig. 3 also shows that relevant components of the extracellular matrix such as elastin, laminin and collagen I, III and IV remained almost unchanged in decellularized lungs, and alveolar and vascular structure appeared well preserved. Data on lung elastance also suggested that the different decellularization processes employed did not induce major changes in the mechanical properties of the whole organ. As shown in Fig. 4, lung elastance values (E_{st} and E_{dyn}) measured in the acellular organs were very close for the constant-pressure and the constant-flow perfusion procedures, being these elastances slightly lower than the ones corresponding to the native lung.

Fig. 5 shows the time course of flow V_{PA} during lung decellularization at constant pressure perfusion (pulmonary vein open to the atmosphere). V_{PA} experienced a considerable reduction when deionized water was perfused and this flow reduction essentially persisted during perfusion of the SDS detergent solution. Final perfusion of PBS considerably increased flow, with a final V_{PA} similar to the one before decellularization. Consistently, the corresponding vascular resistance R_v (Fig. 5) experienced a sudden and considerable increase from 29.1 ± 3.0 cmH₂O/(ml/min) (previous perfusion of ionized water) to a maximum of 664.1 ± 164.3 cmH₂O/(ml/min)

($p < 0.05$), during perfusion of decellularizing media, returning at the end of the process to a value (47.8 ± 6.5 cmH₂O/(ml/min) close to the one prior decellularization ($p > 0.05$).

Decellularization by constant-flow media perfusion (Figs. 6 and 7) resulted in considerable increase in pulmonary artery pressure P_{PA} to values up to 42.4 ± 14.1 cmH₂O and 66.4 ± 2.2 cmH₂O for V_{PA} of 0.2 ml/min and 0.5 ml/min, respectively. However, after final PBS perfusion, P_{PA} resumed values close to the ones at the previous to the application of decellularizing media. As compared with observed for constant-pressure perfusion (Fig. 5), the maximum values of vascular resistance R_v (211.7 ± 70.5 cmH₂O/(ml/min) and 114.4 ± 13.9 cmH₂O/(ml/min) for V_{PA} of 0.2 ml/min and 0.5 ml/min, respectively) increased ($p < 0.05$ in both cases) from pre-decellularization values of 79.5 ± 5.1 cmH₂O/(ml/min) and 49.9 ± 3.3 cmH₂O/(ml/min) for V_{PA} of 0.2 ml/min and 0.5 ml/min, respectively. However, the increases in R_v by constant-flow perfusion were much lower than those achieved by constant-pressure perfusion (Fig. 5). Remarkably, the increase in R_v observed at $V_{PA} = 0.5$ ml/min was particularly low. At the end of constant-flow decellularization, R_v also reached values (57.5 ± 7.9 cmH₂O/(ml/min) and 39.5 ± 3.2 cmH₂O/(ml/min) for V_{PA} of 0.2 ml/min and 0.5 ml/min, respectively) similar to the initial ones ($p > 0.05$ in both cases).

Fig. 8 compares the flow V_{PA} measured throughout decellularization by constant-pressure perfusion ($P_{PA} = 20$ cmH₂O) when the pulmonary vein was open ($V_{PA} = V_{TM} + V_{PV}$) and when it was ligated ($V_{PV} = 0$). Whereas, as expected (Fig. 5), flow significantly varied with time throughout the decellularization process ($p < 0.05$), there was no significant difference whether the pulmonary vein was open or not ($p > 0.05$). Taking into account the circuit scheme in Fig. 1B, showing the distribution of V_{PA} into V_{TM} and V_{PA} , the similarity of flow measured under both conditions indicates that the pathway through the alveolar-capillary membrane was the main route of media transit during decellularization, particularly when deionized water and SDS detergent were infused.

4. Discussion

To the best of our knowledge this is the first study assessing relevant vascular fluid dynamics variables involved in lung decellularization. Measuring the pressure-flow relationship throughout the whole decellularization process under different pressure- and flow-controlled perfusion regimes allowed us to characterize an important process in lung bioengineering – obtaining an acellular scaffold – that is based on media circulation along the vascular-airway network of the organ. Specifically, three main findings were revealed by the study. First, effective vascular resistance showed considerable variations throughout the decellularization process, particularly for pressure-controlled perfusion. Second, flow-controlled perfusion markedly increased pressure inside the vascular system but, given inverse pressure-resistance dependence, vascular pressure was lower than expected from the vascular resistance values measured under pressure-controlled regime. Third, the decellularizing media infused to the pulmonary artery mainly circulated to the airways compartment through the alveolar-capillary membrane with a minor fraction leaving the lung vascular circuit through the pulmonary vein.

There is empirical evidence that lungs can be decellularized by means of different procedures consisting of a combination of general techniques applied for obtaining acellular scaffolds in

organs and tissues (Ott et al., 2010; Petersen et al., 2010; Price et al., 2010; Wallis et al., 2012; Booth et al., 2012; Nichols et al., 2013; Khalpey et al., 2014). Despite this evidence, systematic

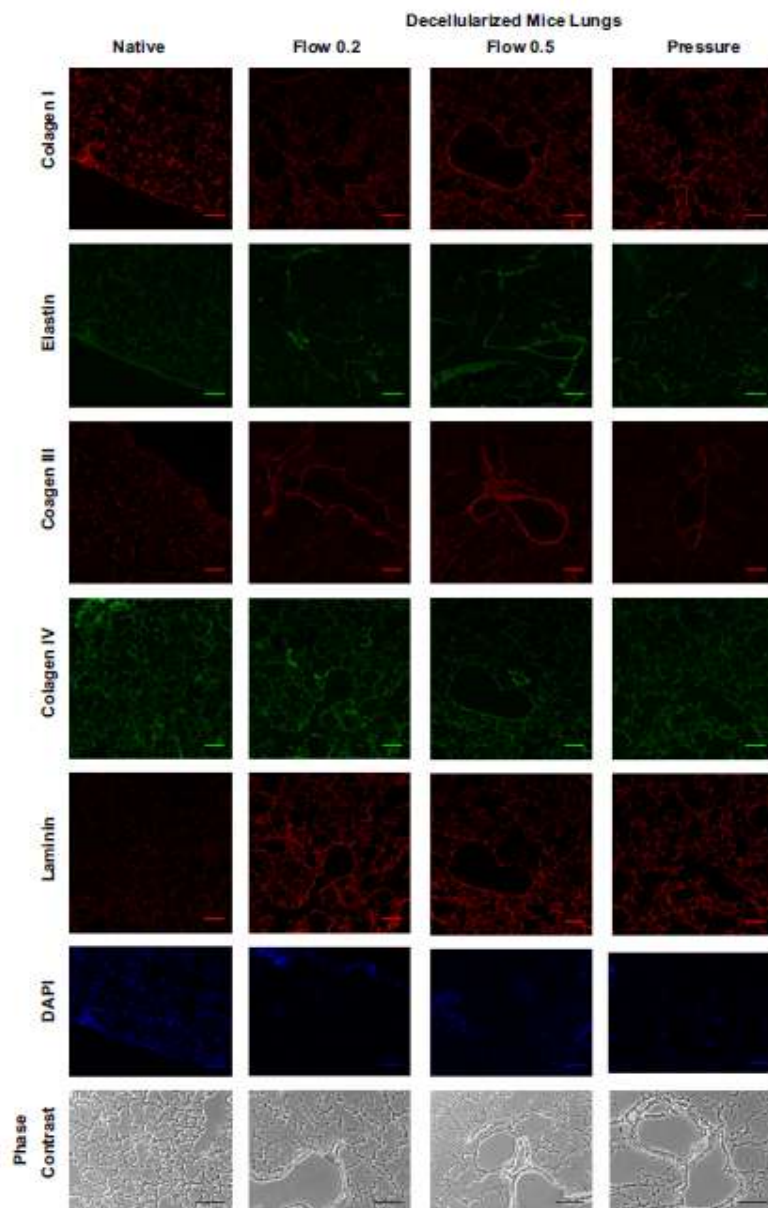


Fig. 3 – Representative image of DAPI staining in native and decellularized mice lungs. Blue dots (absent in the decellularized lung) correspond to cell nuclei. Diffuse blue staining in the acellular lung corresponds to autofluorescence of the extracellular matrix. Immunofluorescent images of native and decellularized by lung slices stained for different components of the extracellular matrix (Collagen I, III and IV, Laminin and Elastin) and phase contrast images. Pressure: decellularization by constant pressure perfusion (20 cmH₂O). Flow 0.2 and Flow 0.5: decellularization by constant flow perfusion (0.2 ml/min and 0.5 ml/min, respectively). Scale bar=100 μm. (For interpretation of the references to color in this figure legend, the reader is referred to the web version of this article.)

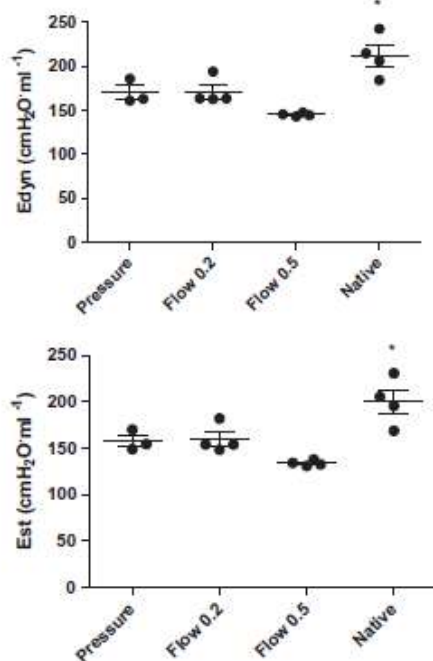


Fig. 4—Static (E_{st}) and dynamic (E_{dyn}) elastances of the whole lungs computed by means of end-inspiratory occlusions during conventional mechanical ventilation. Measurements were carried out in native and decellularized lungs by constant-pressure perfusion (Pressure) and by 0.2 ml/min and 0.5 ml/min constant-flow perfusion (Flow 0.2 and Flow 0.5, respectively). Asterisks indicate $p < 0.05$.

comparison of lung decellularization procedures has not been carried out and hence there is no conclusion of what is the optimal procedure. In fact, comparing the almost infinite combinations of physical, enzymatic and chemical agents to employ, including different possible concentrations of each agent in the media and duration of each step, is hardly feasible. Although this fact could be seen as a drawback, practical experiences have defined different procedures that actually work for obtaining mice (Bonenfant et al., 2013), rat (Melo et al., 2014; Gilpin et al., 2014b), porcine (Price et al., 2014), primate (Bonvillain et al., 2012, 2013) and human (Wagner et al., 2014a, 2014b; Gilpin et al., 2014a; Price et al., 2015) lung scaffolds of suitable quality. Regardless the definition of the specific sequence of decellularizing agents to be applied, which may differ among laboratories, a common issue is that these media are perfused through the organ. The idea is to achieve the widest possible distribution of media within the organ to reach each single cell for decellularization. In most organs (e.g., heart, kidney, lung) the only available route is the circulatory bed of the organ. The lung, however, has an additional possible route for decellularization since the media can be also infused through the trachea. In fact, both routes (trachea and pulmonary artery) alone or combined

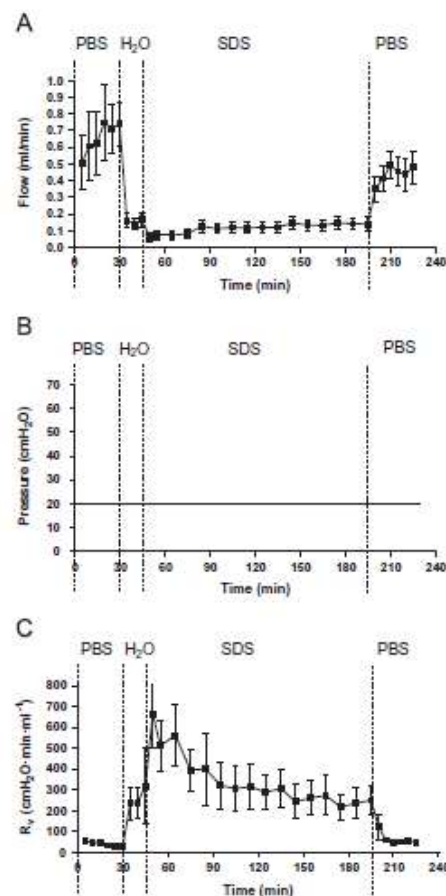


Fig. 5—Pressure (P_{PA}) and flow (V_{PA}) at the pulmonary artery throughout lung decellularization by constant pressure perfusion ($P_{PA} = 20$ cmH₂O), with pulmonary vein open to the atmosphere. Corresponding vascular resistance (R_v). Data are mean \pm SE. PBS (phosphate buffered saline), H₂O (deionized water) and SDS (sodium dodecyl sulfate detergent) indicate the times of perfusion with the different media.

have been used to effectively decellularize lungs (Gimrd et al., 2013; Nonaka et al., 2014a, 2014b; Uriarte et al., 2014; Melo et al., 2014; Wagner et al., 2014a, 2014b; Khalpey et al., 2014; Price et al., 2014). This study was focused on infusing decellularization agents through the vascular bed since is the most conventional route in lungs and the only available in other relevant organs. Perfusion through the pulmonary artery was performed using variable values common in the literature either by applying a reasonably low physiological pressure of 20 cmH₂O (≈ 15 mmHg) at the pulmonary artery (Price et al., 2010) or the corresponding flows under normal conditions (0.2–0.5 ml/min) (Tuchscherer et al., 2006).

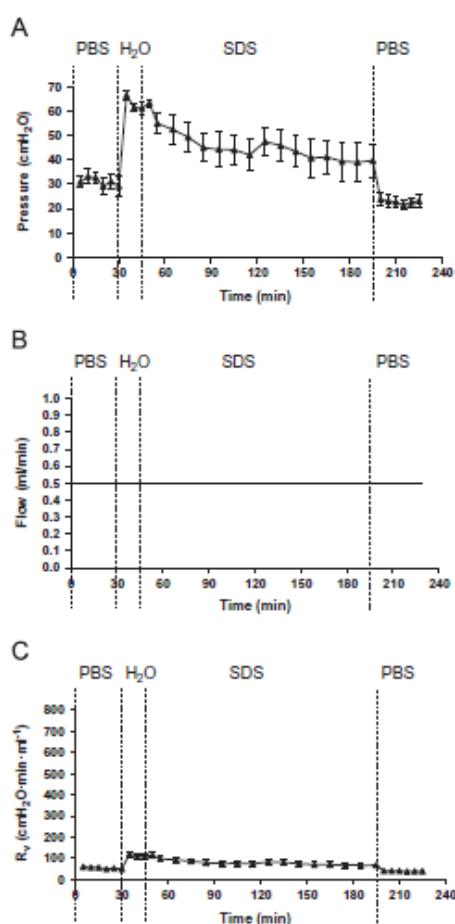


Fig. 6 – Pressure (P_{PA}) and flow (V_{PA}) at the pulmonary artery throughout lung decellularization by constant flow perfusion ($V_{PA}=0.5$ ml/min), with pulmonary vein open to the atmosphere. Corresponding vascular resistance (R_v). Data are mean \pm SE. PBS (phosphate buffered saline), H₂O (deionized water) and SDS (sodium dodecyl sulfate detergent) indicate the times of perfusion with the different media.

Accumulation of cell debris caused by application of deionized water (breaking cell membrane by osmotic shock) caused a \sim 10-fold increase in vascular resistance. Indeed, as shown by Fig. 5, perfusion flow slightly increased throughout the first 30 min of PBS perfusion probably by the elimination of blood components remaining after lung excision. Immediately after application of deionized water, flow was considerably reduced and remained low with mild increase throughout detergent perfusion. Finally, when PBS was applied to washout the circuit, flow increased (and hence vascular resistance decreased) as a result of a reduction in effective viscosity after elimination of SDS (Starov and Zhdanov, 2003; Dhopatkar

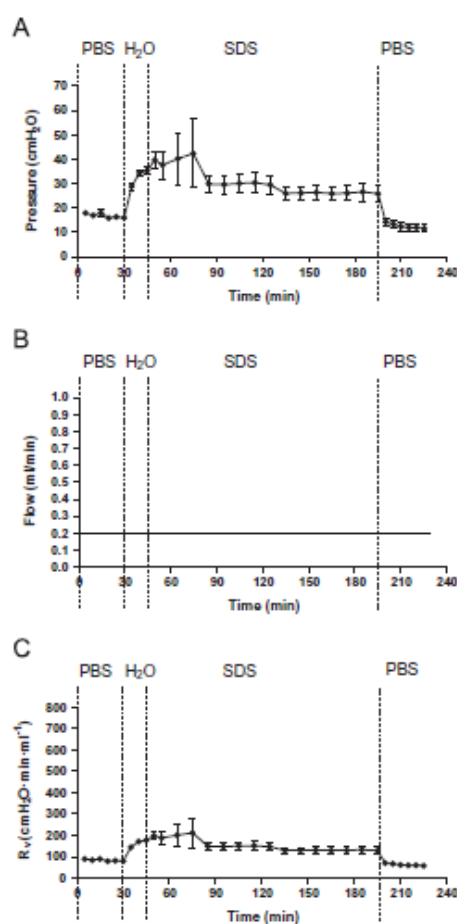


Fig. 7 – Pressure (P_{PA}) and flow (V_{PA}) at the pulmonary artery throughout lung decellularization by constant flow perfusion ($V_{PA}=0.2$ ml/min), with pulmonary vein open to the atmosphere. Corresponding vascular resistance (R_v). Data are mean \pm SE. PBS (phosphate buffered saline), H₂O (deionized water) and SDS (sodium dodecyl sulfate detergent) indicate the times of perfusion with the different media.

et al., 2015), recovering flow and vascular resistance values close to the ones measured prior to starting the decellularization process. It is interesting to note that, as reflected by Fig. 8, virtually all the perfused flow circulates through the alveolar-capillary membrane and only a residual flow is expected to leave the vascular circuit through the pulmonary vein. This fact explains why decellularization by perfusion through the organ vasculature works. Indeed, in case that most media circulated within the vascular circuit, the decellularizing agents would not be able to reach the whole organ, thereby not allowing decellularization of the organ parenchyma and the airway walls.

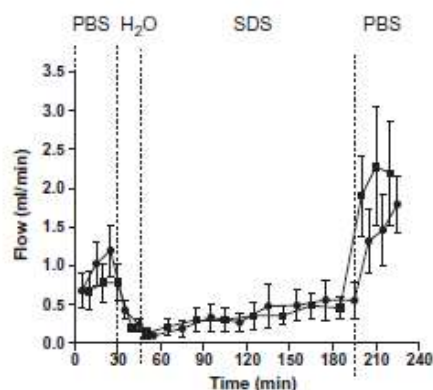


Fig. 8 – Flow through the pulmonary artery (V_{PA}) measured throughout lung decellularization by constant pressure perfusion ($P_{PA}=20$ cmH₂O), with pulmonary vein open to the atmosphere (■) and with ligated pulmonary vein (●). Data are mean \pm SE. PBS (phosphate buffered saline), H₂O (deionized water) and SDS (sodium dodecyl sulfate detergent) indicate the times of perfusion with the different media.

According to the value of effective vascular resistance found during application of deionized water under pressure-controlled regime (Fig. 5), a very high vascular pressure would be expected when maintaining a constant flow. For instance, for a perfusion flow of 0.5 ml/min, if vascular resistance was ≈ 600 cmH₂O/(ml/min) (peak resistance in Fig. 5), pressure during flow-control would reach ≈ 300 cmH₂O. Nevertheless, the peak of pressure (when deionized water was perfused) actually observed (Fig. 6) was much lower (60 cmH₂O), indicating that the effective flow resistance through the alveolar-capillary membrane decreased or that keeping a relatively high flow of 0.5 ml/min allowed to increase the washout of cells debris to an extent inducing vascular resistance decrease and keeping pressure relatively low. Consistently, perfusion with a constant flow of 0.2 ml/min (Fig. 7) induced a peak pressure of ≈ 40 cmH₂O. This negative relationship observed between vascular pressure and resistance – which is the reciprocal expected in a typical non-linear and rigid-wall flow circuit – explains why the lung scaffold is reasonably well preserved regardless of decellularizing the lung under pressure- or flow-controlled conditions (Petersen et al., 2010; Price et al., 2010; Girard et al., 2013).

Although this study was focused on lung decellularization, its main findings regarding the mechanical properties of the vascular circuit during decellularization by perfusion of media through the circulatory bed could be translated into other organs decellularization. In fact, both pressure- and flow-controlled vascular perfusion is employed for obtaining acellular scaffolds of kidney (Orlando et al., 2012; Song et al., 2013), liver (Uygun et al., 2010; Struecker et al., 2014a, 2014b) or heart (Ott et al., 2008; Wainwright et al., 2010; Weymann

et al., 2014) with physiological values of pressure and flow parameters, as done in the present study. The only difference between these organs and the lung is that the systemic capillary membrane is involved instead of the alveolar-capillary membrane. This, however, should not induce a substantial difference among the organs in the fluid dynamics of the perfusate, as reflected by the fact that both pressure- and flow-controlled membrane achieve suitable decellularization with scaffold preservation (Girard et al., 2013; Wagner et al., 2014a, 2014b; Guyette et al., 2014).

5. Conclusion

This study shows that monitoring the fluid dynamics of perfusion throughout decellularization – which is usually overlooked in tissue engineering – provides information that could be relevant for ensuring that the process is kept under a safety range of variables to preserve the organ scaffold. It seems reasonable that mechanical monitoring – actually very easily to perform – should be incorporated into the quality control procedures of automated (Price et al., 2015) and future commercial production lines of acellular lung scaffolds. Moreover, fluid mechanics monitoring can be useful to design optimized automatic procedures for achieving viable scaffolds with reduced process time and hence costing. Indeed, instead of applying a simply pressure- or flow-controlled procedure, as usually to date, it could be possible to design combined strategies for applying the most effective perfusion mode for each of the steps throughout media perfusion.

Acknowledgements

The authors wish to thank Ms. Maeba Polo and Mr. Miguel A. Rodríguez for their excellent technical assistance. This work was supported in part by the Spanish Ministry of Economy and Competitiveness (SAF2011-22576, FIS-PII 1/00089) and the Brazilian Ministry of Education (CAPES, 11514-13-2).

REFERENCES

- Badyrak, S.F., Weiss, D.J., Caplan, A., Macchiarelli, P., 2012. Engineered whole organs and complex tissues. *Lancet* 379 (9819), 943–952.
- Booth, A.J., Hadley, R., Comett, A.M., Dreffs, A.A., Matthes, S.A., Tsui, J.L., Weiss, K., Horowitz, J.C., Fiore, V.F., Barker, T.H., Moore, B.B., Martinez, F.J., Niklason, L.E., Whit, E.S., 2012. Acellular normal and fibrotic human lung matrices as a culture system for in vitro investigation. *Am. J. Respir. Crit. Care Med.* 186 (9), 866–876.
- Bonenfant, N.R., Sokocevic, D., Wagner, D.E., Borg, Z.D., Lathrop, M.J., Lam, Y.W., Deng, B., Desarno, M.J., Ashikaga, T., Loi, R., Weiss, D.J., 2013. The effects of storage and sterilization on decellularized and recellularized whole lung. *Biomaterials* 34 (13), 3231–3245.
- Bonvillian, R.W., Danchuk, S., Sullivan, D.E., Betancourt, A.M., Semon, J.A., Eagle, M.E., Masyuk, J.P., Gregory, A.N., Wang, G., Townley, I.K., Borg, Z.D., Weiss, D.J., Sunell, B.A., 2012. A nonhuman primate model of lung regeneration: detergent-mediated decellularization and initial in vitro recellularization

- with mesenchymal stem cells. *Tissue Eng. Part A* 18 (23–24), 2437–2452.
- Bonvillain, R.W., Scarritt, M.E., Pashos, N.C., Mayeux, J.P., Meshberger, C.L., Betancourt, A.M., Sullivan, D.E., Bunnell, B.A., 2013. Nonhuman primate lung decellularization and recellularization using a specialized large-organ bioreactor. *J. Vis. Exp.* 15 (82), e50825.
- Cortiella, J., Niles, J., Cantu, A., Bretter, A., Pham, A., Vargas, G., Winston, S., Wang, J., Walls, S., Nichols, J.E., 2010. Influence of acellular natural lung matrix on murine embryonic stem cell differentiation and tissue formation. *Tissue Eng. Part A* 16 (8), 2565–2580.
- Crapo, P.M., Gilbert, T.W., Badyal, S.F., 2011. An overview of tissue and whole organ decellularization processes. *Biomaterials* 32 (12), 3233–3243.
- Daly, A.B., Wallis, J.M., Borg, Z.D., Bonvillain, R.W., Deng, B., Ballif, B.A., Jaworski, D.M., Allen, G.B., Weiss, D.J., 2012. Initial binding and recellularization of decellularized mouse lung scaffolds with bone marrow-derived mesenchymal stromal cells. *Tissue Eng. Part A* 18 (1–2), 1–16.
- Dhopatkar, N., Park, J.H., Chari, K., Dhinojwala, A., 2015. Adsorption and viscoelastic analysis of polyelectrolyte-surfactant complexes on charged hydrophilic surfaces. *Langmuir* 31, 1026–1037.
- Farre, R., Granell, S., Rotger, M., Serrano-Mollar, A., Closa, D., Navajas, D., 2005. Animal model of unilateral ventilator-induced lung injury. *Intensive Care Med.* 31, 487–490.
- Garcia, O., Carraro, G., Navarro, S., Bertonecchio, I., McQuilter, J., Driscoll, B., Jeudason, E., Warburton, D., 2012. Cell-based therapies for lung disease. *Br. Med. Bull.* 101, 147–161.
- Gilpin, S.E., Guyette, J.P., Gonzalez, G., Ren, X., Asara, J.M., Mathisen, D.J., Vacanti, J.P., Ott, H.C., 2014a. Perfusion decellularization of human and porcine lungs: bringing the matrix to clinical scale. *J. Heart Lung Transplant.* 33 (3), 298–308.
- Gilpin, S.E., Ren, X., Okamoto, T., Guyette, J.P., Mou, H., Rajagopal, J., Mathisen, D.J., Vacanti, J.P., Ott, H.C., 2014b. Enhanced lung epithelial specification of human induced pluripotent stem cells on decellularized lung matrix. In: Presented at the Fiftieth Annual Meeting of The Society of Thoracic Surgeons, Orlando, FL, Jan 25–29, 2014, 98(5), 1721–1729.
- Girard, E.D., Jensen, T.J., Vadasz, S.D., Blanchette, A.E., Zhang, F., Moncada, C., Weiss, D.J., Finck, C.M., 2013. Automated procedure for biomimetic de-cellularized lung scaffold supporting alveolar epithelial transdifferentiation. *2013 Biomaterials* 34 (38), 10043–10055.
- Guyette, J.P., Gilpin, S.E., Charest, J.M., Tapias, L.F., Ren, X., Ott, H.C., 2014. Perfusion decellularization of whole organs. *Nat. Protoc.* 9 (6), 1451–1458.
- Jensen, T., Rossell, B., Zang, F., Girard, E., Matson, A., Thrall, R., Jaworski, D.M., Hatton, C., Weiss, D.J., Finck, C., 2012. A rapid lung de-cellularization protocol supports embryonic stem cell differentiation in vitro and following implantation. *Tissue Eng. Part C: Methods* 18 (3), 632–646.
- Khalpey, Z., Qu, N., Hemphill, C., Louis, A.V., Ferng, A.S., Son, T.G., Stavoe, K., Penick, K., Tran, P.L., Konhilas, J., Lagrand, D.S., Garcia, J.G., 2014. Rapid porcine lung decellularization utilizing a novel organ regenerative control acquisition bioreactor. *ASAIO J.* 61 (1), 71–77.
- Melo, E., Garreta, E., Luque, T., Cortiella, J., Nichols, J., Navajas, D., Farré, R., 2014. Effects of the decellularization method on the local stiffness of acellular lungs. *Tissue Eng. Part C: Methods* 20 (5), 412–422.
- Nichols, J.E., Niles, J.A., Cortiella, J., 2012. Production and utilization of acellular lung scaffolds in tissue engineering. *J. Cell Biochem.* 113 (7).
- Nichols, J.E., Niles, J., Riddle, M., Vargas, G., Schilgard, T., Ma, L., Edward, K., Lafrancesca, S., Sakamoto, J., Vega, S., Ogedegbe, M., Micak, R., Deyo, D., Woodson, L., McQuitty, C., Lick, S., Beckles, D., Melo, E., Cortiella, J., 2013. Production and assessment of decellularized pig and human lung scaffolds. *Tissue Eng. Part A* 19 (17–18), 2045–2062.
- Nonaka, P.N., Campillo, C., Uriarte, J.J., Garreta, E., Melo, E., de Oliveira, L.V.F., Navajas, D., Farré, R., 2014a. Effects of freezing/thawing on the mechanical properties of decellularized lungs. *J. Biomed. Mater. Res. A* 102, 413–419.
- Nonaka, P.N., Uriarte, J.J., Campillo, N., Melo, E., Navajas, D., Farré, R., Oliveira, L.V., 2014b. Mechanical properties of mouse lungs along organ decellularization by sodium dodecyl sulfate. *Respir. Physiol. Neurobiol.* 15 (200), 1–5.
- Orlando, G., Famey, A.C., Iskandar, S.S., Mirmalek-Sani, S.H., Sullivan, D.C., Moran, E., AbouShwareb, T., De Goppi, P., Wood, K.J., Stratta, R.J., Atala, A., Yoo, J.J., Soker, S., 2012. Production and implantation of renal extracellular matrix scaffolds from: *256(2): 363–370.*
- Ott, H.C., Matthiesen, T.S., Goh, S.K., Black, L.D., Kren, S.M., Netoff, T.L., Taylor, D.A., 2008. Perfusion-decellularized matrix: using nature's platform to engineer a bioartificial heart. *Nat. Med.* 14 (2), 213–221.
- Ott, H.C., Clippinger, B., Conrad, C., Schuetz, C., Pomerantseva, I., Ikononou, L., Kotton, D., Vacanti, J.P., 2010. Regeneration and orthotopic transplantation of bioartificial lung. *Nat. Med.* 16 (8), 927–933.
- Petersen, T.H., Calle, E.A., Zhao, L., Lee, E.J., Gu, J., L. Raredon, M.B., Gavrilov, K., Yi, T., Zhuang, Z.W., Breuer, C., Herzog, E., Niklason, L.E., 2010. Tissue-engineered lungs for in vivo implantation. *30Science* 329 (5991), 538–541.
- Price, A.P., England, K.A., Matson, A.M., Blazar, B.R., Panoskaltis-Mortari, A., 2010. Development of a decellularized lung bioreactor system for bioengineering the lung: the matrix reloaded. *Tissue Eng. Part A* 16 (8), 2581–2591.
- Price, A.P., Godin, L.M., Domek, A., Cotter, T., D'Cunha, J., Taylor, D.A., Panoskaltis-Mortari, A., 2014. Automated decellularization of intact, human-sized lungs for tissue engineering. *Tissue Eng. Part C: Methods* 21, 94–103.
- Price, A.P., Godin, L.M., Domek, A., Cotter, T., D'Cunha, J., Taylor, D.A., Panoskaltis-Mortari, A., 2015. Automated decellularization of intact, human-sized lungs for tissue engineering. *Tissue Eng. Part C: Methods* 21 (1), 94–103.
- Song, J.J., Kim, S.S., Liu, Z., Madsen, J.C., Mathisen, D.J., Vacanti, J.P., Ott, H.C., 2011. Enhanced in vivo function of bioartificial lungs in rats. *Ann. Thorac. Surg.* 92 (3), 998–1005.
- Starov, V.M., Zhdanov, V.G., 2003. Viscosity of emulsions: influence of flocculation. *J. Colloid Interface Sci.* 15 (258), 404–414.
- Song, J.J., Guyette, J.P., Gilpin, S.E., Gonzalez, G., Vacanti, J.P., Ott, H.C., 2013. Regeneration and experimental orthotopic transplantation of a bioengineered kidney. *Nat. Med.* 19 (5), 646–651.
- Struecker, B., Butter, A., Hillebrandt, K., Polenz, D., Reutzel-Selke, A., Tang, P., Lippert, S., Leder, A., Rohn, S., Geisel, D., Denecke, T., Aliyev, K., Jöhrens, K., Raschzok, N., Neuhaus, P., Pratschke, J., Sauer, I.M., 2014a. Improved rat liver decellularization by arterial perfusion under oscillating pressure conditions. *J. Tissue Eng. Regen. Med.*
- Struecker, B., Hillebrandt, K.H., Voigt, R., Butter, A., Schmuck, R.B., Reutzel-Selke, A., Geisel, D., Joehrens, K., Pickerodt, P.A., Raschzok, N., Puhl, G., Neuhaus, P., Pratschke, J., Sauer, I.M., 2014b. Porcine liver decellularization under oscillating pressure conditions: a technical refinement to improve the homogeneity of the decellularization process. *Tissue Eng. Part C: Methods* Epub ahead of print.
- Tuchscherer, H.A., Webster, E.B., Chesler, N.C., 2006. Pulmonary vascular resistance and impedance in isolated mouse lungs: effects of pulmonary emboli. *Ann. Biomed. Eng.* 34 (4), 660–668.

- Uriarte, J.J., Nonaka, P.N., Campillo, N., Palma, R.K., Melo, E., de Oliveira, L.V., Navajas, D., Farré, R., 2014. Mechanical properties of acellular mouse lungs after sterilization by gamma irradiation. *J. Mech. Behav. Biomed. Mater.* 40, 168–177.
- Uygun, B.E., Soto-Gutierrez, A., Yagci, H., Izamis, M.L., Guzzardi, M.A., Shulman, C., Milwid, J., Kobayashi, N., Tilles, A., Berthiaume, E., Hertl, M., Nahmias, Y., Yarmush, M.L., Uygun, K., 2010. Organ reengineering through development of a transplantable recellularized liver graft using decellularized liver matrix. *Nat. Med.* 16 (7), 814–820.
- Wagner, D.E., Bonenfant, N.R., Sokocevic, D., DeSarno, M.J., Borg, Z.D., Parsons, C.S., Brooks, E.M., Platz, J.J., Khalpey, Z.I., Hognson, D.M., Deng, B., Lam, Y.W., Oldinski, R.A., Ashikaga, T., Weiss, D.J., 2014a. Three-dimensional scaffolds of acellular human and porcine lungs for high throughput studies of lung disease and regeneration. *Biomaterials* 35 (9), 2664–2679.
- Wagner, D.E., Bonenfant, N.R., Parsons, C.S., Sokocevic, D., Brooks, E.M., Borg, Z.D., Lathrop, M.J., Wallis, J.D., Daly, A.B., Lam, Y.W., Deng, B., DeSarno, M.J., Ashikaga, T., Loi, R., Weiss, D.J., 2014b. Comparative decellularization and recellularization of normal versus emphysematous human lungs. *Biomaterials* 35 (10), 3281–3297.
- Wainwright, J.M., Czajka, C.A., Patel, U.B., Freytes, D.O., Tobits, K., Gilbert, T.W., Badyak, S.F., 2010. Preparation of cardiac extracellular matrix from an intact porcine heart. *Tissue Eng. Part C: Methods* 16 (3), 525–532.
- Wallis, J.M., Borg, Z.D., Daly, A.B., Deng, B., Ballif, B.A., Allen, G.B., Jaworski, D.M., Weiss, D.J., 2012. Comparative assessment of detergent-based protocols for mouse lung decellularization and re-cellularization. *Tissue Eng. Part C: Methods* 18 (6), 420–432.
- Weiss, D.J., 2014. Concise review: current status of stem cells and regenerative medicine in lung biology and diseases. *Stem Cells* 32 (1), 16–25.
- Weymann, A., Patil, N.P., Sabashnikov, A., Jungebluth, P., Korkmaz, S., Li, S., Veres, G., Soos, P., Bhtok, R., Chaimow, N., Pätzold, I., Czerny, N., Schies, C., Schmack, B., Popov, A.E., Simon, A.R., Karck, M., Szabo, G., 2014. Bioartificial heart: a human-sized porcine model—the way ahead. *3PLoS One* 9 (11), e111591.
- Yusen, R.D., Shearon, T.H., Qian, Y., Kotloff, R., Barr, M.L., Sweet, S., Dyke, D.B., Murray, S., 2010. Lung transplantation in the United States, 1999–2008. *Official J. Am. Soc. Transplant. Am. Soc. Transplant Surg. Am. J. Transplant.* 10 (4 Pt 2), 1047–1068.

Estudo 2.

PLOS ONE

Behavior of vascular resistance undergoing various pressure insufflation and perfusion on decellularized lungs.

--Manuscript Draft--

Manuscript Number:	
Article Type:	Research Article
Full Title:	Behavior of vascular resistance undergoing various pressure insufflation and perfusion on decellularized lungs.
Short Title:	Various pressure insufflation and perfusion on decellularized lungs.
Corresponding Author:	Luis Vicente Franco Oliveira, PhD Nove de Julho University Sao Paulo, Sao Paulo BRAZIL.
Keywords:	Decellularized lung; Vascular resistance; Scaffolds.
Abstract:	<p>Introduction: Bioengineering of functional lung tissue by using whole lung scaffolds has been proposed as a potential alternative for patients awaiting lung transplant. Previous studies have demonstrated that vascular resistance could be altered to optimize the process of obtaining suitable lung scaffolds. Therefore, this work was aimed at determining how lung inflation (tracheal pressure) and perfusion (pulmonary arterial pressure) affect vascular resistance. Methods: This study was carried out using 5 decellularized lungs. The trachea was cannulated and connected to a continuous positive airway pressure (CPAP) device to provide a tracheal pressure ranging from 0 to 15 cmH₂O. The pulmonary artery was cannulated and connected to a controlled perfusion system with continuous pressure (gravimetric level) ranging from 5 to 30 cmH₂O. Effective vascular resistance (R_v) was calculated by ratio of pulmonary artery pressure (PPA) by pulmonary artery flow (V_{PA}). Results: Vascular resistance in the decellularized lungs scaffolds decreased at increasing V_{PA}, stabilizing at a pulmonary arterial pressure greater than 20 cmH₂O. On the other hand, CPAP had no influence on vascular resistance in the lungs scaffolds after being subjected to pulmonary artery pressure of 5 cmH₂O. Conclusion: Compared to positive airway pressure, arterial lung pressure markedly influences the mechanics of vascular resistance in decellularized lungs.</p>
Order of Authors:	Renata Kelly Palma Paula Naomi Nonaka Noelia Campillo Juan J. Uriarte Jessica Juliotti Urbano Daniel Navajas Ramon Farrè Luis Vicente Franco Oliveira, PhD
Opposed Reviewers:	
Additional Information:	
Question	Response
Financial Disclosure Please describe all sources of funding that have supported your work. A complete funding statement should do the following:	RKP and JJU receive grants of the Coordenação de Aperfeiçoamento de Pessoal de Nível Superior (CAPES/PROSUP) and, LVFO received a grant from the Conselho Nacional de Desenvolvimento Científico e Tecnológico (local acronym CNPq) (Research Productivity modality – PQID, process number 307618/2010-2).

<p>Include grant numbers and the URLs of any funder's website. Use the full name, not acronyms, of funding institutions, and use initials to identify authors who received the funding.</p> <p>Describe the role of any sponsors or funders in the study design, data collection and analysis, decision to publish, or preparation of the manuscript. If they had no role in any of the above, include this sentence at the end of your statement: <i>"The funders had no role in study design, data collection and analysis, decision to publish, or preparation of the manuscript."</i></p> <p>If the study was unfunded, provide a statement that clearly indicates this, for example: <i>"The author(s) received no specific funding for this work."</i></p> <p>* typeset</p>	
<p>Competing Interests</p> <p>You are responsible for recognizing and disclosing on behalf of all authors any competing interest that could be perceived to bias their work, acknowledging all financial support and any other relevant financial or non-financial competing interests.</p> <p>Do any authors of this manuscript have competing interests (as described in the PLOS Policy on Declaration and Evaluation of Competing Interests)?</p> <p>If yes, please provide details about any and all competing interests in the box below. Your response should begin with this statement: <i>I have read the journal's policy and the authors of this manuscript have the following competing interests:</i></p> <p>If no authors have any competing interests to declare, please enter this statement in the box: <i>"The authors have declared that no competing interests exist."</i></p> <p>* typeset</p>	<p>"The authors have declared that no competing interests exist."</p>

<p>Ethics Statement</p> <p>You must provide an ethics statement if your study involved human participants, specimens or tissue samples, or vertebrate animals, embryos or tissues. All information entered here should also be included in the Methods section of your manuscript. Please write "N/A" if your study does not require an ethics statement.</p> <p>Human Subject Research (involved human participants and/or tissue)</p> <p>All research involving human participants must have been approved by the authors' Institutional Review Board (IRB) or an equivalent committee, and all clinical investigation must have been conducted according to the principles expressed in the Declaration of Helsinki. Informed consent, written or oral, should also have been obtained from the participants. If no consent was given, the reason must be explained (e.g. the data were analyzed anonymously) and reported. The form of consent (written/oral), or reason for lack of consent, should be indicated in the Methods section of your manuscript.</p> <p>Please enter the name of the IRB or Ethics Committee that approved this study in the space below. Include the approval number and/or a statement indicating approval of this research.</p> <p>Animal Research (involved vertebrate animals, embryos or tissues)</p> <p>All animal work must have been conducted according to relevant national and international guidelines. If your study involved non-human primates, you must provide details regarding animal welfare and steps taken to ameliorate suffering; this is in accordance with the recommendations of the Weatherall report, "The use of non-human primates in research." The relevant guidelines followed and the committee that approved the study should be identified in the ethics statement.</p> <p>If anesthesia, euthanasia or any kind of</p>	<p>Experimental procedures approved by the Ethical Committee for Animal Research of the University of Barcelona.</p>
--	--

<p>animal sacrifice is part of the study, please include briefly in your statement which substances and/or methods were applied.</p> <p>Please enter the name of your Institutional Animal Care and Use Committee (IACUC) or other relevant ethics board, and indicate whether they approved this research or granted a formal waiver of ethical approval. Also include an approval number if one was obtained.</p> <p>Field Permit</p> <p>Please indicate the name of the institution or the relevant body that granted permission.</p>	
<p>Data Availability</p> <p>PLOS journals require authors to make all data underlying the findings described in their manuscript fully available, without restriction and from the time of publication, with only rare exceptions to address legal and ethical concerns (see the PLOS Data Policy and FAQ for further details). When submitting a manuscript, authors must provide a Data Availability Statement that describes where the data underlying their manuscript can be found.</p> <p>Your answers to the following constitute your statement about data availability and will be included with the article in the event of publication. Please note that simply stating 'data available on request from the author' is not acceptable. <i>If, however, your data are only available upon request from the author(s), you must answer "No" to the first question below, and explain your exceptional situation in the text box provided.</i></p> <p>Do the authors confirm that all data underlying the findings described in their manuscript are fully available without restriction?</p>	<p>Yes - all data are fully available without restriction</p>
<p>Please describe where your data may be found, writing in full sentences. Your answers should be entered into the box below and will be published in the form you provide them, if your manuscript is accepted. If you are copying our sample text below, please ensure you replace any instances of XXX with the appropriate details.</p>	<p>Data are available from the http://www.uninove.br/pesquisa and Institutional Data Access / Ethics Committee for researchers who meet the criteria for access to confidential data.</p>

<p>If your data are all contained within the paper and/or Supporting Information files, please state this in your answer below. For example, "All relevant data are within the paper and its Supporting Information files."</p> <p>If your data are held or will be held in a public repository, include URLs, accession numbers or DOIs. For example, "All XXX files are available from the XXX database (accession number(s) XXX, XXX)." If this information will only be available after acceptance, please indicate this by ticking the box below. If neither of these applies but you are able to provide details of access elsewhere, with or without limitations, please do so in the box below. For example:</p> <p>"Data are available from the XXX Institutional Data Access / Ethics Committee for researchers who meet the criteria for access to confidential data."</p> <p>"Data are from the XXX study whose authors may be contacted at XXX."</p> <p>* typeset</p>	
Additional data availability information:	

Cover Letter

Cover Letter

September 25, 2015

Editor-in-Chief

PLOS ONE

Dear,

We submit an original contribution studying biomechanical properties in a tissue engineering application. Specifically, we have for the first time assessed how vascular mechanics is modified during lung decellularization depending on whether perfusion of media through the pulmonary artery is carried out under pressure- or flow-controlled conditions. We found considerable differences in effective vascular resistance, suggesting that mechanical assessment -currently overlooked during organ decellularization- could be useful for optimizing the process of obtaining suitable organ scaffolds, and also as a quality control tool for future high-throughput production.

In our opinion, this novel approach could be of interest for the readership of the PLOS ONE, potentially becoming a well referenced work by authors in the fields of biomechanics and tissue engineering.

We hope that you find value in our work and consider it acceptable for publication in your Journal.

Sincerely,

Luis Vicente Franco Oliveira, PT, PhD



Ramon Farré, PhD



Behavior of vascular resistance undergoing various pressure insufflation and perfusion on decellularized lungs.

Renata Kelly da Palma^{a,b}, Paula Naomi Nonaka^{a,b}, Noelia Campillo^{a,c}, Juan J. Uriarte^{a,d}, Jessica Julioti Urbano^b, Daniel Navajas^{a,c,d}, Ramon Farré^{a,d,e}, Luis V.F.Oliveira^b

a) Unitat Biofísica i Bioenginyeria, Facultat de Medicina, Universitat de Barcelona, Barcelona, Spain

b) Master's and Doctoral Degree Programs in Rehabilitation Sciences, Nove de Julho University, Sao Paulo, Brazil.

c) Institut de Bioenginyeria de Catalunya, Barcelona, Spain.

d) CIBER Enfermedades Respiratorias, Madrid, Spain.

e) Institut Investigacions Biomediques August PiSunyer, Barcelona, Spain.

ABSTRACT

Introduction: Bioengineering of functional lung tissue by using whole lung scaffolds has been proposed as a potential alternative for patients awaiting lung transplant. Previous studies have demonstrated that vascular resistance could be altered to optimize the process of obtaining suitable lung scaffolds. Therefore, this work was aimed at determining how lung inflation (tracheal pressure) and perfusion (pulmonary arterial pressure) affect vascular resistance. **Methods:** This study was carried out using 5 decellularized lungs. The trachea was cannulated and connected to a continuous positive airway pressure (CPAP) device to provide a tracheal pressure ranging from 0 to 15 cmH₂O. The pulmonary artery was cannulated and connected to a controlled perfusion system with continuous pressure (gravimetric level) ranging from 5 to 30 cmH₂O. Effective vascular resistance (R_v) was calculated by ratio of pulmonary artery pressure (P_{PA}) by pulmonary artery flow (V_{PA}). **Results:** Vascular resistance in the decellularized lungs scaffolds decreased at increasing V_{PA} , stabilizing at a pulmonary arterial pressure greater than 20 cmH₂O. On the other hand, CPAP had no influence on vascular resistance in the lungs scaffolds after being subjected to pulmonary artery pressure of 5 cmH₂O. **Conclusion:** Compared to positive airway pressure, arterial lung pressure markedly influences the mechanics of vascular resistance in decellularized lungs.

Key words: Decellularized lung; Vascular resistance; Scaffolds.

INTRODUCTION

In 2012, more than 1300 patients were awaiting lung transplantation in the United States [1] owing to the limited supply of donor lungs. Since lung transplantation is often complicated by chronic rejection and adverse effects associated with immunosuppressive treatment [2, 3], novel alternatives are required. Recently, the engineering of bioartificial organs by using scaffolds with an aim to regenerate functional lung tissue has been proposed as a potential alternative for lung transplantation [4]. However, for the proper functioning of the bioartificial organs, it is imperative that these scaffolds preserve the lung's structure and composition to present an ideal macro- and micro-environment facilitating cell attachment and engraftment for effective repopulation [5].

Given that lung cells are exposed to different physical stimuli during breathing, the lung scaffold should be exposed to ventilation and perfusion stimuli mimicking the ones during normal breathing to provide a physiologically appropriate environment for seeding of stem cells in the decellularized lung. Previous studies from our group demonstrated that effective vascular resistance varies considerably during the process of decellularization. However, data on circulatory resistance of scaffolds as a function of airway and vascular pressures are unavailable. This information is of considerable interest since adequate distribution of cells during scaffold seeding and subsequent cell homing could be modulated by vascular resistance. Monitoring vascular resistance could also be a useful quality control tool for future high-throughput production [6]. Accordingly, this work aimed at determining the mechanism by which lung inflation (tracheal pressure) and perfusion (pulmonary artery) pressure affect vascular resistance.

METHODS

This study was carried out in strict accordance with the recommendations in the Guide for the Care and Use of Laboratory Animals of the National Institutes of Health by using the lungs excised from 5 healthy male Sprague-Dawley rats (250–300 g). The experimental procedures were approved by the Ethical Committee for Animal Research of the University of Barcelona. The rats were anesthetized with intraperitoneal urethane (1 mg/kg, heparin 250 U/kg) and sacrificed by exsanguination through the abdominal aorta. Immediately after euthanasia, the diaphragm was punctured and the rib cage was cut open to reveal the lungs. The lungs were perfused via the right ventricle with phosphate-buffered saline (PBS) containing 50 U/ml heparin (Sigma-Aldrich Co. LLC, St. Louis, MO, USA) and 1 µg/ml sodium nitroprusside – SNP (Fluka Analytical, Sigma-Aldrich Co. LLC, St. Louis, MO, USA) to prevent the formation of blood clots in the lungs. After perfusion was complete, the heart, lungs, and trachea were dissected and removed in bloc and stored in a –80°C freezer until the decellularization process was carried out.

Lung decellularization

The first step in lung decellularization involves thawing the lungs in a water bath at 37°C and freezing them again at –80°C; this cycle was repeated four times. Once the trachea and pulmonary artery were cannulated and placed into the experimental system, the trachea was connected to a continuous positive airway pressure (CPAP) device that was set to provide a tracheal (i.e., transpulmonary) pressure of 10 cmH₂O to inflate the lung close to total lung capacity in an attempt to avoid atelectasis [6]. The following sequence of decellularizing process, the lungs was perfused through the pulmonary

artery: 1) PBS 1× for 30 min, 2) deionized water for 15 min, 3) 1% sodium dodecyl sulfate (SDS) for 150 min, and 4) PBS for 30 min, at a pressure of 20 cmH₂O.

As described in a previous study [10], pulmonary decellularization was carried out by a combination of freezing/thawing methods, and SDS removed cellular debris while preserving the mechanical properties of the structure. No significant changes in the resistance values and elastance of the lungs were observed during conventional mechanical ventilation.

Vascular mechanics

To analyze vascular mechanics in the decellularized lungs, the cannulated trachea was connected to a CPAP device that was set to provide tracheal (i.e., transpulmonary) pressure ranging from 0 to 15 cmH₂O. The cannulated pulmonary artery was connected to a controlled perfusion system with continuous pressure (gravimetric level) ranging from 5 to 30 cmH₂O. A pressure transducer (011-OP229-01; ICU Medical, USA) and a differential pressure transducer (5100J0005H2Y5000; American Sensor Technologies, USA) allowed the measurement of pulmonary artery pressure (P_{PA}) and pulmonary artery flow (\dot{V}_{PA}), respectively, at the entrance of the pulmonary artery. These transducer signals were analogically low-pass filtered, sampled, and stored for subsequent analysis. Hence, continuous measurement of \dot{V}_{PA} and P_{PA} allowed for the assessment of effective vascular resistance (R_v) as $R_v = P_{PA}/\dot{V}_{PA}$.

Statistical analysis

All values are expressed as mean \pm SE. Values of vascular resistance (R_v) and flow (\dot{V}_{PA}) at each pulmonary arterial (5 to 30 cmH₂O) and tracheal pressure (0 to 15 cmH₂O) value were compared by means of paired t-tests.

RESULTS

As shown in Fig. 1, vascular resistance in the decellularized lungs decreased from $\sim 6.7 \text{ cmH}_2\text{O} \cdot \text{min} \cdot \text{ml}^{-1}$ to $\sim 3 \text{ cmH}_2\text{O} \cdot \text{min} \cdot \text{ml}^{-1}$ in response to an increase in pulmonary arterial pressure from 5 to 20 cmH_2O , remaining steady at up to 30 cmH_2O at the entrance of the pulmonary arterial system. Values of vascular resistance did not depend on CPAP.

Fig. 1. Pressure (P_{PA}) and flow (V_{PA}) at the pulmonary artery in the decellularized lung undergone diverse values of pressure perfusion and continuous positive airway pressure. Corresponding vascular resistance (R_v). Data are mean \pm SE.

DISCUSSION

To the best of our knowledge, this is the first study reporting vascular resistance values in decellularized lungs as a function of variations in pulmonary artery and airway pressures. It is known that lack of surfactant in decellularized lungs may cause the alveolar walls to collapse; therefore, in a previous study, we used a CPAP of 10 cmH_2O to keep the lungs inflated during the decellularization process [6]. However, the influence of CPAP on vascular resistance in acellular lungs was not known. In this study, vascular resistance in the acellular lung was found to be almost constant at CPAP ranging from 0 to 15 cmH_2O , provided pulmonary arterial pressure $> 15 \text{ cmH}_2\text{O}$.

Several studies have demonstrated successful transplantation after re-building of the lungs with stem cells; however, the lungs were capable of maintaining gas exchange for a maximum of 7 days [7-9]. It seems clear, however, that the differentiation and maturation of cells in the reseeded graft need to be improved. Therefore, it could be

expected that variations in arterial and alveolar pressures could influence cell adhesion, considering that a reduced flow through the lung circuit would decrease cell distribution. Hence, according to this study, we can suggest that the optimal value of flow and vascular resistance for optimal dynamics is achieved at physiological values of pulmonary arterial pressure (15-30 cmH₂O).

The decellularization process eliminates lung cells, i.e., type II alveolar epithelial cells, which secrete lung surfactant, thereby increasing the lung compliance as described previously [6, 10]. Owing to low lung elastance, this decellularized lung can no longer increase the tension in the alveolar walls to alter vascular resistance, thereby explaining the slight influence of CPAP on vascular resistance.

In conclusion, we demonstrated that compared to positive airway pressure, arterial lung pressure markedly influences the mechanics of vascular resistance in decellularized lungs. This study provides information that could be relevant for future stem cell repopulation by using vascular resistance as a facilitator of cell distribution throughout the pulmonary circuit.

ACKNOWLEDGMENTS

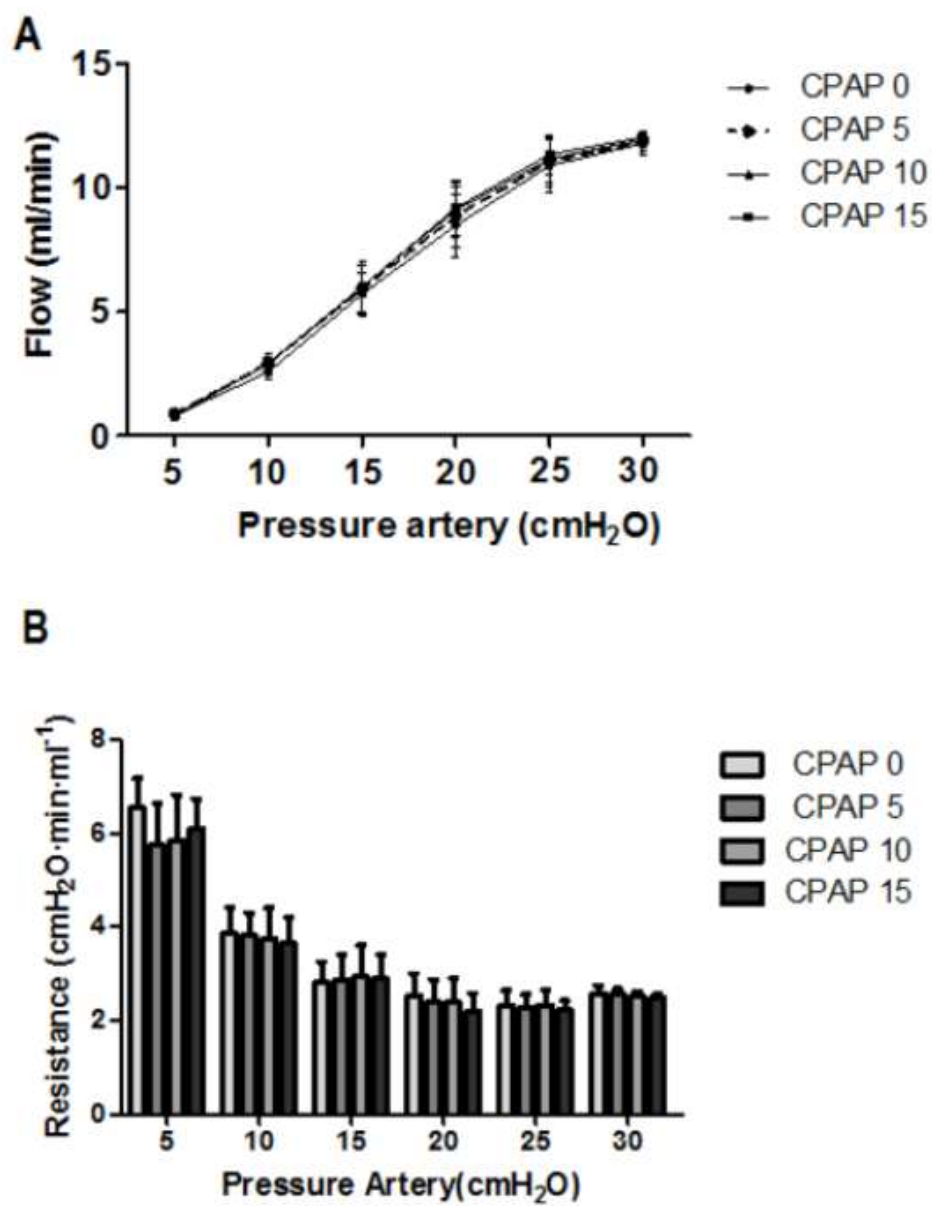
RKP and JJU receive grants of the Coordenação de Aperfeiçoamento de Pessoal de Nível Superior (CAPES/PROSUP) and, LVFO received a grant from the Conselho Nacional de Desenvolvimento Científico e Tecnológico (local acronym CNPq) (Research Productivity modality – PQID, process number 307618/2010-2).

REFERENCES

1. Organ Procurement and Transplantation Network (OPTN). <http://optn.transplant.hrsa.gov> (accessed Online 05 may 2014).
2. Lopez AD, Shibuya K, Rao C, Mathers CD, Hansell AL, Held LS, et al. Chronic obstructive pulmonary disease: current burden and future projections. *Eur Respir J* 2006;27:397-412.
3. Barberà JA, Riverola A, Roca J, Ramirez J, Wagner PD, Ros D, et al. Pulmonary vascular abnormalities and ventilation-perfusion relationships in mild chronic obstructive pulmonary disease. *Am J Respir Crit Care Med* 1994;149:423-429.
4. Daly AB, Wallis JM, Borg ZD, Bonvillain RW, Deng B, Ballif BA, et al. Initial binding and recellularization of decellularized mouse lung scaffolds with bone marrow-derived mesenchymal stromal cells. *Tissue Eng Part A*. 2012 Jan;18(1-2):1-16.
5. Badyaluk SF, Weiss DJ, Caplan A, Macchiarini P. Engineered whole organs and complex tissues. *Lancet* 2012;379:943-52.
6. da Palma RK, Campillo N, Uriarte JJ, Oliveira LV, Navajas D, Farré R. Pressure- and flow-controlled media perfusion differently modify vascular mechanics in lung decellularization. *J Mech Behav Biomed Mater*. 2015 Sep;49:69-79.
7. Petersen TH, Calle EA, Zhao L, Lee EJ, Gui L, Raredon MB, et al. Tissue-engineered lungs for in vivo implantation. *Science*. 2010 Jul 30;329(5991):538-41
8. Ott HC, Clippinger B, Conrad C, Schuetz C, Pomerantseva I, Ikonomou L, et al. Regeneration and orthotopic transplantation of a bioartificial lung. *Nat Med*. 2010 Aug;16(8):927-33
9. Song JJ, Kim SS, Liu Z, Madsen JC, Mathisen DJ, Vacanti JP, et al. Enhanced in vivo function of bioartificial lungs in rats. *Ann Thorac Surg*. 2011 Sep;92(3):998-1005
10. Nonaka PN, Uriarte JJ, Campillo N, Melo E, Navajas D, Farré R, et al. Mechanical properties of mouse lungs along organ decellularization by sodium dodecyl sulfate. *Respir Physiol Neurobiol*. 2014 Aug 15;200:1-5

SUPPORTING INFORMATION

Figure
[Click here to download Figure: Fig1.tif](#)



8. ANEXOS

Comitê de Ética- CEUA- UNINOVE



Comissão de Ética no Uso de Animais- CEUA – UNINOVE
Av. Francisco Matarazzo, 612 – Prédio C – Térreo
ceua@uninove.br

Protocolo de Pesquisa referente ao Projeto nº 0038-2011

Título do Projeto: "Resistência e complacência de pulmões descelularizados durante o processo de recelularização com células tronco"

Orientador: Luis Vicente Franco de Oliveira

Aluno:

Objetivos: Investigar o comportamento das propriedades mecânicas elásticas, viscosas e viscoelásticas de pulmões descelularizados e durante o processo de recelularização com células-tronco.

Os objetivos do trabalho estão claros e contemplam a legislação.

Método: Para a realização do protocolo, inicialmente os animais serão sedados com Diazepam intraperitoneal. Após a sedação, os ratos serão pesados em balança de precisão e posteriormente anestesiados com tiopental sódico e assim, submetidos a eutanásia. O tórax será aberto e a parede torácica removida, os pulmões dos animais serão retirados sendo submetidos ao processo descelularização/recelularização, posteriormente, de quantificação de DNA, quantificação dos componentes da matriz extracelular, microscopia eletrônica de varredura, microscopia multifocal de duplo fóton, avaliação da diferenciação das células tronco por isolamento de RNA, transcrição reversa, PCR e análise por PCR em tempo real, imunofluorescência, análise de citometria de fluxo e análise por Western blot.

Os pulmões serão submetidos a um biorreator para aplicar estímulos físicos realistas sobre os mesmos durante a bioengenharia com células tronco. Os parâmetros mecânicos serão coletados através do método de oclusão ao final da inspiração.

Metodologia de acordo com os procedimentos legais.

Grupo de 03 animais para controle.

Animais (procedência, raça, linhagem, número de animais, peso, sexo): Serão utilizados oito ratos machos da raça Wistar, com peso de 250-300 g, provenientes do biotério de criação da UNINOVE.

Condições de alojamento e nutrição: Os animais serão acondicionados e mantidos em ambiente limpo e seco, com luminosidade natural, respeitando o ciclo claro/escuro de 12h, temperatura e umidade

relativa do ar adequadas. A ração e a água permanecerão *ad libitum* e monitoramento diário para troca de palha e água.

Descrição clara e de acordo com os procedimentos legais

Medidas para evitar estresse e/ou dor nos animais: Não Há.

Procedimento Anestésico e/ou Analgésico (Incluir dose e vias de administração): Anestesiados com tiopental sódico. 5mg, 20mg/Kg de peso corporal. I.p.

Eutanásia: Eutanásia por meio de exanguinação, alternativa ao protocolo padrão da UNINOVE, a câmara de CO₂, de modo a não haver interferência na integridade da estrutura pulmonar e assim, no processo de descelularização e recelularização.

Procedimento dentro do permitido pela legislação

Pertinência e valor científico do estudo proposto: O estudo de propriedades mecânicas dos pulmões seria um importante determinante da função pulmonar e sua medida é fundamental para o estudo dos mecanismos respiratórios. Com isso, este estudo visa investigar o comportamento das propriedades mecânicas elásticas, viscosas e viscoelásticas de pulmões descelularizados por diferentes técnicas de descelularização e durante o processo de recelularização com células-tronco.

O autor descreve claramente a pertinência e valor científico de seu projeto.

Apresentado a este Comitê para análise ética, foi considerado:

Aprovado, sendo que este projeto deverá permanecer arquivado por 05 (cinco) anos nesta Secretaria.

Com pendência (relacionar), devendo o Pesquisador encaminhar as modificações sugeridas, e iniciar a coleta de dados somente após a aprovação do projeto por este Comitê.

Não-Aprovado

São Paulo, 07 de dezembro de 2011



Prof. Dra. Maria Antonietta Leitão Zajac
Presidente da Comissão de Ética no Uso de Animais da
Universidade Nove de Julho

Publicações durante o doutorado

Artigos publicados 1ª autoria:



Short communication

Increased upper airway collapsibility in a mouse model of Marfan syndrome



Renata Kelly da Palma^{a,b}, Ramon Farré^{a,c}, Josep Maria Montserrat^{c,d},
Darya Gorbenko Del Blanco^e, Gustavo Egea^e, Luís Vicente Franco de Oliveira^b,
Daniel Navajas^{a,f}, Isaac Almendros^{a,c,g}

^a Unitat Biofísica i Bioenginyeria, Facultat de Medicina, Universitat de Barcelona - IDIBAPS, Barcelona, Spain^b Master's and Doctoral Degree Programs in Rehabilitation Sciences, Nove de Julho University, São Paulo, Brazil^c CIBER Enfermedades Respiratorias, Buzos, Spain^d Laboratori de la Son, Pneumologia, Hospital Clínic-Facultat de Medicina, Universitat de Barcelona, Barcelona, Spain^e Departament de Biologia Cel·lular, Immunologia i Neurociències, Facultat de Medicina, IDIBAPS - Universitat de Barcelona, Barcelona, Spain^f Institute for Bioengineering of Catalonia, Spain

ARTICLE INFO

Article history:

Accepted 16 December 2014

Available online 23 December 2014

Keywords:

Marfan syndrome
Obstructive sleep apnea
Upper airway collapsibility

ABSTRACT

Marfan syndrome (MFS) is a genetic disorder caused by mutations in the *FBN1* gene that codifies for fibrillin-1. MFS affects elastic fiber formation and the resulting connective tissue shows abnormal tissue laxity and organization. Although an increased prevalence of obstructive sleep apnea among patients with MFS has been described, the potential effects of this genetic disease on the collapsible properties of the upper airway are unknown. The aim of this study was to assess the collapsible properties of the upper airway in a mouse model of MFS *Fbn1*^{C1096G/+} that is representative of most of the clinical manifestations observed in human patients. The upper airway in wild-type and Marfan mice was cannulated and its critical pressure (P_{crit}) was measured *in vivo* by increasing the negative pressure through a controlled pressure source. P_{crit} values from MFS mice were higher (less negative) compared to wild-type mice (-3.1 ± 0.9 cmH₂O vs. -7.8 ± 2.0 cm H₂O) suggesting that MFS increases the upper airway collapsibility, which could in turn explain the higher prevalence of OSA in MFS patients.

© 2014 Elsevier B.V. All rights reserved.

1. Introduction

The Marfan syndrome (MFS) is an autosomal dominant disorder of the connective tissue affecting approximately 1 in 5000 people. Cardiovascular disease (mainly progressive aortic-root dilatation and dissection) is the leading cause of death by MFS, but the disease also causes long bone overgrowth, dislocation of the ocular lens, musculoskeletal and pulmonary dysfunctions (Cañadas et al., 2010). These abnormalities are caused by mutations localized within the *FBN1* gene that encodes fibrillin-1, a component of extracellular microfibrils and therefore of elastic fibers.

OSA is a prevalent disorder characterized by repetitive events of collapse and reopening of the upper airway during sleep. The higher

collapsibility observed in OSA is usually attributed to obesity and other alterations in structural or functional properties of the upper airway (Dempsey et al., 2010). Several studies have documented a higher prevalence of OSA among patients with MFS (Cistulli et al., 2001; Kohler et al., 2009) which has been associated to abnormalities in maxillary morphology and craniofacial structure (Cistulli et al., 2001). Interestingly, there is a study showing that all the MFS patients investigated exhibited increased upper airway collapsibility respect to weight-matched controls. The authors suggested that this abnormally high collapsibility could be caused by MFS-induced changes in the connective tissue (Cistulli and Sullivan, 1995).

Here we use a mouse model of MFS, free of other confounding factors, to investigate whether the potential structural changes in the upper airway associated to MFS could increase its collapsibility explaining in part the higher prevalence of OSA in MFS patients. Accordingly, this murine MFS model could allow interpreting the high occurrence of OSA in MFS patients, being also a useful model of spontaneous collapsibility for studying upper airway mechanics.

* Corresponding author at: Unitat de Biofísica i Bioenginyeria, Facultat de Medicina, Universitat de Barcelona, Casanova 143, 08036 Barcelona, Spain.
Tel.: +34 93 402 4515; fax: +34 93 403 5278.

E-mail address: isaac.almendros@ub.edu (I. Almendros).

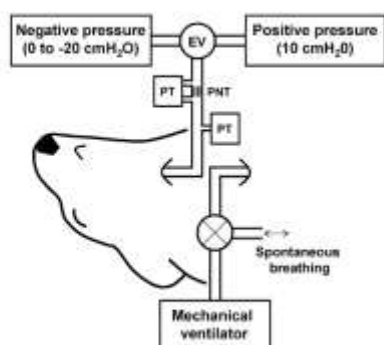


Fig. 1. Schematic diagram of the experimental setup employed. Upper airway collapse and P_{crit} was determined by increasing the negative pressure exerted by the vacuum pump until the cessation of the airflow in the upper airway. PNT: pneumotachograph; PT: pressure transducer; EV: electrovalve.

2. Methods

This study, approved by the Ethical Committee for Animal Research of the University of Barcelona, was carried out on 6 C57BL/6 wild-type (4 females and 2 males) (WT) and 9 mutant $Fbn1^{C1039G/+}$ (MFS) mice (6 females and 3 males), all of them nine month old. The mutant MFS mice harbor a mutation in the *Fbn1* gene where a cysteine is substituted by a tyrosine ($Fbn1^{C1039T/+}$), and mutant mice show representative manifestations of MFS in humans. Before the experiments, all subjects were genotyped by polymerase chain reaction (PCR) assay of genomic DNA.

The experimental setting employed, illustrated in Fig. 1, was able to apply a progressive pressure reduction in the upper airway to induce its collapse, simulating airway closure caused by progressive negative intraluminal inspiratory pressure in patients with OSA. It was adapted from a previously described setup used in rats (Almendros et al., 2008). Briefly, the animals were anesthetized with 10% urethane and subjected to a double intubation at the tracheal level. One cannula was inserted toward the lungs allowing spontaneous breathing. A second cannula was inserted toward the upper airway and was connected to one port of a three-way solenoid electrovalve (L377B03G; Sirai). The other two ports were connected to an adjustable negative pressure source (from 0 to $-20\text{ cmH}_2\text{O}$) and to a constant $10\text{ cmH}_2\text{O}$ positive-pressure source. The pressure exerted at the upper airway cannula was continuously measured by a pressure transducer located in the cannula (176PC14HD2, $\pm 35\text{ cmH}_2\text{O}$). The upper airway airflow was assessed by placing a pneumotachograph (range $\pm 20\text{ ml/s}$) and measuring the change of pressure with a differential pressure transducer (DCX101DS, range $\pm 2.5\text{ cmH}_2\text{O}$). Flow and pressure signals from the transducers were analogically low-pass filtered (Butterworth, 8 poles, 32 Hz), and sampled at a rate of 100 Hz (PCI-6036, National Instruments) by a custom monitoring and recording application (LabView). The valves were controlled electronically to apply either positive or negative pressures to the upper airway.

The upper airway cannula was flushed with air for 3 s prior to each measurement. The upper airway pressure was lowered in a ramp like fashion from $10\text{ cmH}_2\text{O}$ to $-20\text{ cmH}_2\text{O}$. P_{crit} was considered as the pressure at which the upper airway airflow reached zero representing complete collapse. Values of P_{crit} were determined as the mean of 5 individual measurements from each mouse. At the end of P_{crit} measurements in spontaneous breathing conditions, the mouse was paralyzed with an intravenous injection of 1 mg/kg

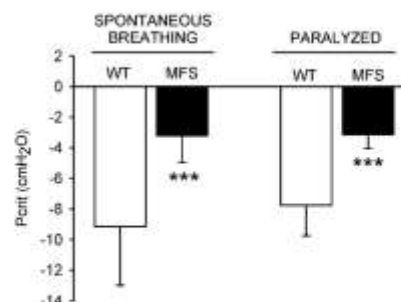


Fig. 2. Critical pressure (P_{crit}) values in wild-type (WT) and Marfan syndrome (MFS) mice under spontaneous breathing and paralyzed conditions. MFS increased the collapsibility of the upper airway as determined by the higher P_{crit} in both conditions. Values are represented as mean \pm SD. *** $p < 0.001$, WT vs. MFS.

pancuronium bromide and was maintained under mechanical ventilation (tidal volume of 0.20 mL at a frequency of 100 breaths/min) (Farre et al., 2005). Just prior to passive P_{crit} measurements, the mechanical ventilator was stopped. The setting employed was able to assess the P_{crit} values in both conditions (spontaneous breathing and paralysis) avoiding any variability related to independent intubations and instrumentalization.

All values are represented as mean \pm SD. A two-way repeated ANOVA was used to test the effects of MFS on P_{crit} values from spontaneously breathing vs. paralyzed mice. To compare the weight of mice, a two-way ANOVA was performed to assess differences between sex and experimental group (WT and MFS). Multiple comparisons between groups were performed by the Student–Newman–Keuls method. Correlation between weight and P_{crit} values was assessed by Pearson's test.

3. Results

The animals' weight was higher ($p = 0.004$) in males for both groups: $29.5 \pm 2.1\text{ g}$ in WT and $27.3 \pm 2.5\text{ g}$ in MFS, compared to females (24.8 ± 2.1 and 22.7 ± 2.4 , respectively). Prior to experiments, both genders were equally and randomly distributed between WT and MFS groups resulting in no difference in the weight between both groups (26.3 ± 3.0 and 24.2 ± 3.3 , respectively, $p = 0.232$).

Values of P_{crit} were not correlated to weight ($p = 0.292$), but differences were found between MFS and WT ($p < 0.001$). In particular, the P_{crit} was higher (less negative values) in MFS ($-3.2 \pm 1.7\text{ cmH}_2\text{O}$) with regard to the WT ($-9.2 \pm 3.8\text{ cmH}_2\text{O}$, $p < 0.001$) in spontaneously breathing mice (Fig. 2). Similar results were obtained between MFS ($-3.1 \pm 0.9\text{ cmH}_2\text{O}$) and WT ($-7.8 \pm 2.0\text{ cmH}_2\text{O}$, $p < 0.001$) in paralyzed mice (Fig. 2). No differences were observed between spontaneous breathing and paralyzed experiments ($p = 0.201$).

4. Discussion

In the present study we used a murine MFS model to investigate the potential changes of upper airway collapsibility in this disease. The murine heterozygous *Fbn1* allele ($Fbn1^{C1039G/+}$) mutant was used because it reproduces in time and shape most of the clinical characteristics occurring in MFS patients (Habashi et al., 2006). The $Fbn1^{C1039G/+}$ mutant is a well-established MFS mouse model with impaired microfibrillar formation, progressive deterioration of aortic wall architecture and skeletal deformity. Laxity and hypermobility joints are associated to this model due to a connective

tissue disorder. Other MFS mouse models, such as homozygous mice presenting a centrally deleted Fbn1 allele (Fbn1^{mgΔ} and Fbn1^{mgR}), were discarded since mice die precociously due to aortic dissection and rupture.

P_{crit} was measured from two different and well-established methods: under spontaneous breathing and paralyzed conditions. P_{crit} values were determined first under anesthesia with spontaneous breathing and immediately later in paralyzed conditions. The mean of P_{crit} from both methods showed similar values as previously reported by others, confirming that active contraction plays a minor role in P_{crit} (Polotsky et al., 2011). Other factors which could modulate the upper airway patency are weight and age (Polotsky et al., 2011). It is well known that the increase of pharyngeal load in obese mice augments the susceptibility to collapsibility of the upper airway (Polotsky et al., 2011). The mutant MFS mice presented equivalent weight with respect to WT mice of the same age (nine months old), and no correlation between weight and P_{crit} values was observed. Therefore, the changes observed in P_{crit} between WT and MFS are mainly attributable to the presence or absence of MFS. In the general population, weight gain is considered a main risk factor of OSA (Dempsey et al., 2010). The results from this work shows that P_{crit} in MFS is reduced independently of weight gain, which could be translated in a higher risk of collapsibility of the upper airway in MFS patients with substantially relatively low body mass index.

This increase in collapsibility can explain the higher prevalence of sleep-disordered breathing described in patients with MFS with regard to the general population (Cistulli and Sullivan, 1995; Kohler et al., 2009). The prevalence of OSA in MFS patients has important clinical implications since OSA can worsen the cardiovascular problems inherent to MFS. In fact, Kohler et al. (2009) showed a strong relationship between the apnea–hypopnea index (AHI) and the aortic root diameter in MFS patients with OSA. Therefore, bearing in mind that aortic dilatation is the main cause of death in MFS patients, OSA could be determinant in the life expectancy of these patients (Kohler et al., 2013). These patient studies also suggested that the apneas and hypopneas associated to MFS were obstructive in nature increasing the collapsibility of the upper airway through osseous and/or connective tissue abnormalities (Kohler et al., 2009). In fact, it has been demonstrated that nasal intermittent positive airway pressure attenuates the progressive dilatation of the aortic root MFS patients suffering OSA (Verbraecken et al., 2003). Although the morphological changes induced in the upper airway associated to MFS need to be studied in more detail, the MFS mouse model used in our study could be of great interest to further research the potential effects of intermittent hypoxia and/or sleep fragmentation in the adverse outcomes associated to MFS. Also, this model provides a translational option to study the consequences of

MFS, without the coexistence of other comorbidities or variables such as weight. Interestingly, P_{crit} could be further increased in the Marfan mice by inducing high-fat diet obesity (Polotsky et al., 2011), providing a model with enhanced spontaneous upper airway collapsibility.

In conclusion, the present work shows new evidence that MFS can increase upper airway collapsibility, suggesting that MFS could produce structural abnormalities in the upper airway being more susceptible to obstructive apneas. Therefore, MFS per se could increase the risk of OSA explaining the higher prevalence observed in patients.

Acknowledgements

This work was supported by Beatriz de Pinós fellowship from the Generalitat de Catalunya (2010 BP.A2 00023) (I.A.); the Spanish Ministry of Economy and Competitiveness (SAF2011-22576) (R.F.), (FIS-P11/00089) (J.M.M.); CAPES (11514-13-2) (R.K.P.) and (BFU2012-33932; National Marfan Foundation (NMF) and Fundación Ramón Areces to G.E.). The authors have no financial conflicts of interest.

References

- Almendra, I., Carreras, A., Ramirez, J., Montserrat, J.M., Navajas, D., Farré, R., 2008. Upper airway collapse and reopening induce inflammation in a sleep apnea model. *Eur. Respir. J.* 32, 399–404.
- Cañadas, V., Villacosta, I., Bruna, E., Fuster, V., 2010. Marfan syndrome. Part I: Pathophysiology and diagnosis. *Nat. Rev. Cardiol.* 7, 256–265.
- Cistulli, P.A., Sullivan, C.E., 1995. Sleep apnea in Marfan syndrome: increased upper airway collapsibility during sleep. *Chest* 108, 631–635.
- Cistulli, P.A., Gotsopoulos, H., Sullivan, C.E., 2001. Relationship between craniofacial abnormalities and sleep-disordered breathing in Marfan syndrome. *Chest* 120, 1455–1460.
- Dempsey, J.A., Veasey, S.C., Morgan, B.J., O'Donnell, C.P., 2010. Pathophysiology of sleep apnea. *Physiol. Rev.* 90, 47–112.
- Farre, R., Granell, S., Rogger, M., Serrano-Mollar, A., Ciosa, D., Navajas, D., 2005. Animal model of unilateral ventilator-induced lung injury. *Intensive Care Med.* 31, 487–490.
- Habashi, J.P., Judge, D.P., Holm, T.M., Cohn, R.D., Loeys, B.L., Cooper, T.K., Myers, L., Klein, E.C., Liu, G., Cai, C., Podowski, M., Neptune, E.R., Halushka, M.K., Bedja, D., Gabrielson, K., Rifkin, D.B., Carta, L., Ramirez, F., Huso, D.L., Dietz, H.C., 2006. Losartan, an AT1 antagonist, prevents aortic aneurysm in a mouse model of Marfan syndrome. *Science* 312, 117–121.
- Kohler, M., Blair, E., Risby, P., Nickol, A.H., Wordsworth, P., Forfar, C., Stradling, J.R., 2009. The prevalence of obstructive sleep apnoea and its association with aortic dilatation in Marfan syndrome. *Thorax* 64, 162–166.
- Kohler, M., Pitcher, A., Blair, E., Risby, P., Senn, O., Forfar, C., Wordsworth, P., Stradling, J.R., 2013. The impact of obstructive sleep apnoea on aortic disease in Marfan syndrome. *Respiration* 86, 39–44.
- Polotsky, M., Elsayed-Ahmed, A.S., Pichard, L., Richardson, R.A., Smith, P.L., Schneider, H., Kirkness, J.P., Polotsky, V., Schwartz, A.R., 2011. Effect of age and weight on upper airway function in a mouse model. *J. Appl. Physiol.* 111, 699–703.
- Verbraecken, J., Paclincx, B.P., Willems, M., Van de Heyning, P., De Backer, W., 2003. Aortic root diameter and nasal intermittent positive airway pressure treatment in Marfan syndrome. *Clin. Genet.* 63, 131–134.

Received: 2013.10.21
Accepted: 2013.11.21
Published: 2013.12.09

Respiratory mechanics study in experimental animal model of venom-induced acute lung injury: A new proposal for an old technique

Authors' Contribution:

- A** Study Design
- B** Data Collection
- C** Statistical Analysis
- D** Data Interpretation
- E** Manuscript Preparation
- F** Literature Search
- G** Funds Collection

Renata Kelly da Palma^{ABCD}, Paula Naomi Nonaka^{ABC}, Nadua Apostólico^{CD},
Nina Teixeira Fonsêca^{BCD}, Jéssica Julioti Urbano^{BCD},
Ezequiel Fernandes Oliveira^{BCD}, Ismael Sousa Dias^{BCD}, Sérgio Roberto Nacif^{BCD},
Rodolfo de Paula Vieira^{BCD}, Luis Vicente F. Oliveira^{BCDEFG}

Experimental Cardiorespiratory Physiology Laboratory, Rehabilitation Sciences Master's and PhD Degree Program, Nove de Julho University, São Paulo, SP, Brazil

Source of support: This work was supported in part by the Conselho Nacional de Desenvolvimento Científico e Tecnológico (Research Productivity modality 307618/2010-2). Paula Naomi Nonaka has a fellowship (2012/04052-2) from Fundação de Amparo à Pesquisa do Estado de São Paulo

Summary

Background:

Accidents involving poisoning can progress to severe clinical conditions with serious repercussions to the respiratory system, which can be measured from the end-inspiratory occlusions after constant flow inflations. Our objective was to demonstrate how the end-inspiratory occlusions after constant flow inflation technique can be used as a new experimental protocol for an animal model submitted to different crude venoms and and/or venom components in the assessment of the behavior of ventilatory mechanics.

Material/Methods:

The animals are inoculated with the toxin, anesthetized, and a tracheostomy is performed, the tracheal cannula is then connected to a pneumotachograph and to a mechanical ventilator which allows the control of tidal volume, air flow and positive end-expiratory pressure (PEEP). Five-second post-inspiration pauses are performed in accordance with the occlusion method. This experimental model allows the study of the mechanical behavior of the respiratory system in cases of poisoning by different animals.

Results:

A previous study seeking to verify the pulmonary mechanics and viscoelastic pressures showed that Est, Edyt, and DeltaP2 increased at 1 h in both venom groups, being significantly higher in V1 than in V0.3, and decreasing progressively, reaching control values at 48 h in V0.3, but remaining altered in V1 at 72 h. DeltaP1 augmented in V1 at 1 h, returning to normal at 72 h.

Conclusions:

Based on previous studies, animal venoms in crude form generate significant lung injury with significant changes in compliance and elastance of the respiratory system and/or isolated lung. However, little is known about the effects of isolated components of these venoms, which should be addressed in future studies.

key words:

respiratory mechanics • venom • toxins • experimental animal model

Full-text PDF:

<http://www.ceml-online.com/download/index/idArt/889928>

Word count:

2290

Tables:

-

Figures:

4

References:

28

Author's address:

Luis Vicente F. Oliveira, Researcher and professor at Rehabilitation Sciences Master's and PhD Degree Program at Universidade Nove de Julho - (UNINOVE), Rua Vergueiro 235, Liberdade, CEP 01504-001 São Paulo, SP, Brazil, e-mail: oliveira.lv@uninove.br

BACKGROUND

The mechanical properties of lung tissue provide important information about pathophysiology since it was realized that lung elastic recoil plays a crucial role in breathing [1].

The study of mechanical properties of lung tissue started from the simple principle evaluation the single-compartment model (Figure 1) proposed by Otis in 1956, which does not consider the slow pressure drop observed after occlusion of the airway at the end of inspiration, the fact that elastance and resistance are frequency-dependent, and hysteresis [2].

Bates et al. [3] proposed the viscoelastic two-compartment model (Figure 2), based on studies from Mount [4]. The mechanical properties of the tissues, however, are now represented by 3 elements: a resistor (R_1 , known as a *dashpot*) and 2 springs. The 3 elements – R_1 , E_1 , and E_2 – together constitute what is known as a *Kelvin body*. The stiffness of the spring E_1 represents the static elastic behavior of the lung, and the series combination of R_1 and E_2 (which together constitute a *Maxwell body*) account for its viscoelastic behavior [5].

If a matrix force deforms the system and bars from the equilibrium elastic point move away to a certain speed, the points of attachment of R_1 damper and springs E_1 and E_2 moves with the same velocity (V). Each point corresponds to a pressure: flow-resistive, elastic, and viscoelastic. The sum of all these pressures corresponds to the total pressure of distension of the system [3].

When the air flow is abruptly interrupted by rapid airway occlusion of the inspiratory valve of the mechanical ventilator and this occlusion is maintained for a long period of time (5 s), the bars of the model remain at the same distance, because inflated volume is stored in lungs. The damper R_1 completes its work at time $t=T_1$ and pressure related to it drops to zero. Spring E_1 is blocked between the bars and continues to exert its elastic force in the opposite direction to its deformation ($Est.V(t)$). The spring E_2 stop at the equilibrium length and the damper R_2 continues to move until $t_2=5$ is reached. After opening the airway, the model returns to its equilibrium point [3].

Therefore, pulmonary mechanics measured from end-inspiratory occlusion has been used since 1956 [6] on both humans [7] and experimental animals [8]. The significance of the measured variables, however, has been only clarified

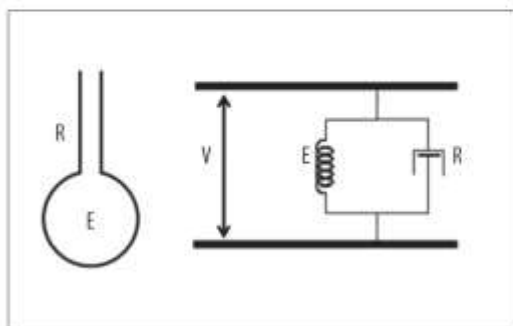


Figure 1. Anatomical and mechanical representation of the single – compartment linear model of the lung.

in a theoretical analysis by Bates et al. [3] through a viscoelastic 2-compartment model.

The elastic, resistive, and viscoelastic pressures are mechanical properties of the respiratory system that play a central role in the diagnosis of pulmonary response to different situations such as asthma [9], chronic obstructive pulmonary disease [10], acute respiratory distress syndrome, and acute lung injury [8]. Alterations in respiratory system components lead to altered lung mechanics, characterized by histological abnormalities, edema, hemorrhaging, inflammation, and increased deposition of matrix extra-cellular proteins [8].

The literature describes the impact on structures of the respiratory system caused by acute or chronic inflammation due to different toxins found in poisonous animals. Among other dysfunctions, an increase in pulmonary vascular permeability is known to induce pulmonary edema, which causes changes in pulmonary compliance and elasticity [11]. Experimental studies involving poisonous animals and addressing the properties of respiratory mechanics have been carried out to gain a better understanding of the physiopathology of the acute and/or chronic inflammatory process, including respiratory distress syndrome induced by different types of toxins, as well as possible treatment strategies [12–17].

Accidents involving poisoning from animal toxins have become increasingly common. Such intoxication can progress to severe clinical conditions with serious repercussions to the respiratory system in humans, as reported in the international scientific literature [18].

According to Cardoso et al. [19], the clinical manifestations of systemic poisoning by snakes include respiratory problems characterized by shortness-of-breath, followed by a mixture of restrictive and obstructive breathing patterns caused by paralysis of the thoracic intercostal muscles and the build-up of secretions in the bronchial tree, progressing to paralysis of the diaphragm. One study reported atelectasis, as well as diffuse hyperemia of the alveolar septa and pulmonary vasculature in general; the histological analysis revealed eosinophil infiltrate and hemorrhage in the respiratory system of domestic animals bitten by the Australian tiger snake [20].

Poisoning caused by scorpions leads to extensive pulmonary edema, which is a serious and often fatal clinical finding, especially in children and the elderly. Andrade et al. [21] found that toxins from the venom of the scorpion *Tityus*

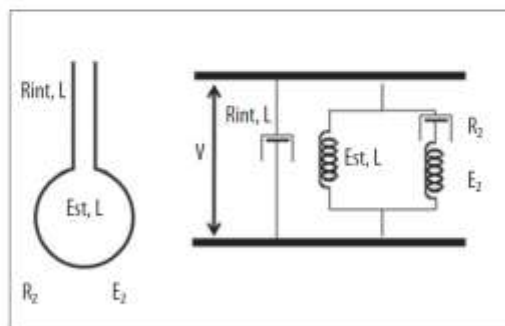


Figure 2. Anatomical and mechanical representation of the viscoelastic model of the lung with two degrees of freedom.

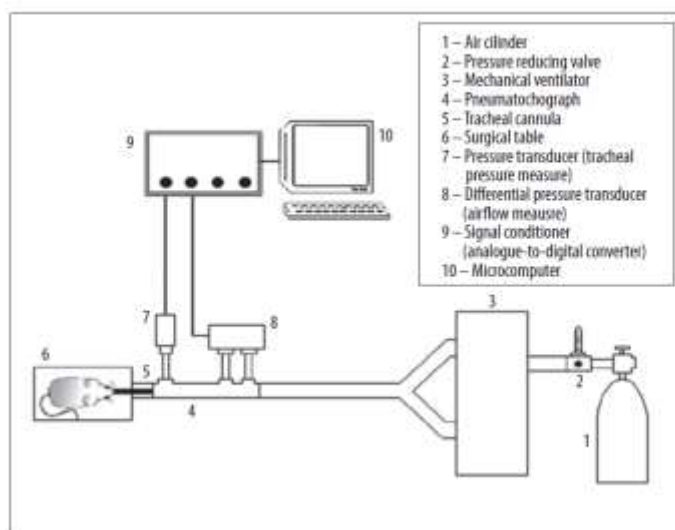


Figure 3. Set up of respiratory mechanics study.

serrulatus inoculated in rats on mechanical ventilation induced a reduction in pulmonary compliance. In another study, the histological analysis of tissue from the pulmonary lobes of animals poisoned by the scorpion *Tityus fasciolatus* revealed congested alveolar capillaries and multifocal petechial hemorrhage, characterized by erythrocytes in the interstitial and intra-alveolar spaces [18].

In an epidemiological study, Bucarechi et al. [22] found that intoxication caused by bites from spiders of the genus *Phoneutria* also resulted in acute pulmonary edema, resulting in the death of one of the severe cases of accidents with humans.

The present study describes how the end-inspiratory occlusions after constant flow inflations technique can be used as a new experimental protocol for an animal model submitted to different crude venoms and and/or venom components to the assessment of the behavior of ventilatory mechanics.

MATERIAL AND METHODS

Experimental protocol

Small animals, such as mice or rats, can be used in this experimental model. First, the mean lethal dose (LD50) of toxin is previously determined by injection of 5 different doses in 5 groups of animals, and recording the death during a 72 h period, considering the pathway [23].

Then the animals are sedated and anesthetized, and inoculated with the dose of the toxin to be studied through a predetermined inoculation pathway, depending on the study protocol. After a previously established poisoning timeframe, the animals are again sedated and anesthetized and properly placed on the surgical table where a tracheostomy and/or orotracheal intubation is performed. For a tracheostomy procedure, a small longitudinal incision is made in the anterior region of the neck. The adjacent tissues are spread until the trachea is exposed. A longitudinal incision is made between the 2 fibrous rings to introduce a cannula of length and diameter appropriate for the specific animal (e.g. 0.5 mm ID for mice and 2.1 mm ID for rats), firmly tied in place.

The tracheal cannula is then connected to a pneumotachograph [24], which is connected to a mechanical ventilator (Samay MVR17, Montevideo, Uruguay or Harvard Apparatus, model 683, South Natick, MA). A pressure transducer is used for measuring tracheal pressure (P_{tr}) (P23 Db, Statham-Gould, Oxnard, CA) and a differential pressure transducer (PT5A, Grass, Quincy, MA) is used for measuring the flow of the airways (\dot{V}). These are coupled to the pneumotachograph, as illustrated in Figure 3.

The signal transducers are connected to a signal conditioner (EMG System do Brasil) with 8 channels of analogical input, 1000 \times amplification, sampled at 250 Hz with a 12-bit analogue-to-digital converter used in the signal processing with the aid of a microcomputer and data acquisition software Windaq/Pro (DATAQ Instruments, Akron, OH).

The flow of the mechanical ventilator is generated by a source of compressed air connected to the ventilator using a pressure-reducing valve. The flow resistance produced by the system (R_{eq}), including the tracheal cannula, must be taken into consideration. The resistance pressure of the equipment will be subtracted from the pulmonary resistive pressures so that the intrinsic values are real [24].

After the tracheostomy, the muscle relaxation will be achieved with curare and the tracheal cannula is connected to the pneumotachograph and ventilator, controlling the tidal volume (TV), air flow (\dot{V}) and positive end-expiratory pressure (PEEP).

After stabilization of the ventilatory parameters, 5-s post-inspiration pauses are performed at the end of inspiration in accordance with the occlusion method [25] for the measurement of the mechanical properties of the respiratory system.

Analysis of curves

In a respiratory system in which the thoracic wall is intact, tracheal pressure (P_{tr}) represents the pressure dissipated by the system and esophageal pressure (P_{es}) represents the pressure generated by the thoracic wall. The pressure

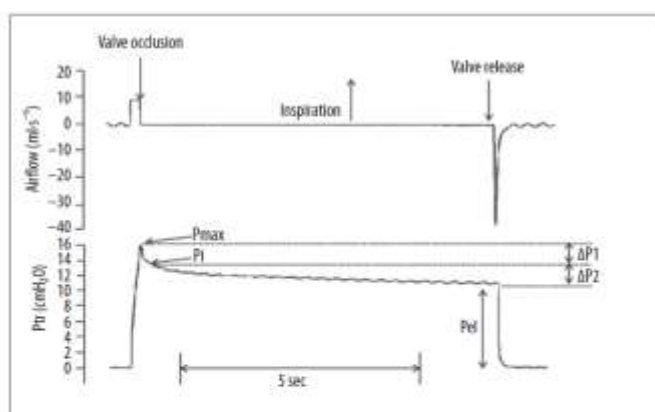


Figure 4. Airflow and tracheal pressure curves in relation to time.

generated by the lungs is obtained by subtracting P_{es} from P_{tr} . When measurements are performed with the thorax open (thoracic wall removed), P_{tr} represents the pressure of the pulmonary parenchyma.

After the occlusion of the airways at the end of inspiration (Figure 4), there is a sudden drop in P_{tr} , beginning with a maximum value (P_{max}) to an inflexion point (P_i), from which the drop in pressure becomes slower, reaching a plateau. This plateau phase corresponds to the elastic retraction pressure of the lungs (P_{el}). The difference in pressure (ΔP_1) that characterizes the initial rapid drop (represented by the difference between P_{max} and P_i) corresponds to the viscous component. The second variation in pressure (ΔP_2), represented by the slow drop, which runs from P_i to the plateau (P_{el}), reflects the pressure dissipated to overcome the viscoelastic component. The sum of ΔP_1 and ΔP_2 is the total variation in lung pressure (ΔP_{tot}). Static elastance (E_{st}) and dynamic elastance (E_{dyn}) are determined by dividing P_{el} and P_i , respectively, by the tidal volume, with ΔE equaling the difference between E_{dyn} and E_{st} .

For the determination of P_i , a nonlinear exponential fall in the 2 curves is used, determining the rapid drop and slow drop. From this, the pressure value in the time from ΔP_1 to ΔP_2 is determined.

RESULTS

This experimental model allows the study of the mechanical behavior of the respiratory system, after end-inspiratory occlusion, in cases of poisoning by different animals. This model allows a better understanding of the physiopathologic repercussions of different toxins in the respiratory system, leading to faster and more efficient clinical interventions.

A previous study investigated the pulmonary mechanics [static (E_{st}) and dynamic (E_{dyn}) elastances, resistive (ΔP_1) and viscoelastic pressures (ΔP_2)], histology, and bronchoalveolar lavage fluid (BALF) from BALB/c mice at 1, 24, 48, and 72 h after intravenous injection of saline or Bothrops jararaca crude venom [0.3 (V0.3) or 1 (V1) $\mu\text{g}\cdot\text{g}^{-1}$]. E_{st} , E_{dyn} , and ΔP_2 increased at 1 h in both V groups, being significantly higher in V1 than in V0.3, decreasing progressively, reaching control values at 48 h in V0.3, but remaining altered in V1 at 72 h. ΔP_1 augmented in V1

at 1 h, returning to normal at 72 h. Histological changes in the V0.3 group included interstitial edema, alveolar collapse, and increased cellularity, which returned to normal at 48 h. These changes were more intense in the V1 group, with alveolar edema and hemorrhage. BALF showed time-dependent neutrophil influx in V0.3 [26].

Another study investigated the effects of *Crotalus durissus terrificus* venom (CdV) on the pulmonary mechanic events [static and dynamic elastance, resistive (ΔP_1) and viscoelastic pressures (ΔP_2)] and histology after intramuscular injection of saline solution (control) or venom (0.6 $\text{mg}\cdot\text{g}^{-1}$). The static and dynamic elastance values were increased significantly after 3 h of venom inoculation, but were reduced to control values in the other periods studied. The ΔP_1 values that correspond to the resistive properties of lung tissue presented a significant increase after 6 h of CdV injection, reducing to basal levels 12 h after venom injection. In ΔP_2 analysis, corresponding to viscoelastic components, an increase occurred 12 h after venom injection, returning to control values at 24 h. CdV also caused an increase of leukocyte recruitment (3–24 h) to the airways wall and to the lung parenchyma. [27].

A recent study evaluated the effects of an intramuscular injection of *Tityus serrulatus* venom (TsV) (0.67 $\text{mg}\cdot\text{g}^{-1}$) on lung mechanics and lung inflammation at 15, 30, 60 and 180 min after inoculation. TsV inoculation resulted in increased lung elastance when compared with the control group ($p < 0.001$); these values were significantly higher at 60 min than at 15 and 180 min ($p < 0.05$). Resistive pressure (ΔP_1) values decreased significantly at 30, 60, and 180 min after TsV injection ($p < 0.001$). TsV inoculation resulted in increased lung inflammation, characterized by an increased density of mononuclear cells at 15, 30, 60 and 180 min after TsV injection when compared with the control group ($p < 0.001$). TsV inoculation also resulted in an increased pulmonary density of polymorphonuclear cells at 15, 30, and 60 min following injection when compared to the control group ($p < 0.001$) [28].

DISCUSSION

Preliminary studies have investigated the effect of animal venoms in crude form on respiratory mechanics after end-inspiratory occlusion and reported acute injury. Silveira

et al. [26] found that intravenous administration of crude venom from *Bothrops jararaca* led to an increase in the elastances and viscoelastic properties of the lung tissue 1 h after induction, with values returning to normal after 48–72 h. Histological analysis revealed interstitial edema, alveolar collapse, and increased cell migration.

A study involving the intramuscular inoculation of the crude venom from the snake *Crotalus durissus terrificus* reported similar results regarding respiratory mechanics, with a significant increase in elastance after 3 h. Viscous and viscoelastic properties also exhibited changes 12–24 h after inoculation. Histological analysis revealed leukocyte migration in the airway walls and pulmonary parenchyma [27].

A study investigating the effects of venom from the scorpion *Tityus serrulatus* on respiratory mechanics [28] also reports acute lung injury, with alterations in the mechanical properties and a considerable increase in both mono- and polymorphonuclear cells 60 min after intramuscular inoculation of the crude venom.

CONCLUSIONS

Based on previous studies, we observed that the viscoelastic 2-compartment model with end-inspiratory occlusion proposed Bates et al. can be used as a new experimental protocol for an animal model submitted to different crude venoms and/or low molecular weight fraction-generated lung injury with significant changes in compliance and elastance of the respiratory system and/or isolated lung. However, little is known about the effects of isolated peptides of these venoms, which should be addressed in future studies.

Conflicts of interest

The authors declare no conflicts of interest.

REFERENCES:

- Suki B, Bates JHT: Lung tissue mechanics as an emergent phenomenon. *J Appl Physiol*, 2011; 110: 1111–18
- Otis AB, McKerrrow CB, Bartlett RA et al: Mechanical factors in distribution of pulmonary ventilation. *J Appl Physiol*, 1956; 8: 427–43
- Bates JHT, DeGraeme D, Chartrand D et al: Volume-time profile during relaxed expiration in the normal dog. *J Appl Physiol*, 1985; 59(3): 732–37
- Mout LE: Ventilation flow-resistance and compliance of rat lungs. *J Physiol Lond*, 1955; 131: 157–67
- Suki B, Bates JHT: Lung tissue mechanics as an emergent phenomenon. *J Appl Physiol*, 2011; 110: 1111–18
- Rattenberg C: Basic mechanics of artificial ventilation. In: *Management of Life-Threatening Pneumonia*, edited by H.C.A. Lassen. London: Livingstone, 1956; 23
- Rossi A, Gottfried SB, Higgins BD et al: Respiratory mechanics in mechanically ventilated patients with respiratory failure. *J Appl Physiol*, 1985; 53: 1849–58
- Santos FB, Nagato LKS, Boechem NM et al: Time course of lung parenchyma remodeling in pulmonary and extrapulmonary acute lung injury. *J Appl Physiol*, 2006; 100: 98–106
- Xisto DC, Farias LL, Ferreira HC et al: Lung parenchyma remodeling in a murine model of chronic allergic inflammation. *Am J Respir Crit Care Med*, 2005; 171(8): 829–37
- Mall MA, Harkema JR, Trojanek JB et al: Development of chronic bronchitis and emphysema in beta-epithelial Na⁺ channel-overexpressing mice. *Am J Respir Crit Care Med*, 2008; 177(7): 730–42
- Bucarechi F, Reinaldo CRD, Hyslop S et al: A clinico-epidemiological study of bites by spiders of the genus *Phoneutria*. *Rev Inst Med Trop*, 2000; 42(1): 17–21
- Peták F, Habre W, Hantos Z et al: Effects of pulmonary vascular pressures and flow on airway and parenchymal mechanics in isolated rat lungs. *J Appl Physiol*, 2002; 92(1): 169–78
- Ober CDN, Aruvigam A, Lachumanan R et al: Pulmonary inflammation and edema induced by phospholipase A2 global gene analysis and effects on aquaporins and Na⁺/K⁺-ATPase. *J Biol Chem Papers*, 2003; 278(33): 31352–60
- Pirrone F, Mazzola SM, Pastore C et al: Activated Protein C Protection from Lung Inflammation in Endotoxin-Induced Injury. *Exp Biol Med (Maywood)*, 2008; 233(11): 1462–68
- Prado CM, da Rocha GZ, Leick-Maldonado EA et al: Inactivation of capsaicin-sensitive nerves reduces pulmonary remodeling in guinea pigs with chronic allergic pulmonary inflammation. *Bras J Med Biol Res*, 2011; 44(2): 130–39
- Carvalho GMC, Oliveira VR, Soares RM et al: Can LASSBio 506 and dexamethasone treat acute lung and liver inflammation induced by microcystin-LR? *Toxicol*, 2010; 56(4): 604–12
- Chao MC, Garcia CS, de Oliveira MB et al: Degree of endothelium injury promotes fibroblastogenesis in experimental acute lung injury. *Respir Neurobiol*, 2010; 173(2): 179–88
- Cardoso JLC, Franca FOS, Wen FH et al: *Animais Peçonhentos no Brasil: Biologia, Clínica e Terapêutica dos Acidentes*. 1^a ed. São Paulo: Sarvier, 2003 [in Portuguese]
- Pinto MCL, Boeboleta LR, Melo MB et al: *Tityus fasciculatus* envenomation induced cardio-respiratory alterations in rats. *Toxicol*, 2010; 55: 1132–37
- Jacoby-Ahner TE, Stephens N, Davern KM et al: Histopathological analysis and *in situ* localisation of Australian tiger snake venom in two clinically envenomed domestic animals. *Toxicol*, 2011; 58(4): 504–14
- Andrade MV, Caramez MP, Abreu EM et al: Lung compliance, plasma electrolyte levels and acid-base balance are affected by scorpion envenomation in anesthetized rats under mechanical ventilation. *Comp Biochem Physiol C Toxicol Pharmacol*, 2004; 138(1): 97–104
- Bucarechi F, Reinaldo CRD, Hyslop S et al: A clinico-epidemiological study of bites by spiders of the genus *Phoneutria*. *Rev Inst Med Trop*, 2000; 42(1): 17–21
- Vieira SLP, Utescher CLA, Ribeiro IA, Jorge MT: Determinação da dose letal 50% (DL₅₀) do veneno padrão de *Crotalus durissus terrificus* inoculado por via intramuscular. *Rev Soc Bras Toxicol*, 1989; Supl.2 [in Portuguese]
- Mortola JP, Noworaj A: Two-sidearm tracheal cannula for respiratory airflow measurements in small animals. *J Appl Physiol*, 1983; 55(1): 250–53
- Chang HK, Mortola JP: Fluid dynamic factors in tracheal pressure measurement. *J Appl Physiol*, 1981; 51: 218–25
- Silveira KSO, Boechem NI, Nascimento SM et al: Pulmonary mechanics and lung histology in acute lung injury induced by *Bothrops jararaca* venom. *Respir Physiol Neurobiol*, 2004; 139: 167–77
- Notaka PN, Amorim CE, Peres ACP et al: Pulmonary mechanic and lung histology injury induced by *Crotalus durissus terrificus* snake venom. *Toxicol*, 2008; 51: 1158–66
- Peres ACP, Notaka PN, Carvalho PTC et al: Effects of *Tityus serrulatus* scorpion venom on lung mechanics and inflammation in mice. *Toxicol*, 2009; 53: 779–85

Available online at www.sciencedirect.com

ScienceDirect

www.elsevier.com/locate/jmbm

Research Paper

Mechanical properties of acellular mouse lungs after sterilization by gamma irradiation [☆]



Juan J. Uriarte^{a,b,c,1}, Paula N. Nonaka^{a,1}, Noelia Campillo^{a,b,d},
Renata K. Palma^a, Esther Melo^{a,b,c}, Luis V.F. de Oliveira^e,
Daniel Navajas^{a,b,d}, Ramon Farré^{a,b,c,*}

^aUnitat de Biofísica i Bioenginyeria, Facultat de Medicina, Universitat de Barcelona, Barcelona, Spain

^bCIBER de Enfermedades Respiratorias, Bunyola, Spain

^cInstitut Investigacions Biomèdiques August Pi Sunyer, Barcelona, Spain

^dInstitut de Bioenginyeria de Catalunya, Barcelona, Spain

^eMaster's and Doctoral Degree Programs in Rehabilitation Sciences, Nove de Julho University, Sao Paulo, Brazil

ARTICLE INFO

Article history:

Received 9 June 2014

Received in revised form

12 August 2014

Accepted 21 August 2014

Available online 28 August 2014

Keywords:

Lung decellularization

Organ scaffold

Gamma irradiation

Pulmonary mechanics

Lung bioengineering

ABSTRACT

Lung bioengineering using decellularized organ scaffolds is a potential alternative for lung transplantation. Clinical application will require donor scaffold sterilization. As gamma irradiation is a conventional method for sterilizing tissue preparations for clinical application, the aim of this study was to evaluate the effects of lung scaffold sterilization by gamma irradiation on the mechanical properties of the acellular lung when subjected to the artificial ventilation maneuvers typical within bioreactors. Twenty-six mouse lungs were decellularized by a sodium dodecyl sulfate detergent protocol. Eight lungs were used as controls and 18 of them were submitted to a 31 kGy gamma irradiation sterilization process (9 kept frozen in dry ice and 9 at room temperature). Mechanical properties of acellular lungs were measured before and after irradiation. Lung resistance (R_L) and elastance (E_L) were computed by linear regression fitting of recorded signals during mechanical ventilation (tracheal pressure, flow and volume). Static (E_{st}) and dynamic (E_{dyn}) elastances were obtained by the end-inspiratory occlusion method. After irradiation lungs presented higher values of resistance and elastance than before irradiation: R_L increased by 41.1% (room temperature irradiation) and 32.8% (frozen irradiation) and E_L increased by 41.8% (room temperature irradiation) and 31.8% (frozen irradiation). Similar increases were induced by irradiation in E_{st} and E_{dyn} . Scanning electron microscopy showed slight structural changes after irradiation, particularly those kept frozen. Sterilization by gamma irradiation at a conventional dose to ensure sterilization modifies acellular lung mechanics, with potential implications for lung bioengineering.

© 2014 Elsevier Ltd. All rights reserved.

[☆]Sources of support: This work was supported in part by the Spanish Ministry of Economy and Competitiveness (SAF2011-22576, FIS-PI11/00089) and by the Conselho Nacional de Desenvolvimento Científico e Tecnológico (Research Productivity modality 307618/2010-2). Paula N. Nonaka had a fellowship (2011/21709-2) from Fundação de Amparo à Pesquisa do Estado de São Paulo.

*Correspondence to: Unitat de Biofísica i Bioenginyeria, Facultat de Medicina, Casanova 143, 08036 Barcelona, Spain.

E-mail address: rfarre@ub.edu (R. Farré).

¹Equally contributed to this work.

<http://dx.doi.org/10.1016/j.jmbm.2014.08.017>

1751-6161/© 2014 Elsevier Ltd. All rights reserved.

1. Introduction

Organ bioengineering has emerged as a potential therapeutic alternative for severe and irreversible diseases. Considerable research efforts are currently devoted to biofabricate organs from acellular scaffolds. Decellularization aims to remove the cellular content leaving the anatomical 3D structure of the organ intact and freed from genetic material from the donor (Gilbert et al., 2006; He and Callanan, 2013). The acellular organ is then used as a non-immunogenic scaffold to rebuild the organ by seeding it with stem/progenitor cells able to adequately repopulate the different niches within the organ (Ross et al., 2009; Uygun et al., 2010).

Lung bioengineering is a field of application particularly active in recent years because of the lack of viable lungs for transplantation and the reduced long term patient survival after the intervention. The investigation is focused on finding the best protocols for lung decellularization (Jensen et al., 2012; Melo et al., 2014a; Wallis et al., 2012), determining whether donor lungs from patients with aged or diseased lungs are suitable and selecting the best types of stem/progenitor cells for lung repopulation (Cortisella et al., 2010; Melo et al., 2014a; Ott et al., 2010; Petersen et al., 2010; Wagner et al., 2014). As knowledge in these issues is advancing and thus the idea of lung biofabrication is progressively seen as a potential alternative for future clinical routines, practical aspects that will be crucial in terms of real life feasibility are progressively being considered. Therefore, it is of great importance to study the best useful procedures – e.g., freezing/thawing (Nonaka et al., 2014a) and storage duration (Bonenfant et al., 2013) – to provide on-the-shelf acellular lungs ready for recellularization.

An important issue to be determined in handling acellular lungs before they are subjected to recellularization is sterilization to suppress any risk of transmission of viruses and bacteria from the donor to the receiver of the transplanted tissue/organ. Indeed, potential transmission of bacterial and viral infections such as HIV and hepatitis C has been reported in applications of tissue engineering (Eastlund, 2006; Kajbafzadeh et al., 2013). Therefore, the effects of different sterilization methods on different types of tissue have been studied to establish the optimal procedures. To this end, it is very important to take into account that aggressive sterilization methods that ensure full elimination of pathogens can also deteriorate structural components in the tissue, specifically its mechanical performance (Gouk et al., 2008; McGilvray et al., 2011).

Sterilization by gamma irradiation is a common procedure in materials and medical devices for clinical application, such as surgical grafts, due to the high penetrability of photons in the irradiated matter, attributed to its homogeneous dose distribution (IAEA, 2008) (Kaminski et al., 2012). However, gamma irradiation on allograft bone and soft tissues may cause structural damage, altering the biomechanical integrity of the tissue, particularly at high radiation doses (Dziedzic-Goclawaska et al., 2005; Nguyen et al., 2007).

The need for testing the mechanical consequences of sterilizing lung scaffolds is particularly relevant since the lung is an organ with high structural and mechanical

complexity that is physiologically subjected to continuous deformation cycling during breathing. Therefore, the mechanical properties of the organ scaffold should be preserved as much as possible after sterilization to ensure optimal organ regeneration. However, there are no data on the mechanical effects induced in lungs, whether native or decellularized, when subjected to a conventional irradiation dose ensuring sterilization of health application material (25–30 kGy). In the only data available to date on the effects of gamma radiation on acellular lungs (Bonenfant et al., 2013) the dose was so low (5 Gy/min for 12 min) that it cannot be taken as an accurate reference for safe sterilization procedures (IAEA, 2008). Regardless of the fact that the radiation dose was low, the authors observed that irradiated acellular lungs presented diffuse heterogeneous thickness, fused septa and spaced alveolar aspect, and laminin and collagen I with a more intense appearance due to agglomeration and tissue thickness (Bonenfant et al., 2013). However, as the authors did not measure any mechanical index, it is unknown whether this low dose (60 Gy) affected tissue mechanics. Therefore, the aim of this study was to evaluate the effects of gamma-irradiation sterilization with a conventional dose (Balsly et al., 2008; Loty et al., 1990) on the mechanical properties of acellular lungs subjected to the physiological conditions of cyclic mechanical stretch typical of ventilation. Since it is not clear whether gamma irradiation at low temperatures could be advantageous (due to reduction of the mobility and reactivity of free radicals) or detrimental for tissues (Gouk et al., 2008), we carried out the irradiation study in acellular lungs kept frozen or at room temperature.

2. Methods

2.1. Lung decellularization

This study was approved by the Ethical Committee for Animal Research of the University of Barcelona. Lungs were obtained from 26 male C57BL/6 mice (7–8 weeks old) intraperitoneally anesthetized with urethane (1.0 g/kg) and sacrificed by exsanguination. The lungs and trachea were excised and stored at -80°C until start of the decellularization protocol. The lungs were decellularized following a variant of previously described procedures in mice (Melo et al., in press; Nonaka et al., 2014a,b). As explained below, decellularizing media were infused by the trachea only, with no perfusion through the pulmonary artery since a previous study showed that this procedure resulted in minor differences in rat lungs (Melo et al., 2014a). Lungs were first subjected to a four-times repeating cycle that consisted in thawing the lungs in a water bath at 37°C and freezing them again at -80°C . Subsequently, all lung samples were cleaned to remove any attached esophageal, lymphatic and connective tissues. The lungs were then submitted to 6–8 washes by tracheal instillation of 2 mL of PBS containing streptomycin (90 mg/mL), penicillin (50 U/mL) and amphotericin B (25 mg/mL) until the liquid extracted from the lungs had a transparent appearance. This step was repeated with 2.5 mL of de-ionized water several times, then treated with tracheal instillation of 2.5 mL of 1% sodium dodecyl sulfate (SDS)

detergent. The lungs were subsequently kept in agitation for 24 h at room temperature in a 50 mL polystyrene conical tube with 20 mL of 1% SDS. The lungs were then rinsed again with 2.5 mL of PBS (with the antibiotic/antimicrobial components described above) and maintained in 20 mL PBS in agitation for 24 h to finish the process for obtaining acellular lung scaffolds.

2.2. Gamma irradiation of decellularized lungs

Baseline respiratory mechanics of all the acellular lungs were measured during conventional mechanical ventilation as described below. Subsequently, 8 of the acellular lungs were selected at random as a control group and frozen at -80°C . The remaining 18 acellular lungs were randomly distributed into two groups ($N=9$ each) for gamma sterilization: one group was irradiated at room temperature (completely thawed) and the other group was irradiated while frozen. To this end, the samples were frozen at -20°C for 5 h and isothermally packed in dry ice. Overnight ^{60}Co gamma irradiation was carried out in a legally certified facility (Arago-gamma, Barcelona, Spain) with an effective measured dose of 31 kGy. After irradiation the amount of dry ice around the frozen lungs was minimally reduced, ensuring that the decellularized lungs remained frozen throughout irradiation. Finally, the frozen acellular lungs (controls and irradiated) were thawed at room temperature and resistance and elastance of all lungs were measured following identical procedure as for the baseline.

2.3. Mechanical ventilation of decellularized lungs

To characterize the mechanical properties of the lung at operating conditions similar to those in physiologically normal breathing, the decellularized lungs were subjected to conventional mechanical ventilation. To this end, the acellular lungs were tracheally intubated using an 18-gauge metallic cannula, suspended vertically by gravity and placed within a chamber similar to the ones typically used in lung bioreactors (32°C and 100% relative humidity). A pneumotachograph (range ± 20 mL/s) was connected to the inlet of the cannula to measure tracheal flow (V) by sensing the pressure drop across the pneumotachograph with a differential pressure transducer (DCXL01DS, range ± 2.5 cmH₂O). Tracheal pressure (P_{tr}) was measured by connecting a pressure transducer (176PC14HD2, ± 35 cmH₂O) on a side port placed between the pneumotachograph and the cannula. The inlet of the pneumotachograph was then connected to the Y piece of a volumetric mechanical ventilator designed for the artificial ventilation of rodents (Farre et al., 2005). The decellularized lungs were subjected to conventional volume-controlled ventilation with a quasi-sinusoidal flow pattern with a tidal volume of 0.20 mL at a frequency of 100 breaths/min. A positive end expiratory pressure (PEEP) of 2 cmH₂O was applied through the ventilator to counteract the absence of physiological negative pleural pressure. Flow and pressure signals from the transducers were analogically low-pass filtered (Butterworth, 8 poles, 32 Hz), sampled at a rate of 100 Hz (PCI-6036, National Instruments) through a custom monitoring and recording application (LabView).

2.4. Measurement of resistance and elastance in decellularized lungs

Lung resistance and elastance were computed from the signals recorded during mechanical ventilation. A first step was to compute the volume signal (V) by digital integration of the flow signal (\dot{V}). Secondly, the tracheal pressure (P_{tr}) signal was corrected by subtracting the pressure drop (P_{can}) caused by the non-linear resistance of the intubation cannula, which had been previously calibrated and characterized ($P_{can}=K_1V+K_2V^2/V$, where K_1 and K_2 are linear and non-linear parameters of the Rohrer model). In a subsequent step, effective lung resistance (R_L) and elastance (E_L) were computed by linear regression of the recorded signals P_{tr} , \dot{V} and V to the conventional respiratory mechanics model $P_{tr}=P_o+E_LV+R_L\dot{V}$, where P_o is a parameter to account for the external PEEP applied by the ventilator. For each decellularized lung, R_L and E_L were computed from data including five ventilation cycles.

To assess acellular lung viscoelasticity, static and dynamic elastances were measured by means of end-inspiratory airway occlusions achieved by pushing the corresponding control button of the mechanical ventilator. A fast initial drop in lung pressure (P_{ci}) from the pre-occlusion value to an inflection point (with pressure P_i) occurs after an end-inspiratory occlusion, and this is followed by a slow pressure decay until a plateau pressure (P_{ei}) corresponding to the elastic recoil pressure of the lung is reached. Accordingly, the lung static elastance (E_{st}) was computed as the plateau pressure (P_{ei}) recorded after 5 s of occlusion minus the PEEP values, divided by the tidal volume. Lung dynamic elastance (E_{dyn}) was computed by dividing the inflection point pressure (P_i) minus the PEEP value by the tidal volume (Bates et al., 1985; Saidiva et al., 1992). For each lung, E_{st} and E_{dyn} were obtained as the mean from 2 end-inspiratory occlusions, the second one performed after allowing 1 min of normal mechanical ventilation following the first occlusion. After mechanical assessment, samples of the acellular lungs were taken to confirm correct decellularization and for imaging.

3. Decellularization assessment

Acellular lungs (as well as some native lungs for comparison) were divided into their lobes and fixed by bronchial infusion of a 3:1 ratio mixture of Optimal Cutting Temperature compound (OCT, Sakura) and PBS and stored at a -80°C freezer. Subsequently, cryosections (12 μm) of frozen lung samples were obtained using a cryostat (Thermo Scientific, HM 560 CryoStar). To verify the absence of cell DNA after the process of decellularization, the cryosections were rinsed with PBS to remove the OCT and then maintained for 10 min in 1 $\mu\text{g/mL}$ of 4', 6-diamidino-2-phenylindole (DAPI, Sigma) fluorescence solution for staining. Sections of interest were observed with a digital camera (CCD-EM C9100, Hamamatsu, Japan) coupled to an inverted fluorescent microscope (TEclipse, Nikon, Tokyo, Japan) and driven by a conventional acquisition software (Metamorph, Molecular Devices, Sunnyvale, CA).

3.1. Lung microscopy

To perform conventional fluorescent imaging, cryosections of the lung ($12\ \mu\text{m}$ thick) obtained from each group were allowed to thaw at room temperature. Several PBS $1\times$ rinses were done in order to remove the OCT. Tissue samples were fixed in 70% ice-cold methanol +30% acetone for 5 min, then blocked with a buffer solution containing PBS $1\times$ and 10% fetal bovine serum (FBS) for 30 min. Primary antibodies were diluted in buffer solution. Diverse slices with different primary antibodies, rabbit anti-collagen I (1:500, Abcam), goat anti-elastin (1:200, Santa Cruz), rabbit anti-collagen III (1:200, Abcam), goat anti-collagen IV (1:200, Santa Cruz) and rabbit anti-laminin (1:25, Sigma), were incubated overnight at $4\ ^\circ\text{C}$. The slices were rinsed three times with the PBS $1\times$, for 5 min each wash. Secondary antibodies, donkey anti-rabbit Cy3 and bovine anti-goat Alexa 488 diluted (1:200, Jackson) in buffer solution, were incubated for 60 min. Three times 5-min rinses with PBS $1\times$ were applied to eliminate unbound secondary antibodies. Finally, coverslips were mounted on each section using a non-fluorescent compound (Fluoromont G, SouthernBiotech).

Images of the regions of interest were obtained with a digital camera (CCD-EM C9100, Hamamatsu, Japan), coupled to an inverted fluorescent microscope (Ti-Eclipse, Nikon, Tokyo, Japan), with a magnification of $10\times$ and operated by a commercial acquisition software (NIS-Elements C Microscope Imaging Software, Nikon Instruments Inc.).

Phase contrast images were obtained after complete OCT elimination and samples were kept in PBS $1\times$ at room temperature during image acquisition. Images were obtained with a digital camera (Mariyn F145, Allied V.T., Germany), operated by Vision Assistant software (National Instruments) and coupled to an inverted optical microscope (TE2000, Nikon, Tokyo, Japan) with a magnification $10\times$.

Decellularized lungs were prepared by following a standard protocol for the preparation of tissue samples for SEM. Briefly, tissue samples were fixed with 2% glutaraldehyde and 2.5% paraformaldehyde in 0.1 M cacodylate buffer for 2 h at room temperature, then rinsed in cacodylate buffer, sliced, and dehydrated through an ethanol gradient. Samples were dehydrated in hexamethyldisilazane for 10 min and dried overnight, then coated with a layer of 14.4 nm of Au using a

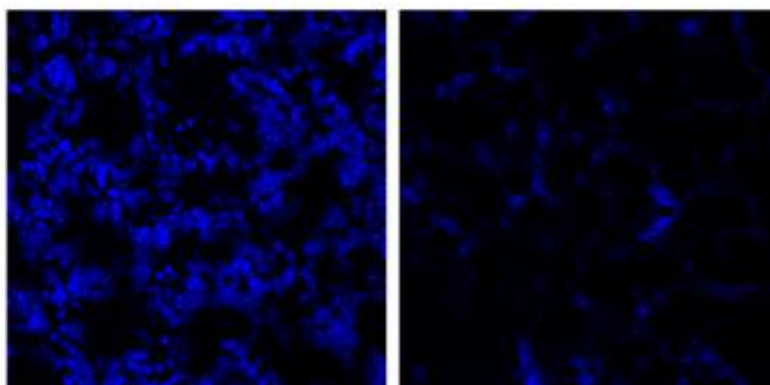


Fig. 1 – Representative image of DAPI staining in a native (left) and acellular lung scaffold (right). Blue dots (absent in the decellularized lung) correspond to cell nuclei. Diffused blue staining in the acellular lung corresponds to autofluorescence of the extracellular matrix. (For interpretation of the references to color in this figure legend, the reader is referred to the web version of this article.)

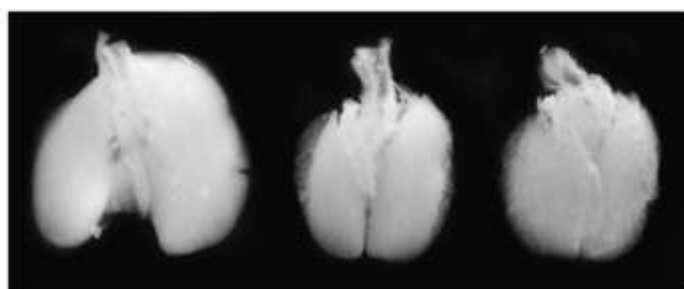


Fig. 2 – Images for whole acellular lungs: non-irradiated (left), irradiated at room temperature (center), and irradiated while kept frozen (right).

sputter coater (SC510, Fisons Instruments, San Carlos, CA) and analyzed using the scanning electron microscope (DSM 940A microscope, Zeiss, Oberkochen, Germany) with an acceleration of 15 kV.

3.2. Statistical analysis

Comparisons between the values obtained for R_t , E_t , E_m and E_{dyn} measured in each group between pre- and post-irradiation

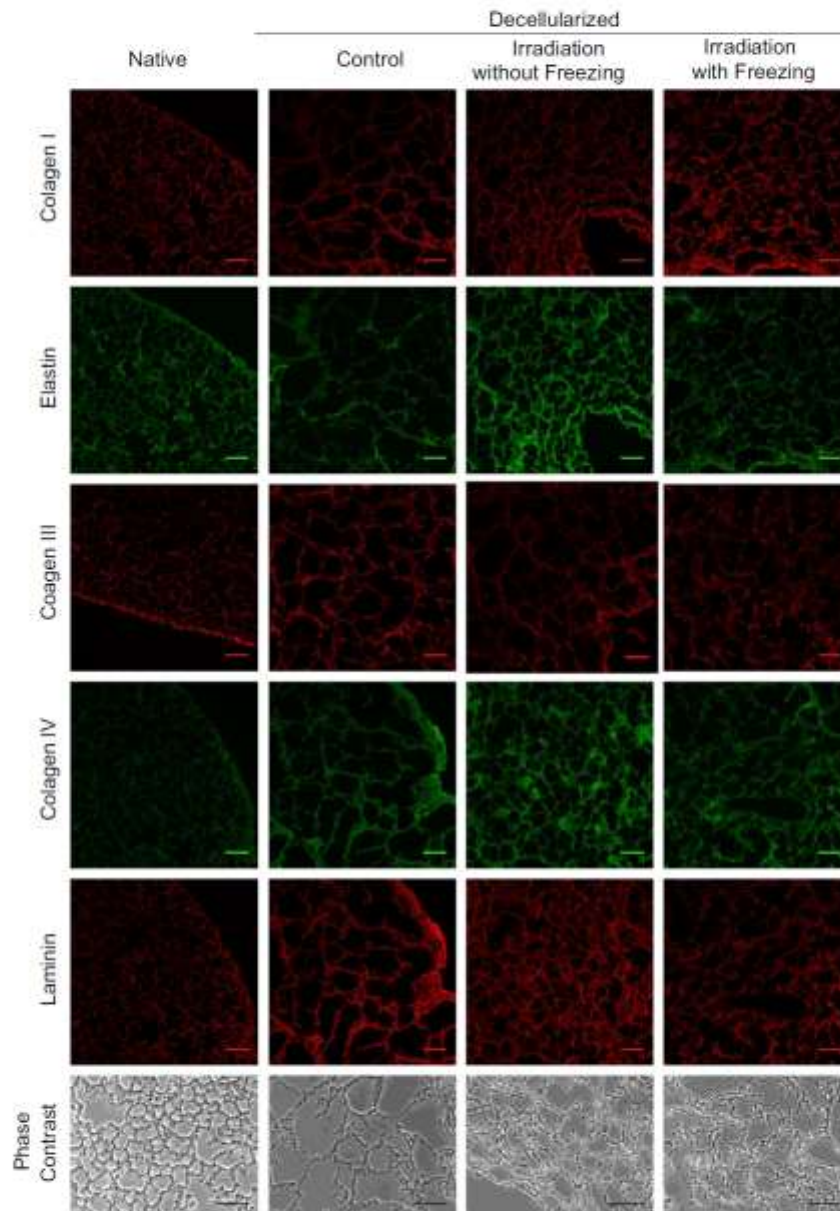


Fig. 3 - Immunofluorescent images of native and acellular (before and after irradiation) lung slices stained for different components of the extracellular matrix (Collagen I, III and IV, Laminin and Elastin) and phase contrast images. Scale bar = 100 μ m.

were carried out by paired Student's *t*-test. The *p* value was considered statistically significant at a 5% level.

4. Results

Scaffolds obtained from the implemented lung decellularization procedure compared with native lungs (Fig. 1), showed lacked cellular nuclei assessed by DAPI. A qualitative macroscopic evaluation of acellular lungs after submission to gamma irradiation sterilization presented changes when compared to non-irradiated control lungs (Fig. 2), with reduction of organ size and apparent damage of the pleura surface. Fig. 3 shows that relevant components of the extracellular matrix (elastin, laminin and collagens I, III and IV) remained almost unchanged in acellular lungs before and after irradiation. Immunostaining

and phase contrast images (Fig. 3) suggest that irradiation maintained the structure although with some degree of reduction in the alveolar spaces. However, observation by SEM (Fig. 4) showed that the different microscopic lung structures were relatively well maintained, presenting possible alterations in irradiated acellular lungs, especially in those irradiated while frozen.

Interestingly, inspiratory occlusions showed no presence of air leak as reflected by the maintenance of plateau pressure (Fig. 5). This figure shows an example of the tracheal pressure recording for the same lung before and after gamma irradiation: the higher pressure plateau after irradiation is a direct consequence of the increase in mechanical impedance. R_L and E_L , obtained from P_{tr} , V and \dot{V} signals during ventilation are depicted in Fig. 6. As expected, no significant differences were observed between pre- and post-evaluation in control group.

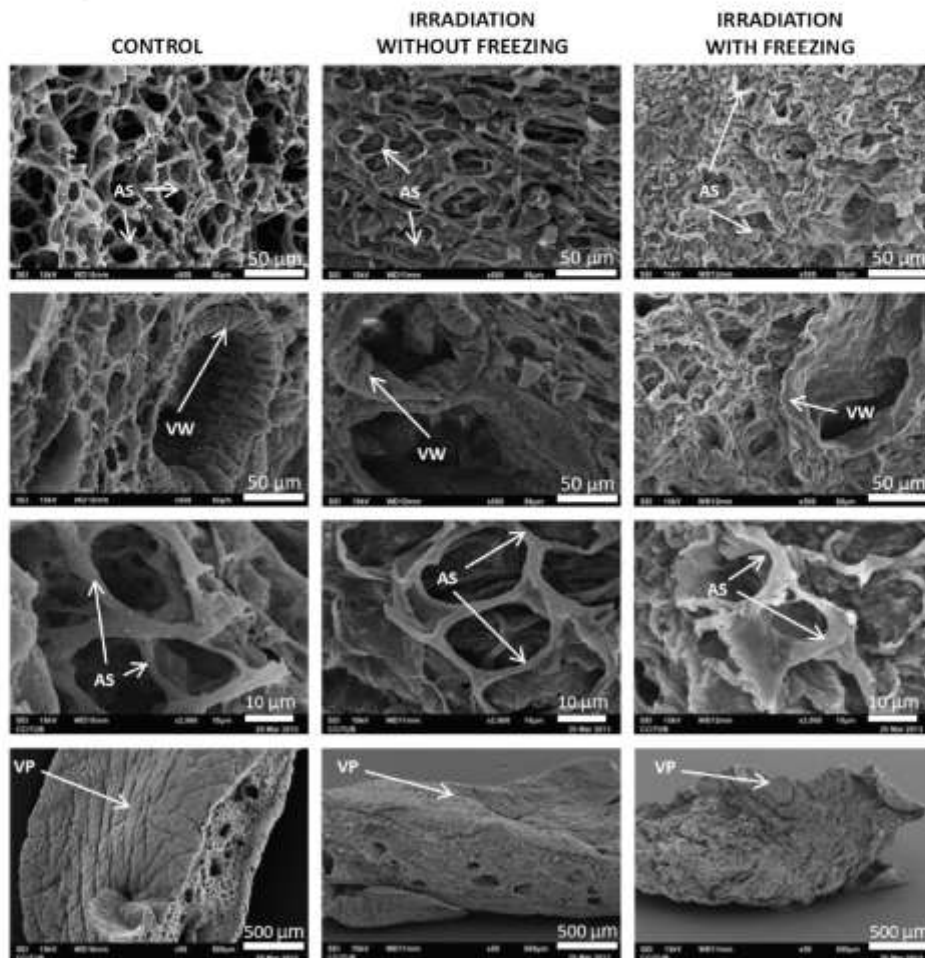


Fig. 4 – Representative examples of SEM images comparing sections of control, and irradiated (without and with freezing) decellularized lungs. AS: alveolar septum; VW: vessel wall; VP: visceral pleura.

This result is consistent with the absence of mechanical effects caused by freezing-thawing the lung scaffold (Nonaka et al., 2014a). However, irradiated lung scaffolds, both while frozen and at room temperature, presented significantly higher mechanical impedance after irradiation. As compared with corresponding pre-irradiation values, R_e increased by 41.1% and 32.8% when irradiation was performed at room temperature and while frozen, respectively. E_e showed a similar behavior, increasing by 41.8% and 31.8%, respectively (Fig. 6). E_{st} and E_{dyn} obtained from inspiratory occlusions (Fig. 7) also showed significant differences between pre- and post-irradiation in both groups (at room temperature and frozen). However, E_{st} and E_{dyn} were slightly higher when acellular lungs were irradiated while

frozen. E_{st} increased by 48.1% in the irradiation without freezing group and 37.3% for the group irradiated while frozen. E_{dyn} also augmented: by 46.9% and 36.8%, respectively.

5. Discussion

Irradiation of acellular lungs with a ^{60}Co -gamma dose typical for sterilization in health applications resulted in a significant increase of the mechanical impedance of the lung scaffold. The increase in lung resistance and reactance was similar regardless of the fact that the gamma irradiation was carried out when the decellularized lungs were frozen or at room temperature.

Sterilization of scaffolds (Rutala and Weber, 2010), a more intense process than disinfection, is essential before any application for tissue engineering in order to ensure safety by eliminating transmission of virus, bacteria or other infectious microorganisms. Being necessary in case of artificial scaffolds because of contamination risk during the whole fabrication process, sterilization is strictly mandatory when using scaffolds from living organs because the existence of potentially infectious organisms always present in the donor. Indeed, even bacteria that are benign in the natural environment of a healthy subject can become pathogenic in the context of a scaffold within a bioreactor. Not every sterilization method used in the health industry is applicable to

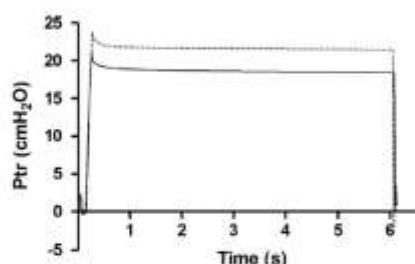


Fig. 5 – Inspiratory occlusion pressure of an acellular lung before (solid line) and after irradiation (dotted line).

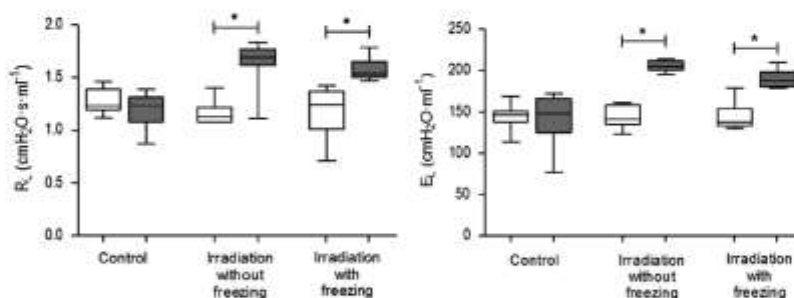


Fig. 6 – Effective resistance (R_e) and elastance (E_e) computed during conventional mechanical ventilation in decellularized lungs before (white box) and after gamma irradiation (gray box). Controls were not irradiated but frozen. Asterisk indicates $p < 0.05$.

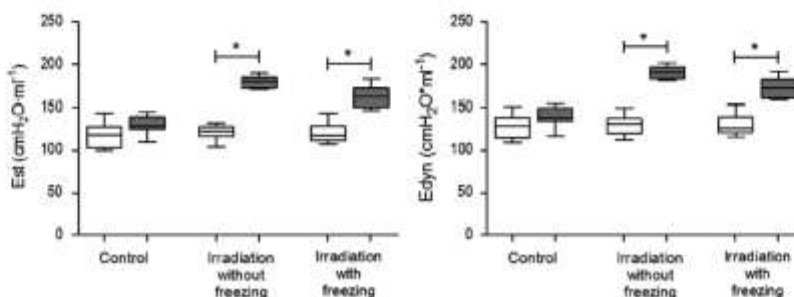


Fig. 7 – Effective static (E_{st}) and dynamic elastances (E_{dyn}) computed during inspiratory occlusions in decellularized lungs before (white box) and after (gray box) gamma irradiation. Controls were not irradiated but frozen. Asterisk indicates $p < 0.05$.

bioscaffolds. The ones involving the use of high temperature, either dry or wet, should be obviously discarded because of their denaturation effects on proteins and other biomolecules in the scaffold. Other sterilization methods such as those based on gamma irradiation, ethylene oxide or other chemical agents could be in principle used. Nevertheless, all sterilization methods have side effects since any action to destroy infectious microorganisms is at the same time potentially affecting the different molecular structures in the scaffold. For instance, it has been described that both ethylene oxide and irradiation can interact with scaffold molecules, potentially degrading its performance. It has been recently suggested that peracetic acid could be a useful chemical agent for sterilizing polymeric scaffolds for tissue engineering (Yoganarasimha et al., 2014), but this agent appeared not to be optimal when used to sterilize lung scaffolds (Bonenfant et al., 2013). Using a chemical agent in an effective way requires that it actually reaches all sites in the structure to be sterilized, which could be compromised in the specific case of lung scaffold given their anatomic complexity (the airway and vascular trees terminate in ~300 million alveoli). From the viewpoint of easily reaching all points of the scaffold structure, gamma irradiation could be particularly suitable for sterilizing lung scaffolds.

It is already known that sterilization by gamma irradiation induces dose-dependent changes in bone and soft tissues. For sufficiently high radiation doses, considerable biomechanical alterations are induced in the integrity of the tissue, e.g. structural damage of the collagen fibers, resulting in significant changes in the mechanical behavior (Nguyen et al., 2007). For instance, liver sterilization by irradiation caused a reduction in the mechanical properties of the organ with a dose of 3 Mrad (30 kGy) (Kajbafzadeh et al., 2013). Gamma irradiation of Allo-derm tissue also caused structural damage such as condensation and increase in thickness of collagen fibers (Gouk et al., 2008). A study regarding the impact of gamma irradiation in acellular pulmonary valves, with a 25–40 kGy dose, showed major reduction in collagen content with fragmentation of the extracellular matrix caused by oxidative damage after irradiation (Sarathchandra et al., 2012).

Gamma irradiation (31 kGy) did induce structural and mechanical alterations in the mouse decellularized lungs. Visual inspection of the acellular lungs showed a reduction of scaffold volume, which was similar for room and low temperature irradiation (Fig. 2). This lung reduction could be due to some degree of alveolar atelectasia (Fig. 3), likely induced by some degree of remodeling in the scaffold fibers, which is consistent with the increase in lung elastance and resistance observed after irradiation. Microscopic examination of the decellularized lung scaffolds (Fig. 4) indicates a different effect of radiation depending on whether it was performed at room temperature or while the scaffold was frozen. When the acellular lungs were irradiated at room temperature, the different lung structures (alveoli, vessel walls and pleura) were very similar to those in non-irradiated lungs. By contrast, irradiation at low temperature considerably altered the microscopic structure, although the different components and compartments of the lung scaffold were maintained (Fig. 3). These differences are not caused by freezing per se since the non-irradiated acellular lungs experienced exactly the same thermal treatment. It is

interesting to note that the apparent alterations in the microstructure of the lung scaffold did not translate into a loss of ventilatory function, as illustrated by Fig. 5 showing no airleaks during the postinspiratory pause employed to measure static elastance. It is also remarkable that irradiation (either at low or room temperatures) did not modify the degree of inhomogeneity/viscoelasticity of the acellular lungs, as indicated by the invariance of the ratio E_{dyn}/E_{st} (within the range 1.06–1.08 in all groups) and by the similar values obtained for E_{dyn} and E_{st} .

The mechanisms determining how sterilization by irradiation specifically modifies the different sub-structures in the acellular lung scaffold are unknown. However, it has been described that gamma radiation causes damage to the collagen fibers, inducing free-radical-mediated cross-linking or degradation and fragmentation via direct peptide chain scission (Dziedzic-Goclawska et al., 2005). Accordingly, these alterations could result in significant modification of mechanical properties in the tissue, in particular the increase in impedance found in the acellular lungs after irradiation. This collagen damage induced by high doses of gamma irradiation can be associated mainly to peptide chain scission in dry scaffolds whereas in hydrated state (which was the case in all our investigated samples) it seems to be linked to intermolecular cross-linking (Sun et al., 2009). The finding that acellular lungs irradiated at room temperature were slightly less affected than those irradiated while frozen and data reporting that irradiation at low temperature increases resistance of bacteria and viruses (Dziedzic-Goclawska et al., 2005), adds support in favor of irradiation at room temperature, which is easier from a practical viewpoint and, therefore, could be suitable for sterilizing acellular lungs.

In conclusion, application of gamma irradiation with a dose high enough to expect full sterilization induced an increase in the mechanical impedance of decellularized lungs. However, the changes observed were not severe since the microscopic structure of the lung compartment maintained its integrity and the acellular lung could be normally ventilated. Future research should be addressed to ascertain whether the molecular effects of such a maximal irradiation could be detrimental for cell repopulation of the scaffold in lung bioengineering. Interestingly, given that dose selection should strike a balance between high and low values to inactivate potentially existing pathogens and to preserve the mechanical and biological tissue properties, respectively, future specific analysis could allow to reduce the irradiation dose in lung bioengineering to values below 30 kGy, with subsequent decrease in mechanical alterations. According to our data on scaffold mechanics, sterilization by irradiation, a standardized method, cheap and commercially available, should not be discarded as a routine procedure for this particular application of regenerative medicine.

Acknowledgments

The authors wish to thank Maebis Polo and Miguel A. Rodríguez for their excellent technical contribution. This work was supported in part by the Spanish Ministry of Economy and Competitiveness (SAF2011-22576, FIS-PI11/00089) and by the Conselho Nacional de Desenvolvimento Científico e Tecnológico (Research

Productivity modality 307618/2010-2). Paula Naomi Nonaka had a fellowship (2011/21709-2) from Fundação de Amparo à Pesquisa do Estado de São Paulo.

REFERENCES

- Baisly, C.R., Cotter, A.T., Williams, L.A., Gaskins, B.D., Moore, M.A., Wolfenbarger Jr., L., 2008. Effect of low dose and moderate dose gamma irradiation on the mechanical properties of bone and soft tissue allografts. *Cell Tissue Bank* 9 (4), 289–298, <http://dx.doi.org/10.1007/s10561-008-9069-0>.
- Bates, J.H., Rossi, A., Milic-Emili, J., 1985. Analysis of the behavior of the respiratory system with constant inspiratory flow. *J. Appl. Physiol.* 58 (6), 1840–1848.
- Bonenfant, N.R., Sokocevic, D., Wagner, D.E., Borg, Z.D., Lathrop, M.J., Lam, Y.W., Weiss, D.J., 2013. The effects of storage and sterilization on de-cellularized and re-cellularized whole lung. *Biomaterials* 34 (13), 3231–3245, <http://dx.doi.org/10.1016/j.biomaterials.2013.01.031>.
- Cortiella, J., Niles, J., Cantu, A., Brettler, A., Pham, A., Vargas, G., Nichols, J.E., 2010. Influence of acellular natural lung matrix on murine embryonic stem cell differentiation and tissue formation. *Tissue Eng. Part A* 16 (8), 2565–2580, <http://dx.doi.org/10.1089/ten.tea.2009.0730>.
- Dziedzic-Goclawska, A., Kaminski, A., Uhrzynska-Tyszkiewicz, I., Stachowicz, W., 2005. Irradiation as a safety procedure in tissue banking. *Cell Tissue Bank* 6 (3), 201–219, <http://dx.doi.org/10.1007/s10561-005-0338-x>.
- Eastlund, T., 2006. Bacterial infection transmitted by human tissue allograft transplantation. *Cell Tissue Bank* 7 (3), 147–166, <http://dx.doi.org/10.1007/s10561-006-0003-z>.
- Farre, R., Granell, S., Rotger, M., Serrano-Mollar, A., Closa, D., Navajas, D., 2005. Animal model of unilateral ventilator-induced lung injury. *Intensiv. Care Med.* 31 (3), 487–490, <http://dx.doi.org/10.1007/s00134-004-2534-8>.
- Gilbert, T.W., Sellaro, T.L., Badyak, S.F., 2006. Decellularization of tissues and organs. *Biomaterials* 27 (19), 3675–3683, <http://dx.doi.org/10.1016/j.biomaterials.2006.02.014>.
- Gouk, S.S., Lim, T.M., Teoh, S.H., Sun, W.Q., 2008. Alterations of human acellular tissue matrix by gamma irradiation: histology, biomechanical property, stability, in vitro cell repopulation, and remodeling. *J. Biomed. Mater. Res. B Appl. Biomater.* 84 (1), 205–217, <http://dx.doi.org/10.1002/jbm.b.30862>.
- He, M., Callanan, A., 2013. Comparison of methods for whole-organ decellularization in tissue engineering of bioartificial organs. *Tissue Eng. Part B Rev.* 19 (3), 194–208, <http://dx.doi.org/10.1089/ten.TEB.2012.0340>.
- International Atomic Energy Agency (2008). Trends in Radiation sterilization of Health care products; Vienna.
- Jensen, T., Roszell, B., Zang, F., Girard, E., Matson, A., Thrall, R., Finck, C., 2012. A rapid lung de-cellularization protocol supports embryonic stem cell differentiation in vitro and following implantation. *Tissue Eng. Part C Methods* 18 (8), 632–646, <http://dx.doi.org/10.1089/ten.TEC.2011.0584>.
- Kajbafzadeh, A.M., Javan-Farazmand, N., Monajemzadeh, M., Baghaye, A., 2013. Determining the optimal decellularization and sterilization protocol for preparing a tissue scaffold of a human-sized liver tissue. *Tissue Eng. Part C Methods* 19 (8), 642–651, <http://dx.doi.org/10.1089/ten.TEC.2012.0334>.
- Kaminski, A., Jastrzebska, A., Grazka, E., Marowska, J., Gut, G., Wojciechowski, A., Uhrzynska-Tyszkiewicz, I., 2012. Effect of gamma irradiation on mechanical properties of human cortical bone: influence of different processing methods. *Cell Tissue Bank* 13 (3), 363–374, <http://dx.doi.org/10.1007/s10561-012-9308-2>.
- Loty, B., Courpied, J.P., Tomeno, B., Postel, M., Forest, M., Abelanet, R., 1990. Bone allografts sterilized by irradiation. Biological properties, procurement and results of 150 massive allografts. *Int. Orthop.* 14 (3), 237–242.
- McGilvray, K.C., Santoni, B.G., Turner, A.S., Bogdansky, S., Wheeler, D.L., Puttlitz, C.M., 2011. Effects of (60)Co gamma radiation dose on initial structural biomechanical properties of ovine bone–patellar tendon–bone allografts. *Cell Tissue Bank* 12 (2), 89–98, <http://dx.doi.org/10.1007/s10561-010-9170-z>.
- Melo, E., Garreta, E., Luque, T., Cortiella, J., Nichols, J., Navajas, D., Farre, R., 2014a. Effects of the decellularization method on the local stiffness of acellular lungs. *Tissue Eng. Part C Methods* 20 (5), 412–422, <http://dx.doi.org/10.1089/ten.TEC.2013.0325>.
- Melo, E., Cardenes, N., Garreta, E., Luque, T., Rojas, M., Navajas, D., Farré, R., 2014b. Inhomogeneity of local stiffness in the extracellular matrix scaffold of fibrotic mouse lungs. *J. Mech. Behav. Biomed. Mater.* 37, 186–195.
- Nguyen, H., Morgan, D.A., Forwood, M.R., 2007. Sterilization of allograft bone: effects of gamma irradiation on allograft biology and biomechanics. *Cell Tissue Bank* 8 (2), 93–105, <http://dx.doi.org/10.1007/s10561-006-9020-1>.
- Nonaka, P.N., Campillo, N., Uriarte, J.J., Garreta, E., Melo, E., de Oliveira, L.V., Farre, R., 2014a. Effects of freezing/thawing on the mechanical properties of decellularized lungs. *J. Biomed. Mater. Res. A* 102 (2), 413–419, <http://dx.doi.org/10.1002/jbm.a.34708>.
- Nonaka, P.N., Uriarte, J.J., Campillo, N., Melo, E., Navajas, D., Farré, R., Franco Oliveira, L.V., 2014b. Mechanical properties of mouse lungs along organ decellularization by sodium dodecyl sulfate. *Respir. Physiol. Neurobiol.* 200, 1–5.
- Ott, H.C., Clippinger, B., Conrad, C., Schuetz, C., Pomerantseva, I., Ikonomou, L., Vacanti, J.P., 2010. Regeneration and orthotopic transplantation of a bioartificial lung. *Nat. Med.* 16 (8), 927–933, <http://dx.doi.org/10.1038/nm.2193>.
- Petersen, T.H., Calle, E.A., Zhao, L., Lee, E.J., Gui, L., Raredon, M.B., Niklason, L.E., 2010. Tissue-engineered lungs for in vivo implantation. *Science* 329 (5991), 538–541, <http://dx.doi.org/10.1126/science.1189345>.
- Ross, E.A., Williams, M.J., Hamazaki, T., Terada, N., Clapp, W.L., Adin, G., Batich, C.D., 2009. Embryonic stem cells proliferate and differentiate when seeded into kidney scaffolds. *J. Am. Soc. Nephrol.* 20 (11), 2338–2347, <http://dx.doi.org/10.1681/asn.2008111196>.
- Rutala, W.A., Weber, D.J., 2010. Guideline for disinfection and sterilization of prion-contaminated medical instruments. *Infect. Control Hosp. Epidemiol.* 31 (2), 107–117, <http://dx.doi.org/10.1086/650197>.
- Saldiva, P.H., Zin, W.A., Santos, R.L., Eidelman, D.H., Milic-Emili, J., 1992. Alveolar pressure measurement in open-chest rats. *J. Appl. Physiol.* 72 (1), 302–306.
- Sarathchandra, P., Smolenski, R.T., Yuen, A.H., Chester, A.H., Goldstein, S., Heacock, A.E., Taylor, P.M., 2012. Impact of gamma-irradiation on extracellular matrix of porcine pulmonary valves. *J. Surg. Res.* 176 (2), 376–385, <http://dx.doi.org/10.1016/j.jss.2011.10.011>.
- Sun, K., Tian, S.Q., Zhang, J.H., Xia, C.S., Zhang, C.L., Yu, T.B., 2009. ACL reconstruction with BPTB autograft and irradiated fresh frozen allograft. *J. Zhejiang Univ. Sci. B* 10 (4), 306–316, <http://dx.doi.org/10.1631/jzus.B0820335>.
- Uygun, B.E., Soto-Gutierrez, A., Yagci, H., Izamis, M.L., Guzzardi, M.A., Shulman, C., Uygun, K., 2010. Organ reengineering through development of a transplantable recellularized liver graft using decellularized liver matrix. *Nat. Med.* 16 (7), 814–820, <http://dx.doi.org/10.1038/nm.2170>.
- Wagner, D.E., Bonenfant, N.R., Parsons, C.S., Sokocevic, D., Brooks, E.M., Borg, Z.D., Weiss, D.J., 2014. Comparative decellularization and recellularization of normal versus emphysematous human lungs. *Biomaterials* 35 (10),

- 3281–3297, <http://dx.doi.org/10.1016/j.biomaterials.2013.12.103>.
- Wallis, J.M., Borg, Z.D., Daly, A.B., Deng, B., Ballif, B.A., Allen, G.B., Weiss, D.J., 2012. Comparative assessment of detergent-based protocols for mouse lung de-cellularization and re-cellularization. *Tissue Eng. Part C Methods* 18 (6), 420–432. <http://dx.doi.org/10.1089/ten.TEC.2011.0567>.
- Yoganarasimha, S., Trahan, W.R., Best, A.M., Bowlin, G.L., Kitten, T.O., Moon, P.C., Madurantakam, P.A., 2014. Peracetic acid: a practical agent for sterilizing heat-labile polymeric tissue-engineering scaffolds. *Tissue Eng. Part C Methods*, <http://dx.doi.org/10.1089/ten.tec.2013.0624>. PMID: 24341350.

Received: 2014.10.23
Accepted: 2014.11.12
Published: 2014.11.24

Decellularized Lung Scaffolds for Bioengineered Organs

Authors' Contribution:
Study Design: A
Data Collection: B
Statistical Analysis: C
Data Interpretation: B
Manuscript Preparation: E
Literature Search: F
Funds Collection: G

ABG 1 Jéssica Julioti Urbano
BDE 2 Nadua Apostólico
BDE 2 Renata Kelly da Palma
DE 2 Ezequiel Fernandes Oliveira
BD 3 Juan J. Uriarte
AEG 2 Luis Vicente Franco de Oliveira

1 Physical Therapy School, Scholarship Scientific Initiation CNPq, Nove de Julho University, São Paulo, Brazil
2 Master Degree and PhD Post Graduation Program in Rehabilitation Sciences, Nove de Julho University, São Paulo, Brazil
3 Unit of Biophysics and Bioengineering, Faculty of Medicine, University of Barcelona, Barcelona, Spain

Corresponding Author: Luis Vicente Franco de Oliveira, e-mail: oliveira.lvf@uninove.br

Source of support:

The Cardiorespiratory Experimental Laboratory receives funding from Nove de Julho University (Brazil) and, IJU receive grants of the Conselho Nacional de Desenvolvimento Científico e Tecnológico (CNPq) (protocol number 166879/2013-4) and, NA receive grants from the Fundação de Amparo à Pesquisa do Estado de São Paulo (FAPESP) (protocol number 2013/21765-5), and, RKP receive grants from Coordenação de Aperfeiçoamento de Pessoal de Nível Superior (CAPES) (protocol number BEX 11514/13-2). LVFD received a grant from the Conselho Nacional de Desenvolvimento Científico e Tecnológico (local acronym CNPq) (Research Productivity modality – PQID, process number 30761B/2010-2)

Background: Lung transplantation is a treatment provided to patients in terminal respiratory diseases. While opportunities for organ transplantation are somewhat limited, the list of patients awaiting donation is increasing. Therefore, new strategies are required to increase the availability of organs. The development of bioengineered lungs is one potential therapeutic alternative to functional organ transplantation. Intensive research, carried out by several groups, has explored the possibility of using tissue engineering to produce completely decellularized organs.

Material/Methods: This study aimed to demonstrate in an experimental animal model the decellularization process of lungs in order to prepare scaffolds for artificial recreation of organs. For the successful creation of a bioengineered lung, it is necessary that the organ remains viable and contains a functional architecture that allows adequate ventilation, perfusion, and gas exchange.

Results: Cells and nuclear material were removed during the decellularization process, but the architecture of the alveolar septum remained unchanged. An scanning electron microscope study confirmed that the alveolar cells, red blood cells, and cellular proteins previously present in the native lung were absent in the decellularized structure. Quantitative trials showed that collagen had been retained in the extracellular matrix, while elastin was partially exhausted. High-resolution micro-computed tomography revealed that the lung architecture, arterial weft, and microcirculation remained intact.

Conclusions: Decellularization is part of the bioengineering process, and various ionic, nonionic, and zwitterionic detergents have been used during decellularization. The variety of methods used in these studies also reinforces the need for a standard decellularization protocol that could advance the development of bioengineered organs.

MeSH Keywords: Bioengineering • Lung • Tissue Scaffolds

Full-text PDF: <http://medscitechnol.com/abstract/index/idArt/892838>

1936 2 15



Background

Lung transplantation is a treatment provided to patients in advanced stages of significant respiratory diseases such as chronic obstructive pulmonary disease, idiopathic pulmonary fibrosis, primary pulmonary hypertension, interstitial lung disease, and cystic fibrosis. While opportunities for organ transplantation are somewhat limited, the list of patients with respiratory disease awaiting donation is increasing; a situation that is exacerbated by an aging population. Therefore, new strategies are required to increase the availability of organs for transplantation [1].

The development of bioengineered lungs is a potential therapeutic alternative to functional organ transplantation. Intensive research, carried out by several groups, has explored the possibility of using tissue engineering to produce completely decellularized organs. However, despite advances in the reconstruction of tissue and structures *in vitro*, engineered organs that have vascular networks capable of exchanging nutrients and gases and are appropriate for transplantation have yet to be produced. Specific advances in decellularization have enabled the production of scaffolds consisting of extracellular matrix (ECM) of natural origin, which are required for the process of organ engineering. These scaffolds provide appropriate biological signals and maintain the microarchitecture of the tissue so that the new organ can integrate successfully with the circulatory system of the recipient [2,3].

The decellularization technique has previously been used to successfully engineer a variety of tissues, including tissue of the bone, esophagus, arteries, bladder, trachea, and heart [4,5]. However, compared to other organs, the structure of the lung is extremely complex, and this has hindered the progress of bioengineered lungs [6,7].

Before complex bioengineered tissues such as those of the lung can be used in clinical applications, further developments will be necessary, such as advances in the standard procedures used for differentiation of cells, production of a matrix that meets the needs of the lung, and the development of application methods in the injured lung tissue [2].

Despite the complexity of the task, by using the appropriate protocols, the lung can be completely decellularized, and an extracellular structure can be obtained.

Material and Methods

Below, an animal experiment using lungs obtained from male Sprague-Dawley rats (300–500 g) is described. These rats were maintained at 20°C ($\pm 2^\circ\text{C}$), with a relative humidity of

55% ($\pm 10\%$), and a 12-h day/night cycle. To extract the lungs, the rats were anesthetized with urethane (1 mg/kg, intraperitoneal injection), phosphate-buffered saline (PBS) 1 \times was infused through the right ventricle, and the rats were killed by exsanguination. Subsequently, the trachea, esophagus, and lungs were extracted and stored at -80°C until the process of decellularization was begun. This protocol was approved by the Ethical Committee for Animal Experimentation of our institution (process number 0030/2011 CEUA-UNINOVE) and University of Barcelona.

Lung decellularization

The first step of decellularization was to increase cellular injury and facilitate cell loss through four cycles of thawing and freezing, with 10-min freezing at -80°C and then 10-min thawing to 40°C . The second step involved cleaning the lungs, whereby they were slowly perfused with PBS 1 \times via the trachea until an increased amount of blood cells was eliminated. Subsequently, the lungs were first perfused with autoclaved distilled H_2O , and then with a detergent, 1% sodium dodecyl sulfate (SDS). Next, the lungs were placed in a sterile flask with 1% SDS and agitated for approximately 20 h. The following day, washing with detergents was repeated, but with no agitation, by placing the lungs in new flasks with sterile 1% SDS for 20 h.

The next step involved perfusing PBS 1 \times through the trachea until the detergent remaining in the lung was eliminated and, after removal of detergent, perfusing PBS 1 \times containing amphotericin 2% (photosensitive) and penicillin/streptomycin 2% sterile. The lungs were then placed in a sterile flask containing PBS 1 \times , antibiotics 2%, and antifungals 2%, and agitated for approximately 20 h. Following this period, the washing procedure was repeated without agitation and the lungs were stored (Figures 1 and 2).

Preparation of decellularized lungs slices

A mixture of Optimal Cutting Temperature compound (OCT, Sakura) and PBS in a ratio of 3: 1 was infused into the trachea of the decellularized lungs before they were submitted to rapid freezing in liquid nitrogen. The samples were stored at -80°C before cryosections (40–100 μm) of the frozen lungs samples were obtained by using a cryomicrotome and placed in cell culture plates or elastic membranes. The slices were then washed with PBS containing antibiotics to remove OCT.

Quantification of DNA in decellularized lungs

The process of staining with 4',6-diamidino-2-phenylindole (DAPI) (Sigma-Aldrich) was used to verify the absence of nuclei or DNA after decellularization. For staining, a solution of DAPI (5 mg/mL; 14.3 mM for dihydrochloride or 10.9 mM for

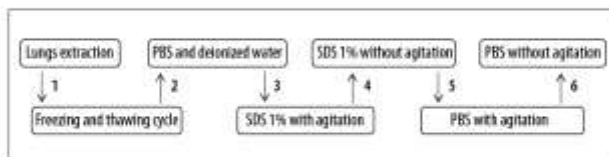


Figure 1. Steps of the decellularization process.



Figure 2. (A, B) Lungs during the decellularization process; (C) Decellularized lung of rat.

dilactate) was made by dissolving 10 mg of DAPI in 2 mL of deionized water, after sonication for 2 h. By producing images of these samples, the appropriate areas of the sample were checked to ensure that they were free from cells following decellularization. The samples were separated by electrophoresis on 3% low melting point (LMP) agarose gel with ethidium bromide at 60 V for 1 h, and observed under ultraviolet transillumination [8].

Quantification of the components of the extracellular matrix in the decellularized lungs

Collagen, elastin, laminin, and glycosaminoglycans (GAGs) were quantified in the decellularized lungs. For comparison, the same process was repeated using fresh non-decellularized lungs as a control. Collagen was quantified by oxidation of 4-OH-L-proline to pyrrole and reaction with p-dimethylaminobenzaldehyde (with the absorbance read at 560 nm). Elastin was measured by using a Fastin Elastin quantitative dye-binding kit (Bicolor Ltd.) according to the manufacturer's instructions. Laminin was measured by using a laminin ELISA kit (Genomics Insight) on samples homogenized with protease inhibitors (Roche). GAGs were determined by using a dimethyl methylene blue assay. Total protein was determined by using the Bradford method (Sigma-Aldrich).

Scanning electron microscopy

The decellularized lung samples were analyzed by using scanning electron microscopy (SEM), following the application of a standard protocol for the preparation of tissue samples. The tissue samples were fixed with 2% glutaraldehyde and 2.5% paraformaldehyde in 0.1 M cacodylate buffer for 2 h at room temperature, and then rinsed in cacodylate buffer, before being sliced and dehydrated through an ethanol gradient. The samples were then dehydrated in hexamethyldisilazane for 10 min and dried overnight. Finally, samples were sputter coated with gold and analyzed by using SEM.

Two-photon microscopy

Samples were visualized by multi-photon microscopy to detect autofluorescence in the tissue, and by second harmonic generation microscopy to detect fibrillar collagen. The fluorescence emission in the spectral region of 500–650 nm was recorded for detecting the bands of autofluorescence of the lung. The second harmonic generation was analyzed by using excitation at 800 nm and with a 400 ± 14 nm bandpass filter. Various locations in the apex of the lobe and in the broncho-alveolar region were analyzed. At each location, z-stacks were acquired from the external surface of the lung by using a z range of 1–150 μ m total depth, and by using a 40×0.75 NA, water immersion objective.

Results

For decellularization of the rat lung, Ott et al. [4] developed a system of pulmonary arterial infusion using 0.1% SDS and the application of pressure via physiological perfusion of the lung tissue. The process resulted in intact structures with vasculature, airways, and acellular alveolar. When using SDS at 0.1%, nuclear remnants were found in the cartilaginous rings of the trachea. However, while higher concentrations of SDS (0.5%) produced complete decellularization of the rings, impairment of membrane architecture was observed in the small vessels and alveolar septa. Therefore, 0.1% SDS has been used in subsequent experiments.

Petersen et al. [9] used a solution containing CHAPS in 1 M phosphate buffer while maintaining a perfusion pressure under 20 mmHg for 2–3 h. Cells and nuclear material were removed during decellularization (for example, quantification confirmed that 99% of DNA was removed), but the architecture of the alveolar septum remained unchanged. An SEM study confirmed that the alveolar cells, red blood cells, and cellular proteins previously present in the native lung were absent in the decellularized structure. Quantitative trials showed that

collagen had been retained in the extracellular matrix, while elastin was partially exhausted by the decellularization process (40% of elastin remained in the acellular matrix and more than 90% of GAG was removed). High-resolution micro-computed tomography revealed that the lung architecture, arterial wall, and microcirculation remained intact.

Price et al. [10] decellularized the lungs of mice, removed together with the trachea and heart. The lungs were perfused with distilled water, Triton X-100, and SDS to remove cellular material. More complete decellularization was achieved by infusion of solutions through the trachea and the right ventricle than by an independent route. After decellularization, lungs were ventilated with the aim of assessing the effects of process on the extracellular matrix. Following evaluation, the lung matrix, including collagen and elastin, was found to be intact.

A study published by our group demonstrated that freezing and thawing, a process commonly used in decellularization, did not induce significant changes in the ventilatory mechanical properties of decellularized lungs. Therefore, we demonstrated that the lung could be frozen and thawing during the decellularization process without changing its viscosity or elasticity for future recellularization [11].

Nonaka et al. characterized the behavior of the mechanical properties throughout the different steps of lung decellularization process using a conventional protocol based on SDS. Lungs resistance and elastance were measured along decellularization steps and were computed by linear regression fitting of tracheal pressure, flow, and volume during mechanical ventilation. The authors concluded although a variation in extracellular matrix stiffness observed during the decellularization process, this variation can be considered negligible overall because the resistance and elastance returned to basal values at the final process [12].

Discussion

For the successful creation of a bioengineered lung, it is necessary that the organ remains viable and contains a functional architecture that allows adequate ventilation, perfusion, and gas exchange. Decellularization is part of the bioengineering

References:

1. Yusen RD, Shearon TH, Qian Y et al: Lung Transplantation in the United States, 1999-2008. *Am J Transplantation*, 2010; 10(2): 1047-68
2. Nichol JE, Niles JA, Cortella I: Design and development of tissue engineered lung: Progress and challenges. *Organogenesis*, 2009; 5: 57-61
3. Arenas-Herrera JE, Ko IK, Atala A, Yoo JJ: Decellularization for whole organ Bioengineering. *Biomed Mater*, 2013; 8(1): 014106
4. Ott HC, Clippinger B, Conrad C et al: Regeneration and orthotopic transplantation of a bioartificial lung. *Nat Med*, 2010; 16: 927-33
5. Gilberta TW, Sellaro TL, Badyalok SF: Decellularization of tissues and organs. *Biomaterials*, 2006; 27: 3675-83
6. Price AP, Godin LM, Domek A et al: Automated Decellularization of Intact, Human-Sized Lungs for Tissue Engineering. *Tissue Eng Part C Methods*, 2014; [Epub ahead of print]

process, and various ionic, nonionic, and zwitterionic detergents have been used during decellularization.

Non-ionic detergents are used in decellularization protocols owing to their positive effects on tissue structure. Of these detergents, Triton X-100 is most frequently used. Non-ionic detergents disturb lipid-lipid and lipid-protein interactions, but keep intact protein-protein interaction so that the proteins in the tissue remain functional after treatment [13].

Ionic detergents can solubilize cytoplasmic and nuclear cellular membranes; however, they can also denature proteins by dysregulation of protein-protein interactions [13]. The most commonly used ionic detergents are SDS, sodium deoxycholate, and Triton X-200. Compared to other detergents, SDS more fully removes nuclear residues and cytoplasmic proteins. However, while it alteration the structure of native tissue, SDS does not necessarily promote the removal of collagen tissue [14].

Zwitterionic detergents, such as 3-[[3-cholamidopropyl] dimethyl ammonio]1-propanesulfonate (CHAPS), have nonionic and ionic properties, but have a greater tendency for denaturing proteins than do ionic detergents [15].

Several studies comparing different methods of lung decellularization were published with the use of temperature variation, via of the infusion line, and use of various detergents, however, the most efficient protocol for obtaining a lung scaffold is still unclear [4,9-12].

Conclusions

Previous studies showed that, by using the appropriate protocol, the lungs can be completely decellularized to obtain a preserved extracellular scaffold. The variety of methods used in these studies also reinforces the need for a standard decellularization protocol that could advance the development of bioengineered organs. Although significant progress has been made towards the production of bioengineered organs, many questions remain regarding their potential future application. In particular, further research will be necessary to overcome the difficulty of using differentiated cells and to resolve issues around limited availability and proliferation capacity.

7. He M, Callanan A: Comparison of Methods for Whole-Organ Decellularization in Tissue Engineering of Bioartificial Organs. *Tissue Eng Part B Rev*, 2013; 19(3): 194–208
8. Cortiella J, Niles J, Cantu A et al: Influence of acellular natural lung matrix on murine embryonic stem cell differentiation and tissue formation. *Tissue Eng Part A*, 2010; 16(8): 2565–80
9. Petersen TH, Calle EA, Zhao L et al: Tissue-engineered lungs for in vivo implantation. *Science*, 2010; 329(5991): 538–41
10. Price AP, England KA, Matson AM et al: Development of a decellularized lung bioreactor system for bioengineering the lung: the matrix reloaded. *Tissue Eng Part A*, 2010; 16: 2581–91
11. Nonaka PN, Campillo N, Uriarte JJ et al: Effects of freezing/thawing on the mechanical properties of decellularized lungs. *J Biomed Mater Res A*, 2013; 102(2): 413–19
12. Nonaka PN, Uriarte JJ, Campillo N et al: Mechanical properties of mouse lungs along organ decellularization by sodium dodecyl sulfate. *Respir Physiol Neurobiol*, 2014; 200: 1–5
13. Seddon AM, Cumow P, Booth PJ: Membrane proteins, lipids and detergents: not just a soap opera. *Biochim Biophys Acta*, 2004; 1666: 105–17
14. Woods T, Gratzel PF: Effectiveness of three extraction techniques in the development of a decellularized bone-anterior cruciate ligament-bone graft. *Biomaterials*, 2005; 26: 7339–49
15. Dahl SL, Koh J, Prabhakar V, Niklason LE: Decellularized native and engineered arterial scaffolds for transplantation. *Cell Transplant*, 2003; 12: 659–66

Received: 2014.11.28
 Accepted: 2014.12.22
 Published: 2015.01.07

Mathematical Models for Measuring Mechanical Properties in Experimental Animal Lung: A Literature Review

 Authors' Contribution:
 Study Design: A
 Data Collection: B
 Statistical Analysis: C
 Data Interpretation: D
 Manuscript Preparation: E
 Literature Search: F
 Funds Collection: G

ABG 1 Nadua Apostólico
BDG 1 Jessica Julioti Urbano
BDE 1 Renata Kelly da Palma
ABF 1 Rodolfo de Paula Vieira
AF 2 Glauber Sá Brandão
AF 3 Juan Jose Uriarte
AEG 1 Luis Vicente Franco Oliveira

 1 Experimental Cardiorespiratory Physiology Laboratory, Master's and Doctoral Degree Programs in Rehabilitation Sciences, Nove de Julho University, São Paulo, SP, Brazil
 2 Department of Education, University of the State of Bahia (UNEB), Salvador, BA, Brazil
 3 Unit of Biophysics and Bioengineering, Faculty of Medicine, University of Barcelona, Barcelona, Spain

Corresponding Author: Luis Vicente Franco de Oliveira, e-mail: oliveira.lvf@uninove.br

Source of support: The Experimental Cardiorespiratory Physiology Laboratory receives funding from Nove de Julho University (Brazil), support from the Conselho Nacional de Desenvolvimento Científico e Tecnológico (CNPq) (protocol number 166879/2013-4), and grants from the Fundação de Amparo à Pesquisa do Estado de São Paulo (FAPESP) (protocol number 2013/021765-5) and the Coordenação de Aperfeiçoamento de Pessoal de Nível Superior (CAPES) (BEX number 11514/protocol 13-2)

The mechanical properties of the respiratory system are important determining factors of their function and might be impaired in lung disease. Mathematical models are used for studying the physiology and pathology of human respiratory mechanics, but these parameters can also be used in animal testing with small animals, such as mice or rats. Depending on the experiment, a tracheostomy or endotracheal intubation should be performed: the tracheal cannula is connected to a pneumotachograph and a mechanical ventilator, which allows minute volume control, airflow, and positive end-expiratory pressure (PEEP). After stabilizing the ventilatory parameters, the mechanical properties are measured 10–15 times in each animal, and can be used in the equation of motion as the end-inspiration occlusion method. All data were analyzed using specific software. The lungs and the chest wall are usually treated as linear dynamic systems that can be expressed by differential equations, and thereby allow the determination of system parameters that reflect the mechanical properties. The unicompartimental linear model is sufficient to detail the mechanical behavior of the respiratory system in different physiological conditions. The use of mice to create a model of airway diseases has been essential to better understand the mechanical action of lung diseases.

MeSH Keywords: **Bioengineering • Biomedical Engineering • Lung • Respiratory Mechanics**
Full-text PDF: <http://medscitechnol.com/abstract/index/idArt/893173>
 4145
  —
  4
  40


Background

The lungs and the chest wall are usually treated as a linear dynamic system that can be expressed by differential equations, and thereby allow the determination of system parameters that reflect the mechanical properties. However, different models that include nonlinear characteristics and multiple compartments have been used in several approaches, especially in patients with acute lung injury requiring mechanical ventilation [1].

Bates et al. proposed the viscoelastic 2-compartment model, based on studies by Mount. The mechanical properties of the tissues, however, are now represented by 3 elements: a resistor (R_1 , known as a *dashpot*) and 2 springs. The 3 elements – R_1 , E_1 , and E_2 – together constitute what is known as a *Kelvin body*. The stiffness of the spring E_1 represents the static elastic behavior of the lung, and the series combination of R_1 and E_2 (which together constitute a *Maxwell body*) account for its viscoelastic behavior. This is different from the principle of the single compartment proposed by Otis in 1956, which does not consider the slower pressure drop observed after occlusion of the airway at the end of inspiration, as described in Figure 1 [2-4].

Ventilatory volume, flow, and pressure measurements of the respiratory system in physiological and pathological conditions allow the evaluation of the mechanical behavior of the system, and of its components in isolation [5,6].

Pulmonary ventilation requires mechanical work to overcome opposing forces. These forces include elastic and viscoelastic lung tissue resistive forces generated by the flow of air in the airways. This air flow is also responsible for plastic-elastic hysteresis forces, inertial forces (e.g., dough-dependent tissues and gases), and gravitational forces (which are typically included in the measurements of elastic forces) [7].

The main determinants of the mechanical integrity of lung tissue fibers are collagen, elastin, and proteoglycans, but cells may also contribute to the mechanical tissue [8]. However, 2 main structures contribute to the elastic behavior of the pulmonary parenchyma: tissue fibres and alveolar lining. The lungs always tend to shrink and collapse because of the elastic recoil force resulting from elastin and collagen fibers and their geometrical arrangement, which tends to return them to their minimum volume [9].

Another important factor contributing to the elastic characteristics of lung tissue is the surface tension of the liquid film lining the alveoli. The surfactant causes a change in the surface tension as a function of the alveolar volume, and contributes to increased lung compliance and decreased respiratory activity [9].

Tissue resistance is determined by the energy losses caused by viscosity (i.e., friction) relative to the movement of the lungs and by the speed of displaced air. The larger the dissipated power to overcome frictional resistance of the fabric during expiration, the lower the elastic force available to overcome the pulmonary resistance. In normal individuals, tissue resistance corresponds to 20% of lung resistance and airway resistance accounts for the remainder [10].

Mathematical Models

Mathematical models seek to represent the behavior of the respiratory system in different physiological conditions, and have contributed to a better understanding of respiratory mechanics. Using complex models, especially in the presence of disease, allows better interpretation of physical mechanisms that enable detailed analysis of signals [10].

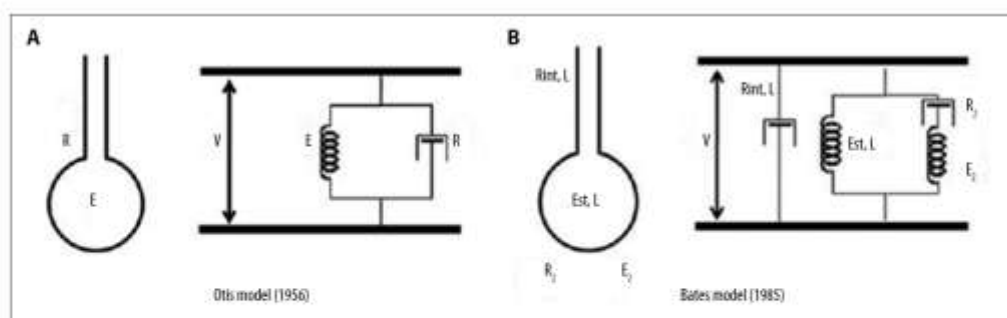


Figure 1. Anatomical and viscoelastic representation: (A) Single-compartment linear lung model; (B) Bicompartimental lung model with 2 degrees of freedom.

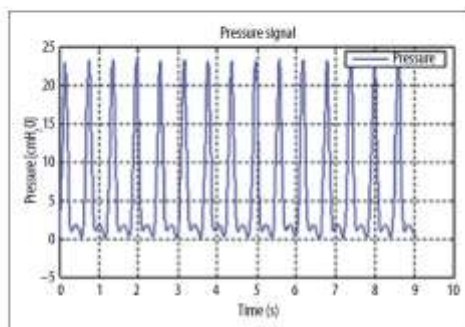


Figure 2. Tracheal pressure curve in related to time – Equation of motion.

Equation of Motion

In the early 20th century, Rohrer analyzed the influence of elastic and resistive inertive components to study the physical phenomena involved in the mechanical motion of the respiratory system [11].

The equation of motion (Equation 1, Figure 2) is the sum of resistive pressure (P_{res}) in relation to airflow in the airways; inertive pressure (P_{in}) in relation to the time derivative of the flow; the elastic pressure (P_e) in relation to the volume (V) above the functional residual capacity (FRC); and residual end-expiratory pressure (P_0). This constitutes the unicompartamental linear model in which P_{atm} is the opening pressure of airway, R is the resistance, E is the elastance, I_n is inertance of the respiratory system, V' is the flow, and P_0 is the time derivative of the flow [12].

$$P_{atm} = R \cdot V' + E \cdot V + I_n \times V' + P_0$$

The pressure applied to the respiratory system of a patient under mechanical ventilation is the sum of the pressure generated by the ventilator – measured at the airway opening (i.e. mouth) – and the pressure generated by the respiratory muscles, which can be described by the movement equation as follows:

$$P_{st} = P_{AO} + P_{mus} = V' \times R + V/C + k$$

in which P_{st} is the pressure of the respiratory system, P_{AO} is the pressure at the airway opening, P_{mus} is the pressure generated by the respiratory muscles, V is the volume, V' is the flow, R is the airway resistance, C is the compliance of the respiratory system, and k is a constant representing the positive end-expiratory pressure (PEEP) or, when associated with auto-PEEP, PEEP full.

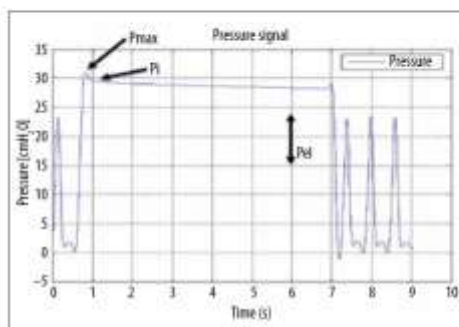


Figure 3. Tracheal pressure curve related to time – End-inspiratory airway occlusion.

When the respiratory activity of the patient is entirely passive (i.e., ventilation is controlled), the pressure developed by the respiratory muscles is negligible and the pressure required to move the air into and outside of the respiratory system can be described by the following simplified motion equation:

$$P_{st} = P_{AO} = V' \times R + V/C + k$$

Based on the characteristics of the forces to be overcome, the motion equation can be split into 2 components: the resistive component and the elastic component.

" $V' \times R$ " corresponds to the pressure dissipated through the air and the endotracheal tube that overcomes the friction forces generated by the flow of gas, which with the V determines the resistance of the respiratory system.

" V/C " corresponds to the pressure that must be applied to the system to overcome the elastic forces; V/C depends on inflation in excess of the residual volume, and reflects the compliance of the respiratory system volume.

End-Inspiratory Airway Occlusion

Respiratory mechanics are evaluated by the viscoelastic properties analyzed using parameters obtained by mechanical ventilation, based on the end-inspiratory airway occlusion method, described by Bates et al. [13,14]. After connecting the tracheostomy on a ventilator with a constant tidal volume (VT), airflow (V'), and PEEP, the lungs will be ventilated and subjected to 10 inspiratory pauses, with each lasting 6 seconds for the measurements.

According to Figure 3, after the occlusion of the end-inspiratory airway, a sudden fall in tracheal pressure from the maximum value (P_{max}) to a turning point (P_i) occurs in which the

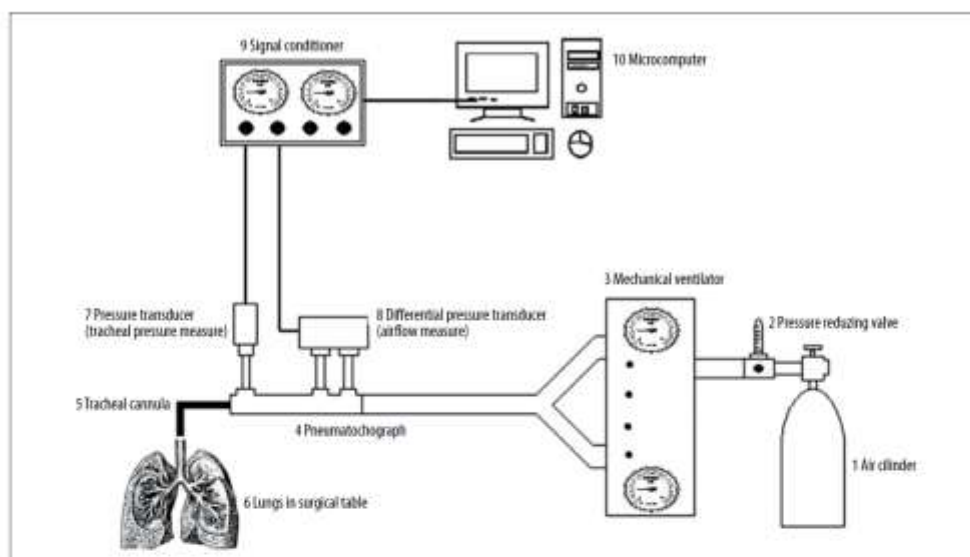


Figure 4. Respiratory mechanics study model setup.

pressure decay slows and reaches a plateau. This plateau phase corresponds to the elastic recoil pressure of the lungs (P_{el}). The pressure difference (ΔP_1), which characterizes the initial rapid decline represented by the difference between the initial P_{max} and P_i , is the viscous component [15].

Briefly, after end-inspiratory occlusion, there is an initial fast drop in PL (ΔP_1) from the pre-occlusion value down to an inflection point (P_i) followed by a slow pressure decay (ΔP_2) until an apparent plateau is reached [3]. ΔP_1 selectively reflects pressure dissipated against pulmonary resistance in normal animals and humans and ΔP_2 reflects viscoelastic properties (stress relaxation) and/or homogeneities of lung tissues, together with a miniscule contribution from the pendelluft in normal situations [16].

The second variation of pressure (ΔP_2), represented by the slow fall of P_i to the plateau (P_{el}), reflects the pressure dissipated to overcome the viscoelastic component. The sum of ΔP_1 and ΔP_2 provides the total pressure in the lungs (ΔP_{tot}). The static elastance (E_{st}) and dynamic elastance (E_{dyn}) can then be obtained by dividing P_{el} and P_i , respectively, by tidal volume; E is the difference between E_{dyn} (i.e., static compliance) and E_{st} (i.e., dynamic compliance) [17].

To obtain the P_i , the nonlinear fit to 2-exponential decay curves, which determine the time of fast decay and slow decay, and the pressure value at the time of passage $\Delta P_1 + \Delta P_2$ are used. To this end, *MicracalOrigin* 6.0 software is used for analysis.

To obtain the analyzed parameters, the following formulas are used:

$$\begin{aligned} \Delta P_1 &= P_{max} - P_i \text{ Est} = P_{el}/VC \\ \Delta P_2 &= P_i - P_{el} \text{ Edyn} = P_i/VC \\ \Delta P_{tot} &= \Delta P_1 + \Delta P_2 \Delta E = E_{dyn} - E_{st} \end{aligned}$$

Multiple Occlusion Method

In the multiple occlusion technique, airway occlusion is performed several times at different expiration points. From the moment the Hering-Breuer reflex is triggered, the pressure graph shows that a plateau is the elastic recoil pressure at the time of occlusion.

When the volume remaining in the lung is above the FRC at the time of occlusion, this volume is plotted against the other pressures. The slope of the resulting plot of the volume and pressure, which is calculated by linear regression, represents the intercept, and compliance of the respiratory system (C_{rs}) represents the axis of the volume, and shows how much lung volume was increased at the end of expiration. Thus, to evaluate passive respiratory mechanics, it is necessary to accurately measure volume, flow, and pressure [18]. The absence of muscle relaxant administration is the main advantage of this method [19].

Expiration Relaxed Method

This technique consists of the occlusion of air at the end of each inhalation pathway, which may be spontaneous. While occlusion is maintained, the relaxation of the elastic pressures of the respiratory muscles is measured, and is used to obtain the values of complacency. When the airway opens and relaxes, expiration occurs, but if no other forces are being generated, the resistive pressure can be calculated [20]. It has been demonstrated that cardiac surgery increases the pulmonary complacency, thus altering the expiratory flow [21].

When the occlusion is released, relaxed exhalation and a single compartment may represent the respiratory system. The downward portion of the cycle, when flow volume has increased, is the expiratory time constant of the respiratory system, which indicates the time needed to vent 63% of the lung volume [20,21].

Forced Oscillation Technique

The forced oscillation technique (FOT) is a complementary tool that allows translational and experimental evaluation of pulmonary function in rats. This technique is comprehensive, detailed, accurate, and reproducible, and provides mechanical measurements of the respiratory system by analyzing pressure – volume signals obtained in response to predetermined criteria, a small amplitude, and waveform oscillating flow (also referred to as the disturbance or input signal) that are typically applied in opening the patient's airway [22].

Its simplest form would be a single sinusoidal waveform with a well-defined frequency. More complex disorders typically consist of a superposition of a selection of specific waveforms of (mutual) frequencies that cover a broad spectrum. The decomposition of the input signals and output to the multi-frequency components using the Fourier transformation allows the calculation of the input impedance of the respiratory system (Z_{rs} ; the transfer function between the input signals and the output in each frequency) [22].

Therefore, the forced oscillation technique allows simultaneous evaluation of respiratory mechanics in a range of frequencies in a single manoeuvre. Advanced mathematical models (e.g., the constant phase model) for impedance data allow a division of the response-dependent parameters (central and peripheral) airways and lung parenchyma tissue [23].

Experimental Protocol

Small animals such as mice or rats can be used in this experimental model. The animals must first be sedated and

anaesthetized, and then placed on a surgical table where a tracheostomy and/or endotracheal intubation are performed.

For the tracheostomy procedure, a small longitudinal incision is created in the anterior neck. The tissues surrounding the trachea are exposed where the longitudinal incision is made between the 2 fibrous cannulae to introduce the appropriate length and diameter tubes for the individual animal (e.g., 0.5 mm in diameter for mouse rings and 2.1 mm in diameter for rats). Then, the animals were paralyzed with pancuronium bromide (0.1 mg/kg i.v.), and ventilated with frequency of 100 breaths/min, tidal volume of 0.2 ml, and flow of 1 ml/s, and PEEP 2 cmH₂O, and a constant-flow for mice and for rats with frequency of 100 breaths/min, tidal volume of 0.2 ml, and flow of 2 ml/s and PEEP 2 cmH₂O.

A pneumotachograph (1.5 mm ID, length=4.2 cm, distance between side ports=2.1 cm) was connected to the tracheal cannula for the measurement of air flow (V'). The pneumotachograph is connected to a ventilator (Samay MVR17, Universidad de la Republica, Montevideo, Uruguay or Harvard Model 683, Harvard Apparatus, South Natick, MA) [16]. A pressure transducer (-P23 Db Statham Gould, Oxnard, CA) measures the tracheal pressure and a differential pressure transducer (PT5A; Grass, Quincy, MA) measures airway flow (V'). These devices are attached to the pneumotachograph, as illustrated in Figure 4.

The signal transducers are connected to a signal conditioner (EMG System Sao Paulo, Brazil), which has an 8-channel analogue input, 1000x amplification, sampled at 250 Hz with an analogue-digital 12-bit converter used in signal processing with the aid of a microcomputer, and data acquisition software Windaq/Pro (DATAQ Instruments, Akron, OH). The ventilator flow is generated by a compressed air source connected to the fan by a pressure-reducing valve. The flow resistance produced by the system (r_{eq}), including the endotracheal tube, must be taken into consideration.

The pressure resistance of the equipment is subtracted from pulmonary resistive pressure so that the intrinsic values are real. After the tracheotomy, muscle relaxation is achieved with curare, and the tracheal cannula is connected to a pneumotachograph. A fan controls the tidal volume, air flow (V'), and PEEP. After stabilizing the ventilatory parameters, the mechanical properties were measured 10–15 times in each animal. All data were analyzed using specific software.

Model of Acute Lung Injury Using Venom and Respiratory Mechanics

A previous study investigated the pulmonary mechanics [i.e., static (E_{st}) and dynamic (E_{dyn}) elastances, resistive (ΔP_1)

and viscoelastic pressures (DeltaP2), measured by the occlusion method at the end of inspiration from BALB/c mice at 1, 24, 48, and 72 h after intravenous injection of saline or *Bothrops jararaca* crude venom [0.3 (V0.3) or 1 (V1) microg-g(-1)]. [23]

Est, Edyn, and DeltaP2 increased at 1 h in both V groups, being significantly higher in V1 than in V0.3, decreasing progressively, reaching control values at 48 h in V0.3, but remaining altered in V1 at 72 h. DeltaP1 augmented in V1 at 1 h, and returning to normal at 72 h. This model allows a better understanding of the pathophysiological effects of different toxins in the respiratory system, which leads to faster and more efficient clinical interventions [23].

Another study investigated the effects of venom of the rattlesnake *Crotalus durissus terrificus* (CdtV) on the events of pulmonary mechanics [static compliance and dynamic resistance (DP1) and viscoelastic pressures (DP2)] and histology after intramuscular injection of saline (control) or venom (0.6 mg/g) [24]. The values of static and dynamic elastance were significantly increased after 3 h of venom inoculation, but were reduced to the control values in other periods that were studied. The DP1 values, which correspond to the resistive properties of the lung tissue, showed a significant increase 6 h after the CdtV injection and decreased to the basal levels 12 h after venom injection. In the DP2 analysis, viscoelastic components had a corresponding increase 12 h after the injection of the venom, and returned to the control values within 24 h. The CdtV also increased leukocyte recruitment (3–24 h) in the wall of the lung parenchyma and air routes [24].

A recent study evaluated the effects of an intramuscular injection of venom of the scorpion *Tityus serrulatus* (TsV) (0.67 mg/g) on lung mechanics and lung inflammation at 15, 30, 60, and 180 min after inoculation. The TsV injection increased lung elastance, compared to the lung elastance in the control group ($P < 0.001$). These values were significantly higher at 60 min than at 15 min and 180 min ($P < 0.05$) [25].

The values of resistive pressure (DP1) decreased significantly by 30, 60, and 180 min after TsV injection ($P < 0.001$). The TsV injection increased lung inflammation, which was characterized by an increased density of mononuclear cells 15, 30, 60, and 180 min after the TsV injection, compared to lung inflammation in the control group ($P < 0.001$) [25].

The TsV injection also increased the density of lung polymorphonuclear cells 15, 30, and 60 min after injection, compared to the polymorphonuclear cell density in the control group ($P < 0.001$) [25]. A study involving blooms of toxic cyanobacteria due to microcystin exposure investigated the mechanical changes through the occlusion method at the end of inspiration at 2:08 h and at 1, 2, and 4 days after the injection of the

toxin. The authors concluded that microcystin led to a rapid rise in lung impedance and an inflammatory response with interstitial edema and inflammatory cell recruitment in mice [26].

Experimental Model of Respiratory Mechanics and Chronic Lung Disease

A study in rats using TOF methacholine-induced bronchospasm (12.5 mg/mL) showed increased resistance of the baseline end-expiratory pressure when measurements were performed with increasing pressures of 3–9 cmH₂O. When bronchodilators were administered, airway resistance was reduced as an effect of higher volume and pressure; this finding reflects the viscoelasticity of the tissue parameter and possibly lower resistance of the airway [27].

In a study by Fernandes et al. [28], 12 adult Wistar rats were randomly divided into 2 groups of 6 animals each: a Pentobarbital (PENTO group) and a Dexmedetomidine (DMED group). During mechanical ventilation, the respiratory mechanical parameters were similar in both groups. The absence of histological changes supported these results. For analysis, the lung mechanical occlusion method at the end of inspiration was used. The average constant inspiratory flows and volumes, as well as lung, and chest wall Est, Ptot, P1, and P2, were similar in both groups. Dexmedetomidine does not alter the parameters of respiratory mechanics and lung histology in normal rats, but caused respiratory depression with hypercapnia and hypoxemia.

Lino et al. [29] investigated a potential correlation between formaldehyde (FA) inhalation and asthma; however, the exact role of the FA remains controversial. The effects of FA inhalation after ovalbumin (OVA) sensitization were investigated using a parameter of respiratory function, as assessed by the end-inspiratory occlusion method. They concluded that exposure to FA before OVA sensitization reduces respiratory mechanics.

In a study by Aristoteles et al. [30], guinea pigs were exposed to repeated OVA inhalation to obtain an experimental model of asthma. For 4 days, the animals were administered 1400 W [specific inducible nitric oxide synthase (iNOS) inhibitor], commencing on the last inhalation. A slice of the distal lung respiratory function was evaluated using the oscillatory force technique wherein the tissue resistance (Rt) and tissue elastance (Et) were evaluated before and after the OVA challenge (0.1%); the lung slices were subjected to histopathological studies. The authors found that animals that had been exposed to OVA showed an increased response in Rt and maximum Et in the distal lung tissue ($P < 0.001$). The 1400 W administration reduced all of these responses in the alveolar septa ($P < 0.001$). Exposed animals that received ovalbumin alpha-amino acid

N(ω)-hydroxy-nor-L-arginine (nor-NOHA) decreased by Rt, Et after challenge with antigen-positive iNOS cells, and 8-iso-prostane and NF- κ B ($P < 0.001$) in lung tissue [30].

Hyperinflation reduces elastic recoil and expiratory airflow limitation. It also increases respiratory work and oxygen demand, thereby hurting gas exchange and increasing the consumption of oxygen by cells, which leads to a progressive inability to perform physical activities.

Fusco et al. [31] evaluated pulmonary function before and after lung volume reduction surgery in an experimental rat model. The equation of motion, adapted to the respiratory system, was used to obtain the values of resistance and elastance of the respiratory system. They found that the elastance of animals subjected to bi-lobectomy and papain was higher than the elastance of animals subjected to papain without undergoing surgery; it was statistically equal to the physiological solution with and without surgery. The authors conclude that the elasticity of the respiratory system of animals with emphysema undergoing lung volume reduction through bi-lobectomy returned to levels equivalent to the control group values.

Experimental Model of Respiratory Mechanics and Atelectasis

An experimental model of atelectasis was created in rats, in which a sphygmomanometer is wrapped around the thorax or abdomen of the animal and the cuff is inflated for 5 s. The pulmonary mechanics were obtained through the occlusion technique at the end of inspiration before and after compression. The sample was divided into 2 groups: group A and group B atelectasis (control). The authors showed that in group A the respiratory mechanics remained unchanged, but in group B there was an increase in the resistive and viscoelastic pressures and increased static and dynamic elastance [32].

Trauma Induced by Mechanical Ventilation and Respiratory Mechanics

In 1994, Kano [12] proposed an index characterized by the percentage of dependent elastance in the total volume elastance (% E2), which identifies recruitment when this index is less than zero and hyperinflation when the index is greater than 30. Use of this index is important in preventing injury induced by mechanical ventilation. However, these studies did not consider the influence of the presence of 1 element or an inertive element. Dependent flow resistance may result in estimated elastance indexes and may be derived from them [33].

Pulmonary Mechanics in Animals Exposed to Environmental Pollution

A study published in 2014 aimed to investigate the time-dependency of lung impairment in animals that underwent a single exposure to residual oil fly ash (ROFA), simulating the situation of someone visiting a polluted place for a day. In conclusion, the authors demonstrated that the exposure to low doses of ROFA rapidly compromised pulmonary mechanics and histology, and the pathophysiological findings resolved 5 days after exposure [34]. In this study, the end-inspiratory pressure occlusion was used to evaluate lung mechanics.

Arsenic is a significant global environmental health problem. Exposure to arsenic in early life has been shown to increase the rate of respiratory infections during infancy, reduce childhood lung function, and increase the rates of bronchiectasis in early adulthood. In this article, lung mechanics were measured using the forced-oscillation technique and that technique generates measures of airway resistance (Raw), tissue damping (G), and elastance (H). Further details are provided in the Supplemental Material (pp. 3–4). The authors conclude in animals developmentally exposed to both arsenic and influenza had additive deficits in lung mechanics in early life and additive effects on airway responsiveness in adulthood [35].

Organs Bioengineering and Mechanical Properties

Study involving bioengineered organs, based on the scaffold of decellularized organs and using cycles of freeze/thaw in a conventional decellularization protocol, showed a slight increase in static elastance (15%) and dynamic elastance (15.7%). Fifteen lungs were decellularized and measured using the motion equation technique, so that the resistance ($p < 0.01$) and elastance ($p < 0.05$) increased significantly. The percentage of variation reached 79% resistance to A and reached a range of 28–35% for elastance E (34.3%), EL static (28.1%), and EL dyn (30.1%). However, data obtained using the technique of end-inspiratory occlusion, as well as static and dynamic elastance, showed no significant increase [36].

However, the increase in elastance has physiological implications in the performance of the scaffold when subjected to conventional lung ventilation during repopulation. This small change in elastance can be attributed to a small, induced formation of ice crystals at a non-uniform rate with changes within the scaffold, which determine the 3D architecture in most bronchi and alveoli with volume changes during breathing. Studies indicate that the technique of freezing/thawing has no relevant small effect on lung mechanical properties in decellularized lung scaffolds using the equation of motion technique

as the end-inspiratory occlusion method for assessing pulmonary mechanical properties [37].

The significant increase in resistance and elastance parameters observed after the first wash with sodium dodecyl sulphate (SDS), in which the lung becomes more translucent as the cellular material was washed out, can be attributed to the presence of cellular debris, which generated the apparent mucus [36]. Use of the equation of motion model containing the volume-dependent elastance can help unravel the elastic nonlinearities when subjected to opening and closing cycles of the airways in the respiratory system [38,39].

A study by Uriarte et al. [40] aimed to evaluate the effects of sterilization by gamma irradiation of lung scaffolds on the mechanical properties of an acellular organ when subjected to mechanical ventilation manoeuvres in bioreactors. The mechanical properties of decellularized lungs were measured before and after irradiation using the occlusion method at the end of inspiration. The lungs showed higher resistance (RL) and elastance (EL) after irradiation than before irradiation.

The RL increased 41.1% with room temperature irradiation and 32.8% with frozen irradiation, and EL increased by 41.8% with room temperature irradiation and 31.8% with frozen irradiation. Irradiation induced similar increases in static and dynamic elastance. Gamma radiation applied at a conventional dosage to ensure sterility modifies the mechanical properties of a decellularized organ and has potential implications for lung bioengineering [40].

Conclusions

Mathematical models represent the intrinsic nature of the system and the unicompartamental linear model sufficiently explains the mechanical behavior of the respiratory system in different physiological conditions. The use of mice to create a model of airway disease has been essential in better understanding the mechanisms of lung diseases.

Conflicts of interest

The authors declare no financial or other conflict of interest regarding this article.

References:

- Carvalho AR, Zin WA: Respiratory system dynamical mechanical properties: modeling in time and frequency domain. *Biophys Rev*, 2011; 3: 71-84
- Mount LE: The ventilation flow-resistance and compliance of rat lungs. *J Physiol*, 1955; 127(1): 157-67
- Bates JHT: Understanding lung tissue mechanics in terms of a mathematical model. *Monaldi Arch Chest Dis*, 1993; 48(2): 134-39
- Otis AB, Mckenrow CB, Bartlett RA et al: Mechanical factors in distribution of pulmonary ventilation. *J Appl Physiol*, 1956; 8: 427-43
- Zin WA, Gomes RFM: Mathematical models in respiratory mechanics. *Crit Care Med*, 1996; 10: 391-400
- Zin WA: Métodos e técnicas para monitorização das propriedades elásticas e resistivas dos pulmões e da parede torácica na insuficiência respiratória aguda. *Jornal de Pneumologia*, 1990; 16: 91-96 [in Portuguese]
- Dunsmore SE, Rannels DE: Extracellular matrix biology in the lung. *Am J Physiol*, 1996; 270(1 pt 1): 13-27
- Romero PV, Cañete C, Aguilar JL et al: In: Milic-Emili J (ed.), *Applied physiology in respiratory mechanics*. Milano: Springer, 1998; P57-72
- Robatto FM: Lung tissues mechanics. In: Milic-Emili J (ed.), *Applied physiology in respiratory mechanics*. Milano: Springer, 1998; P50-56
- Zin WA, Rocco PRM: *Mecânica respiratória*. Cap. 46. P. 514-526 in: Aires MM (ed.), *Fisiologia*. Rio de Janeiro: Guanabara Koogan S, 1999; A. 934 [in Portuguese]
- Mead J: Mechanical properties of lung. *The American of Physiology Society*, 1961; 41(2): 281-330
- Kano S, Lanteri CJ, Duncan AW, Sly PD: Influence of nonlinearities on estimates of respiratory mechanics using multilinear regression analysis. *J Appl Physiol* (1985), 1994; 77: 1185-97
- Bates JHT, Deamer D, Chartrand D et al: volume-time profile during relaxed expiration in the normal dog. *J Appl Physiol* (1985), 1985; 59(3): 732-37
- Mount LE: Ventilation flow-resistance and compliance of rat lungs. *J Physiol*, 1955; 131: 157-67
- Gotthardt SB, Higgsd, Rossi A, Carli F et al: Interrupter technique for measurement of respiratory mechanics in anesthetized humans. *J Appl Physiol* (1985), 1985; 59(2): 647-52
- Saldiva PHN, Zin WA, Santos RIB et al: Alveolar pressure measurement in open-chest rats. *J Appl Physiol*, 1992; 72: 302-6
- Martins MA, Saldiva PH, Zin WA: Evoked bronchoconstriction: testing three methods for measuring respiratory mechanics. *Respir Physiol*, 1989; 77(3): 41-53
- Zin WA, Pengelly LD, Milic-Emili J: Single-breath method for measurement of respiratory mechanics in anesthetized animals. *J Appl Physiol Respir Environ Exerc Physiol*, 1982; 52(5): 1266-71
- Gappa M, Colin AA, Goetz I, Stoks I: Passive respiratory mechanics: the occlusion techniques. *Eur Respir J*, 2001; 17: 141-48
- Bates JHT, Irvin CG: Measuring lung function in mice: the phenotyping uncertainty principle. *J Appl Physiol*, 2003; 94: 1297-306
- Bates JHT: *Lung mechanics. An inverse modeling approach*. Cambridge University Press, New York, 2009
- Hantos Z, Daroczy B, Suki B et al: Input impedance and peripheral inhomogeneity in dog lungs. *J Appl Physiol*, 1992; 72: 168-78
- Silveira KS, Boehem NT, do Nascimento SM et al: pulmonary mechanics and lung histology in acute lung injury induced by *Bothrops jararaca* venom. *Respir Physiol Neurobiol*, 2004; 139(2): 167-77
- Nonaka PN, Amorim CF, Peres ACP et al: Pulmonary mechanic and lung histology injury induced by crotalus durissus terrificus snake venom. *Toxicol*, 2008; 51: 1158-66
- Peres ACP, Nonaka PN, Carvalho PTC et al: Effects of tityussmilestus scorpion venom on lung mechanics and inflammation in mice. *Toxicol*, 2009; 53: 779-85
- Soares RM, Cagido VR, Ferraro RB et al: Effects of microcystin-ir on mouse lungs. *Toxicol*, 2007; 50(3): 330-38
- McGovern TK, Robichaud A, Fereydoonzad L et al: Evaluation of Respiratory System Mechanics in Mice using the Forced Oscillation Technique. *J Vis Exp*, 2013; (75): e50172
- Fernandes FC, Ferreira HC, Cagido VR et al: Effects of dexmedetomidine on respiratory mechanics and control of breathing in normal rats. *Respir Physiol Neurobiol*, 2006; 154(3): 342-50

29. Lina-dos-Santos-Franco A, Gimenes-júnior JA, Ugras-de-Oliveira AP et al: Formaldehyde inhalation reduces respiratory mechanics in a rat model with allergic lung inflammation by altering the nitric oxide/cyclooxygenase-derived products relationship. *Food Chem Toxicol*, 2013; 59: 733-38
30. Aristoteles LR, Righetti RF, Pinheiro NM et al: Modulation of the oscillatory mechanics of lung tissue and the oxidative stress response induced by arginase inhibition in a chronic allergic inflammation model. *BMC Pulm Med*, 2013; 13: 52
31. Fusco IB, Fonseca MH, Pêgo-Fernandes PM et al: Cirurgia de redução do volume pulmonar em modelo experimental de enfisema em ratos. *J Bras Pneumol*, 2005; 31(1): 34-40 [in Portuguese]
32. Contador RS, Chagas PS, Vasconcelos FP et al: Evaluation of respiratory mechanics and lung histology in a model of atelectasis. *Respir Physiol Neurobiol*, 2003; 137(1): 61-68
33. Nève V, Leclerc F, de La-Roque ED et al: Overdistention in ventilated children. *Crit Care*, 2001; 5(4): 196-203
34. Carvalho GMC, Nagato LKS, Fagundes SS et al: Time course of pulmonary burden in mice exposed to residual oil fly ash. Published on *Frontiers in physiology*. September 2014, Volume 5, Article 366
35. Ramsey KA, Foong RE, Sly PD et al: Early life arsenic exposure and acute and long-term responses to influenza A infection in mice. *Environ Health Perspect*, 2013; 121(10): 1187-93
36. Nonaka PN, Campillo N, Uriarte JJ et al: Effects of freezing/thawing on the mechanical properties of decellularized lungs. *J Biomed Mater Res A*, 2014; 102(2): 413-19
37. Nonaka PN, Uriarte JJ, Campillo N et al: Mechanical properties of mouse lungs along organ decellularization by sodium dodecyl sulfate. *Respir Physiol Neurobiol*, 2014; 200: 1-5
38. Vassiliou MP, Petri L, Amygdalou A et al: Linear and nonlinear analysis of pressure and flow during mechanical ventilation. *Intensive Care Med*, 2000; 26: 1057-64
39. Bersten AD: Measurement of overinflation by multiple linear regression analysis in patients with acute lung injury. *Eur Respir J*, 1998; 12: 526-32
40. Uriarte JJ, Nonaka PN, Campillo N et al: Mechanical properties of acellular mouse lungs after sterilization by gamma irradiation. *J Mech Behav Biomed Mater*, 2014; 40: 169-77